



**Abatement of Heavy Metals from Aqueous Solution using Modified
Bentonite and Biochar Derived from *Lepironia Articulata***

Asadullah

A Thesis Submitted in Fulfillment of the Requirements for the Degree of
Doctor of Philosophy in Chemical Engineering
Prince of Songkla University

2019

Copyright of Prince of Songkla University



Abatement of Heavy Metals from Aqueous Solution using Modified
Bentonite and Biochar Derived from *Lepironia Articulata*

Asadullah

A Thesis Submitted in Fulfillment of the Requirements for the Degree of
Doctor of Philosophy in Chemical Engineering
Prince of Songkla University
2019
Copyright of Prince of Songkla University

This is to certify that the work here submitted is the result of the candidate's own investigations. Due acknowledgement has been made of any assistance received.

.....Signature
(Assoc. Prof. Dr. Luponng Kaewsichan)
Major Advisor

.....Signature
(Mr. Asadullah)
Candidate

I hereby certify that this work has not been accepted in substance for any degree, and is not being currently submitted in candidature for any degree.

.....Signature

(Mr. Asadullah)

Candidate

Thesis Title	Abatement of Heavy Metals from Aqueous Solution using Modified Bentonite and Biochar Derived from <i>Lepironia Articulata</i>
Author	Mr. Asadullah
Major Program	Chemical Engineering
Academic Year	2018

ABSTRACT

Heavy metal once released from industries have adverse effects on environment as a whole. Adsorption technique through cost effective adsorbents was said to be more effective comparing with commonly used conventional wastewater treatment methods. Current study initially aimed to produce organic and inorganic clay adsorbents and further to modify them using surfactant and alkali to get higher surface area and more developed surface functional groups. Bentonite clay adsorbent was modified using benzylhexadecyldimethyl ammonium chloride (BCDMACl) surfactant to increase its surface functional groups and cation exchange capacity (CEC) value. *Lepironia articulata* was taken as biomass to prepare hydrochar (HC) using hydrothermal carbonization (HTC) method. The HTC temperature was kept at (180, 200, 220, and 240 °C) and the residence time was varied at (2, 4, 6, 12, and 24 h), respectively. HC produced was used as precursor for the preparation of modified biochar (LABC). Modification of LAHC to LABC was performed in a tubular reactor under slow pyrolysis conditions at 700 °C. KOH was used as a chemical activating agent by keeping the HC to chemical ratio of (1:3). All the adsorbent materials before and after modification were characterized using Scanning electron microscopy (SEM) and energy dispersive X-ray (EDX), Fourier transform infrared spectroscopy (FTIR), and Brunauer–Emmett–Teller (BET), Cation exchange capacity (CEC), proximate analysis, thermogravimetric analysis (TGA), higher heating value (HHV), Wettability were evaluated by contact angle, to determine the elemental composition of materials X-ray fluorescence (XRF) was used. The surface area of modified biochar (LABC) was remarkably increased to 820.54 m² g⁻¹ for LABC from 69.23 m² g⁻¹ due to chemical activation. To investigate the performance of biochar after modification, batch

experiments were performed with aqueous solutions of chromium (VI), Nickel (II), and Zinc (II). The maximum adsorption capacity and the removal of Cr(VI), Ni(II), and Zn(II) were calculated to be 27.24 mg g⁻¹ and 98.86% at pH 2.0, respectively. The Cr(VI), Ni(II), and Zn(II) adsorption isotherm on the *Lepironia articulata* biochar (LABC) was tested with Langmuir, Freundlich, Dubinin–Radushkevich and Temkin isotherm models, and the Langmuir isotherm showed the best fit. From thermodynamic parameters ΔH° , ΔG° , and ΔS° , calculate at variable temperatures (20, 40, and 60 °C), the adsorption of Cr(VI) was concluded to be endothermic, spontaneous, and increased disorder. In addition, HTC was revealed to be effective technique for the preparation of carbon materials with variable physico-chemical properties and consequently HCs could be applied in numerous different applications e.g. as alternative low-cost adsorbent for pollutant removal from water, pre-cursor for energy generation, fertilizer and soil amendments etc. Further its use to prepare modified biochar has increased its efficiency for the removal of Cr (VI), Ni (II), and Zn (II) from aqueous solution and laboratory wastewater. Preparation of monolith by binding of modified organic (biochar) and inorganic (bentonite) has successfully proved to be efficient adsorbents, particularly when used in continuous operation. Almost 99% of the heavy metals were removed from aqueous solution through continuous operation in a fixed bed glass column with random packing. Variation in flow rate and bed height suggested the highest removal with flow rate 5 mL/min with a bed height of 4 cm. It was also observed that when using methylcellulose in combination with PVDF binder can not only enhance the strength and durability it can also retain its porous structure, surface area and restrict the excess use of PVDF which make it much cost effective as well. Sustainable development towards obtaining such adsorbents from inexpensive product LA can bring new material for various applications. The liquid and gas products produced from the HTC process are still to be considered for variable by-products from the same species.

Keywords: Hydrochar, hydrothermal carbonization, modification, surfactant, adsorbent

ACKNOWLEDGMENT

In the Name of **ALLAH**, THE benevolent and THE clement, all the praises and thanks to **ALLAH**, for the blessing of life and wisdom for never neglecting me, who gave me courage every time during my research work and in whole life.

Countless salutation upon The Holy Prophet HAZRAT MUHAMMAD (صلى الله عليه وسلم), the city of knowledge and blessing for an entire creature who has guided his Ummah to seek knowledge from cradle to grave, and enabled me to win the honor of life.

I owe my deep gratitude to my advisor **Assoc. Prof. Dr. Lupong Kaewsichan**, Faculty of Engineering, Prince of Songkla University, for his precious advice, guidance, and thoughtful suggestions during my research work. His kind interest in the research work, passions, cooperation, efforts and moral encouragement towards the inculcation of the constant hard working which will always serve me as an inspiration throughout the course of life.

I am very thankful to **Assoc. Prof. Dr. Pakamas Chetpattananondh**, **Assoc. Prof. Dr. Kulchanat Prasertsit**, Faculty of Engineering, Prince of Songkla University for their kind suggestions and guidance in the proposal examination as well as during the entire duration of the research. I am also sincerely thankful to **Assoc. Prof. Dr. Sukritthira Ratanawilai**, Associate department head for graduate studies, Faculty of Engineering, Prince of Songkla University for her continuous help and support. I would also like to extend my gratitude towards the countless and valuable support by all faculty members and staff of the department of chemical engineering, faculty of Engineering, Prince of Songkla University, Hatyai, Thailand.

Words are inadequate to express my special thanks to the staff and scientists of chemical engineering department (**Ms. Pornpimon Sansuk**, **Ms. Keerattaya Charoenmark**, **Mr. Somkid Geenapong**, **Mr. Tanakorn Kiatkwanboot**, **Ms. kanjana Kantakapan**, **Mr. Narong Apayanugool**) and all other faculty and staff for their countless help and support throughout the duration of research work.

I expand my specials thanks to all friends and brothers, Dr. Surat Semmad, Miss. Kanogwan Tohdee and her entire family, Dr. Faisal Usman Sheikh, Zulifqar Ali Jumani, Syed Haseeb Sultan, Muhammad Amin, Ustad Muhammad Jafri, Khurshid

Baloch, Lala Khan for their moral support and for stimulating a fun-filled environment during the stay in Prince of Songkla University and Hat-Yai city.

I take this opportunity to sincerely acknowledge the Graduate School, Prince of Songkla University, Songkhla, Thailand, for providing financial assistance in the form of TEH-AC scholarship which braced me to perform my lab work and in attending the conference, comfortably. I would also like to acknowledge the research grant provided by the graduate school. I would also like to thank the department of Chemical Engineering, Faculty of Engineering, and Prince of Songkla University for providing me all the assistance related to the Ph.D. thesis.

Finally, I owe my love and gratitude to my beloved father (late) whose encouragement and motivation throughout my life has enlightened my career. I am proud that I am continuing my journey towards his footprints. I also appreciate the hard work and support that I received by my mother, my dearest brothers, sisters and special thanks to my wife, daughter, and son, for complete support and prayers in the achievement of this goal, for their love, encouragement, supporting, patience and attention throughout my life.

I would like to appreciate the people for their help and support during my research. My thanks and gratitude goes to my principal advisor Assoc. Prof. Dr. Lupong Kaewsichan. He gave an opportunity, motivation, and stimulation throughout my work. I sincerely thank all committee members **Assoc. Prof. Dr. Nurak Grisdanurak, Asst. Prof. Dr. Suratsawadee Kungsanant, Assoc. Prof. Dr. Ram Yamsaengsung, and Assoc. Prof. Dr. Kanda Panthong** for their support and invaluable comments on my research. Also, I would like to acknowledge the financial support of Ph.D. scholarship, Prince of Songkla University.

Asadullah

TABLE OF CONTENT

Contents	Page
ABSTRACT	v
ACKNOWLEDGMENT	viii
LIST OF FIGURES	xii
LIST OF TABLES	xv
1. INTRODUCTION	1
1.1 Theoretical background.....	1
1.2 Biomass	4
1.2.1 <i>Lepironia articulata</i> (LA)	4
1.3 Clay minerals.....	6
1.3.1 Bentonite properties and composition	6
1.4 Problem statement	7
1.5 Research objectives	8
1.6 Scope of Work.....	9
2. LITERATURE REVIEW	10
2.1 Adsorption.....	10
2.2 Adsorbents.....	11
2.2.1 Preparation of hydrochar and modified biochar adsorbents	11
2.2.2 Modification of natural bentonite	14
2.3 Properties and characteristics of adsorbents.....	20
2.3.1 Cation exchange capacity (CEC).....	20
2.3.2 Surface functional groups.....	21
2.4. Kinetics and modeling	21
2.4.1 Adsorption kinetics	21
2.4.2 Adsorption isotherm models	23
2.4.3 Fixed bed Column breakthrough curve analysis and modeling	26
3. MATERIALS AND METHODOLOGY	31
3.1 Materials.....	31
3.1.1 Chemicals	31
3.1.2 Biomass (<i>lepironia articulata</i>)	31
3.2 Methodology	31

TABLE OF CONTENT (Conitnue)

3.2.1 Preparation of HC.....	32
3.2.2 Pyrolysis of LAHC into modified biochar	33
3.2.3 Modification of bentonite using (BCDMCL) surfactant	34
3.2.4 Analysis and instrumentation.....	35
3.2.5 Batch adsorption experiments.....	41
3.2.6 Continuous adsorption experiments.....	42
4. RESULTS AND DISCUSSION	44
4.1 Characterization of adsorbents	44
4.1.1 Surface structure and morphology of adsorbents	44
4.1.2 Surface functional groups (SFG).....	47
4.1.3 Hydrochar yield	49
4.1.4 Proximate and ultimate analysis	50
4.1.5 Contact angle and wettability.....	50
4.2 Chemical characterization of adsorbents.....	51
4.2.1 Cation exchange capacity (CEC).....	51
4.3 SEM-EDX after adsorption	51
4.4 Batch adsorption experiments	52
4.4.1 Effect of pH on the removal of heavy metals	53
4.4.2 Effect of initial metal concentration.....	55
4.4.3 Effect of time.....	59
4.4.4 Effect of temperature	59
4.4.5 Batch adsorption kinetics	60
4.4.6 Adsorption isotherm.....	62
4.4.7 Adsorption thermodynamics	66
4.5 Continuous adsorption experiments using fixed-bed column	68
4.5.1 Effect of flow rate.....	68
4.5.2 Effect of bed height	69
4.5.3 Breakthrough curve calculations and modeling	70
4.6 Desorption and recycling	72

TABLE OF CONTENT (Continue)

5. CONCLUSION AND RECOMMENDATIONS	74
5.1 Conclusion.....	74
5.2 Future recommendation.....	75
REFERENCES	76
APPENDIX	85
VITAE	99

LIST OF FIGURES

Figure 1. 1 Lepironia articulata (LA).....	5
Figure 1. 2 Structure of bentonite	7
Figure 2. 1 Basic adsorption terms	11
Figure 2. 2 Schematic diagram of the hydrothermal carbonization process showing from the starting material (plant derived) to the final carbon product	12
Figure 2. 3 Schematic graphic of BCDMACl (surfactant) modified bentonite (Tohdee et al., 2018)	17
Figure 2. 4 Chemical structure of PVDF	18
Figure 2. 5 Chemical structure of Methylcellulose (Source:	19
Figure 3. 1 Schematic flow diagram of the conversion of Lepironia articulata into hydrochar and modified biochar	32
Figure 3. 2 Schematic diagram of HTC process a) hydrothermal reactor b) Heating coil jacket c) pressure gauge d) thermocouple e) safety pressure relieve valve f) Temperature controller.....	33
Figure 3. 3 Pyrolysis process a) tubular reactor b) heating box with coils c) Temperature controller (3 cycle).....	34
Figure 3. 4 Swelling of modified (left) and unmodified bentonite (right).....	37
Figure 3. 5 Contact angle analysis using (OCA 15EC) contact angle analyser.....	38
Figure 3. 6 Gerhardt (Germany) ammonia distiller to calculate CEC	40
Figure 3. 7 Incubator shaker for batch adsorption experiments.....	42
Figure 3. 8 Schematic diagram of fixed bed continuous adsorption process a) Liquid tank b) Peristaltic pump c) control valve d) Rotameter e) fixed bed reactor.....	43
Figure 4. 1 Biomass LA converted into LAHC and LABC.....	44
Figure 4. 2 SEM images of A) LAHC B) LABC	45
Figure 4. 3 FTIR spectrum of raw biomass lepironia articulata along with LAHCs...47	47
Figure 4. 4 FTIR spectra of biomass (LA), hydrochar (LAHC), and modified biochar (LABC)	48
Figure 4. 5 SEM-EDX spectrum of LABC before and after adsorption of Cr at 333K , pH 2,.....	52

Figure 4. 6 SEM-EDX of Cr(VI) and Ni(II) in multi-system after adsorption using LABC	52
Figure 4. 7 Effect of pH on the removal of Cr(VI) and on the capacity	54
Figure 4. 8 The effect of pH on the percent removal of Ni(II) (initial metal concentration of 50 mg L^{-1} and hydrochar dosage of 20 g L^{-1})	54
Figure 4. 9 Removal efficiency of Ni (II) with variable initial Concentration of adsorbate	56
Figure 4. 10 Adsorption capacity $q_e \text{ (mg g}^{-1}\text{)}$ at different initial Ni(II) concentration $C_e \text{ (mg L}^{-1}\text{)}$ using hydrochar	56
Figure 4. 11 Effects of initial metal concentration (mg L^{-1}) on the removal of Cr(VI) & q_e at pH 2 with adsorbent dose 0.3 g/ 50 mL of LABC and LAHC at selected temperatures	57
Figure 4. 12 Removal of Cr(VI), Ni(II), and Zn(II) at different initial metal concentration (mg/L)	57
Figure 4. 13 The adsorption capacity of Ni(II), Cr(VI), and Zn(II) adsorption onto LABC-MB monolith	58
Figure 4. 14 Removal of Cr (VI), Ni (II) against the initial metal concentration (mg/L) using NB and MB	58
Figure 4. 15 Effects of contact time on the removal of Cr(VI) at selected adsorption Temperatures. The pH was held at 2, the dosage of adsorbent was $0.3\text{g}/50\text{ml}$ of the solution, and initial metal concentration was 50 mg L^{-1}	59
Figure 4. 16 Pseudo-second order model fit shown with experimental data at different temperatures and initial metal concentration a) 50 mg L^{-1} b) 100 mg L^{-1} c) 150 mg L^{-1} d) 200 mg L^{-1}	61
Figure 4. 17 Linearized pseudo-second-order kinetics plots for adsorption of Cr(VI) by LABC at different initial metal concentration ($50 \text{ mg L}^{-1} - 200 \text{ mg L}^{-1}$); different temperatures a) 293 K b) 313 K c) 333 K ; at pH 2 and dosage $0.3 \text{ g}/50 \text{ mL}$	61
Figure 4. 18 Freundlich adsorption (a) and Langmuir adsorption isotherm (b) for removal of Ni(II) using LAHC	63
Figure 4. 19 The fitted adsorption isotherms are shown with experimental data for selected	64

Figure 4. 20 Breakthrough curves for heavy metal adsorption on the LABC-MB monolith at 5 mL/min flow rate at constant inlet metal concentration of 100 (mg/L) and a bed height of 2 cm	69
Figure 4. 21 Breakthrough curves for heavy metal adsorption on the LABC-MB monolith at 15 mL/min flow rate at constant inlet metal concentration of 100 (mg/L) and a bed height of 2 cm	69
Figure 4. 22 Breakthrough curves for heavy metal adsorption on the LABC-MB monolith at 2 cm bed height and at constant inlet metal concentration of 100 (mg/L) and flow rate 5 mL/min.....	70
Figure 4. 23 Breakthrough curves for heavy metal adsorption on the LABC-MB monolith at 4 cm bed height and at constant inlet metal concentration of 100 (mg/L) and flow rate 5 mL/min.....	70

LIST OF TABLES

Table 1. 1 The MCL standard for the most hazardous heavy metals	2
Table 1. 2 Elemental composition of <i>lepironia articulata</i> (LA)	5
Table 4. 1 Surface area, cation exchange capacity against the sample and process condition	46
Table 4. 2 Lignocellulosic component and hydrochar yield by varying reaction parameters	49
Table 4. 3 Proximate and ultimate analysis of HC at different HTC temperature.....	50
Table 4. 4 Collected parameters in the kinetic models	62
Table 4. 5 Langmuir and Freundlich isotherm parameters for the sorption of Ni(II) ions onto hydrochar.....	64
Table 4. 6 Collected parameters for the fitted isotherm models	65
Table 4. 7 Maximum sorption capacities of some adsorbents of hexavalent chromium	65
Table 4. 8 Thermodynamic parameters of the adsorption of Cr(VI) onto <i>Lepironia</i> <i>articulata</i> -derived	68
Table 4. 9 Adams-Bohart, Thomas, and Yoon-Nelson model results from linear regression analysis	72

1. INTRODUCTION

This chapter contains the theoretical background of the industrial and domestic waste contaminants present in effluent particularly heavy metals and their causes and impacts on the environment and human. Further explains about what were the possible methodologies adopted by scientists and manufacturer to overcome this problem in the past. The hydrothermal technique as a new methodology to get valuable adsorbent is explained here thoroughly, the modification into biochar is coupled with that using alkali as a chemical modifier. Natural clay (bentonite) is also briefly discussed to be used as an inorganic sorbent for heavy metal recovery in this study. The problem statement was explained to present the overall structure of why we need to conduct this study. Objects are given at the end of the chapter to give a brief know how about what are the next steps to be conducted to overcome the above issues related to heavy metal recovery.

1.1 Theoretical background

Environmental issues concerning wastewater pollution is the biggest problem to sort out in the global scenario. Wastewater discharged from industries contain any kinds of contamination along with them, which could suffer human and aquatic life by creating environmental pollution. Different kind of water pollution detecting in industrial effluent which most of the time is discharged untreated directly into the rivers, ponds, and lakes etc. Among all these contaminants heavy metals play a leading role in damaging the aquatic, human and agriculture life in large scale due to its high level of toxicity. Heavy metals are commonly referred to as those metals which hold a specific density of above than 5 g/cm^3 and unfavorably affect the living organisms and the environment (Järup, 2003). Heavy metal pollution takes place in many industrial effluents such as those produced by metal plating facilities, mining operations, leather tanning, battery manufacturing processes, the glass production industry, and production of paints and pigments, and (Argun, Dursun, Ozdemir, & Karatas, 2007). This wastewater usually includes Cr, Ni, Cu, Cd, Pb, and Zn. These inorganic heavy metals are considered to be not biodegradable and their existence in lakes and streams leads to bioaccumulation in living organisms, causing health problems in human beings, animals and plants. Taking excessive human intake of these metals by a human may

lead to severe corrosion and mucosal irritation, kidney failure, brain damage and memory loss, widespread capillary damage, central nervous system irritation followed by depression, and renal damage. Table 1.1 shows the possible side effects of these contaminants to human health and their allowable maximum contaminant level (MCL).

Table 1. 1 The MCL standard for the most hazardous heavy metals (Tripathi & Rawat Ranjan, 2015)

Heavy Metal	Major sources	Toxicity	MCL (mg/L)
Arsenic (As)	Pesticide , fungicide , metal smelters	Skin manifestation, visceral cancers, vascular disease	0.05
Cadmium (Cd)	Welding, electroplating, Pesticide, fertilizer, nuclear fission plant	Kidney damage, renal disorder, a human carcinogen	0.01
Chromium (Cr)	Mines, mineral sources	Headache, diarrhea, nausea, vomiting, carcinogenic	0.05
Copper (Cu)	Mining, chemical industry, Food, Metal piping, pesticide production	Liver damage, wilson disease, insomnia	0.25
Nickel (Ni)	Welding, electroplating, steel	Dermatitis, nausea, chronic asthma, coughing, a human carcinogen	0.2
Zinc (Zn)	Plumbing, refineries, brass metal plating, Food packaging	Depression, lethargy, neurological signs, and increased thirst	0.8
Lead (Pb)	Paint, pesticide, smoking, mining burning of coal, automobiles	Damage the fetal brain, circulatory system and nervous system	0.006
Mercury (Hg)	Pesticide, packaging, batteries	Rheumatoid arthritis and disease of kidney	0.00003

A range of treatment technologies are available with different success level to remove the heavy metal ions from water, including basic precipitation, ion exchange, chelation extraction, chemical coagulation, flocculation, plant adsorption, chemical precipitation, ion exchange, electrochemical processes, evaporation, flotation, extraction and membrane processes and so on (Ajaykumar, Darwish, & Hilal, 2009;

Harper & Kingham, 1992; Kulkarni & Kaware, 2014; Syafalni, Abdullah, & Abustan, 2013). Every technique has their advantages and disadvantages associated with them. Besides being currently the most inexpensive method, precipitation introduces large quantities of undesirable waste sludge. Ion exchange can effectively remove heavy metal ions from solution, but the high cost of synthetic resin make it still expensive for this purpose (Seki, Saito, & Aoyama, 1997).

Comparatively, the adsorption process is considered a better alternative in water and wastewater treatment because of convenience, the simplicity of design, and ease of operation. Adsorption is broadly used in practice to remove constituents from fluid phases (gases or liquids) for being a phase transfer process. It can also be observed as a natural process in different environmental compartments. In water treatment for the removal of inorganic wastes/ heavy metals, adsorption has proved to be an efficient elimination process for a multiplicity of solutes (Worch, 2012). Different kinds of adsorbent have been utilized by researchers from time to time to obtain optimum results in terms of heavy metal recovery from wastewater. Activated carbon is one of the largest use adsorbent for the treatment of contaminated water. Besides the high manufacturing cost and environmental problems during manufacturing, activated carbon also generates a huge amount of waste in the form of solids. Hydrochar prepared via an inexpensive and ease in operation hydrothermal carbonization is said to be a remarkable ingredient in the field of adsorption, soil amendments, carbon sequestration, and energy generation. HTC technique allows the wide range of starting materials to be converted into valuable carbon materials with surface functional features and well-developed porosity. Various scientists have used this technique to remove heavy metals from wastewater in cost-effective way (Kang et al., 2016; Zhou, 2016; Zhu *et al.*, 2014). Besides its ease of operation hydrothermal process doesn't generate flue gases at all. The byproduct obtained in terms of liquid product can also be utilized as fertilizer and pesticide after applying a few additional separation procedures. Due to low surface area and pore volume, it is further recommended to do pyrolysis of hydrochar in the presence of alkali to modify it into biochar. Bentonite, on the other hand, has very good results obtained by a scientist for the removable of heavy metal (Aljlil & Alsewailem, 2014; Tohdee, Kaewsichan, & Asadullah, 2018). Next investigations were made afterward

for the modification of bentonite using surfactants and acids (Al-Shahrani, 2014; Asadullah; Kaewsichan, Lupong; Three, 2018). The overall effect of modified bentonite and biochar has posed huge popularity in the wastewater treatment and the removal of heavy metals (Díaz-Nava, Olguín, & Solache-Ríos, 2012).

1.2 Biomass

Biomass being inexpensive, easily available, and having valuable features to be used for a variety of applications. Biomass has also been used as a precursor for the manufacturing of modified biochar, activated carbon, hydrochar etc. Many of the researchers have obtained such valuable products from different biomass materials i.e. rice husk, kikar tree, grass, empty palm fruit bunch (EFB), orange peel, sugar cane bagasse, tobacco stalk, shrimp waste, municipal solid waste (MSW) (Cai *et al.*, 2016; Chen *et al.*, 2017; Kang *et al.*, 2012; Kannan, Garipey, & Raghavan, 2017; Puccini *et al.*, 2017; Tran *et al.*, 2016). Later on, their potential for being active adsorbent for the removal of heavy metal from wastewater was successfully verified by a number of batch and continuous adsorption experiments. The major contaminants removed were, Zn, Pb, Ni, Cr, Cu, Ar etc. The search to find more valuable, fast growing, and widely available biomass for the production of biochar are still on high demand.

1.2.1 *Lepironia articulata* (LA)

Lepironia articulata, also identified as grey sedge, is a tall tightly rhizomatous macrophyte that forms huge dense meadows of flora (Fig. 1.1). It cultivates in transient wetlands and the boundaries of freshwater marshlands. A fast-growing tropical grass from sedge family is known for its usefulness in the small home industry for handicrafts manufacturing in the southern part of Thailand. *Lepironia* is highly ornamental and has huge potential as a designer water feature plant. This native sedge is an emergent aquatic plant which grows in dense clumps. It has a large, securely anchored root system.



Figure 1. 1 *Lepironia articulata* (LA)
Source: <http://www.export-forum.com>

It is utmost important to identify the elemental composition of biomass before processing to get useful carbonaceous material. The biomass is generally composed of K, Si, Cl, and Ca etc. Various useful functional groups could be enhanced during carbonization process once the basic elements are identified. LA is enriched with such elements which could be further modified through a series of carbonization and chemical modification techniques. Detail elemental composition of LA calculated in his study is given in table 1.2.

Table 1. 2 Elemental composition of *lepironia articulata* (LA)

S.No.	Element	Concentration (%)	S.No.	Element	Concentration (%)
1	Na	0.206	11	Cr	0.004
2	Mg	0.064	12	Mn	0.021
3	Al	0.108	13	Fe	0.22
4	Si	0.645	14	Ni	0.002
5	P	0.035	15	Cu	0.013
6	S	0.278	16	Zn	0.004
7	Cl	0.658	17	Ga	0.001
8	K	0.937	18	Br	0.004
9	Ca	0.115	19	Rb	0.002
10	Ti	0.008			

The potential of LA as adsorbent was not identified yet. Furthermore, due to its lack of utilization as a potential candidate for variable products in environmental remediation and sustainable energy potential, the use is very limited. With a minimum effort, its growth can be extremely high once taking into account as potential biomass candidate.

1.3 Clay minerals

Clay minerals have many applications in the industrial sector. They can be used as sorbents, catalysts, carriers for the catalysts, and molecular sieves. Because of their low penetrability, clay minerals play a significant role as physical barriers, for the sequestration of metal-rich wastes; but chemical barrier too, as some types of clay minerals, are significant to overcome the environmental dispersion of heavy metals by removing them from wastewater. The popularity of clay mineral has increased due to its wide used as an adsorbent and ion exchange in wastewater treatment especially for the removal of organic pollutants, nutrients, and heavy metals. Compared to poly aluminium chloride, zeolite and bentonite, are some of the prospective alternatives, as they have high specific surface areas with a net negative charge, which can be electrically rewarded for by organic and inorganic cations from the wastewater. Their sorption capabilities come from their high surface areas and exchange capacities. Bentonite is an extremely effective natural clay mineral, mainly in granulated form, used for the sludge dewatering and purification of wastewater.

1.3.1 Bentonite properties and composition

The basis of bentonite is recognized to the modification of volcanic ash or glass, but later on, the term is extended to include a montmorillonite composition which was formed in a different manner. Commonly, two types of bentonite are well known, the calcium bentonite and sodium bentonite. Calcium bentonite which developed from volcanic ash deposited in freshwater environments and is known to be a low-swelling type. While sodium bentonite is derived from volcanic ash that is deposited in marine environments known to be the high-swelling type (Dwairi and Al-Rawajfeh, 2012). The non-metallic type clay named smectites is primarily composed of hydrated sodium calcium aluminum silicate. Smectites are commonly named as sodium montmorillonite

("sodium bentonite" or "wyoming bentonite") or montmorillonite and swelling bentonite ("Western bentonite"). Its complex chemical structure is made up of the three-layer set, one layer of Al octahedron sandwiched between two layers of SiO₄ tetrahedral (Fig 1.2). Because of large availability, low price, and adsorption capabilities of bentonite has increased its use for water and wastewater treatment due to its capability of absorbing all kinds of pollutants including heavy metals from wastewater, (Guimaraes *et al.*, 2009). This outstanding capability is due to the presence of the mineral montmorillonite (Khenifi *et al.*, 2009).

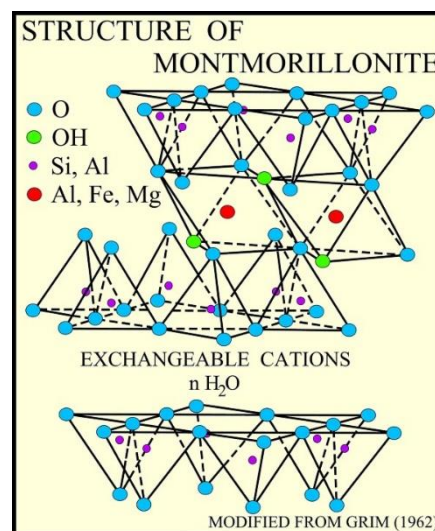


Figure 1. 2 Structure of bentonite

Source:<https://koiorganisationinternational.org/blog-entry/clay-necessary-koi-ponds>

Apart from that, bentonite is a natural material which is very useful for wastewater treatment due to the vital compounds it contains such as iron, aluminum, and clay materials which are useful for the treatment of wastewater. Additionally, being cheaper than chemicals, bentonite gives economic benefits to environmental concerns and operators. However, commercially available coagulants are mostly chemical-based, which may create an adverse impact on the environment (Ozcan *et al.*, 2007)

1.4 Problem statement

Heavy metals sources are not biodegradable or renewable, and the natural reserves are widely being consumed. Therefore, it is overbearing that those elements considered dangerous to the environment or those of economic value and technological importance

are inhibited and improved through suitable treatments at their point of origin. Variety of conventional techniques have predominated disadvantages which overcome their benefits. The generation of bulk solid waste, handling of harmful chemicals to be used for this purpose, high associated cost, and unavailability of raw material etc. are the problems which are identified to avoid conventional technique to be used for the treatment of wastewater for the removal of heavy metals. Hydrochar produced from the wet process of biomass has got a huge attraction towards its effectiveness as an adsorbent and being inexpensive. However, low surface and pore volume have limited its benefits on using it for heavy metal removal on large scale. Treating hydrochar into biochar using slow pyrolysis process and alkali treatment is said to be the most beneficial technique for the preparation of efficient adsorbent for the removal of heavy metals from wastewater.

1.5 Research objectives

This research will aim to further characterize the *lepironia articulata* hydrochar (LAHC), unmodified *lepironia articulata* biochar (ULABC), modified biochar (LABC) and modified bentonite (MB) and investigate some parameters that would favor their adsorption abilities of heavy metals from aqueous solution and laboratory wastewater. Batch adsorption experiments will identify the efficiency of prepared adsorbents. Further binding of adsorbents will be made to prepare monolith and identify its applicability and efficiency through continuous adsorption in a fixed bed column study. The following objectives are summarized to achieve the goals in terms of preparation, modification, characterization, application, and modeling. Further key objectives of the study are given below:

1. Hydrothermal carbonization (HTC) of *lepironia articulata* (LA) to convert into hydrochar, the effect of variable temperature, holding time, water to biomass (WTB) ratio and their assessment on HCs yield, surface functional groups, surface area, and porosity.
2. Modification of HC into LABC by mixing with KOH using a slow pyrolysis process at high temperature. How much can be gained by modifying the hydrochar into modified biochar? This would be analyzed through batch adsorption experiments by varying adsorbate initial concentration, adsorbent loading, pH, time, and temperature.

3. Modification of bentonite using BCDMCl surfactant.
4. To conduct batch adsorption experiments to verify the effectiveness of LAHC, ULABC, LAHB, MB for having good selective properties for the removal of heavy metals from aqueous solution.
5. Binding of LABC and MB into a monolith using variable binders PVDF and methylcellulose. Characterization of the LABC-MB-monolith to check its wettability and contact angle, swelling, compact strength, and surface morphology.
6. Conducting continuous adsorption experiments for the removal of heavy metals from aqueous solution and laboratory wastes using fixed bed packed column. Adsorbent LABC-MB-monolith and powdered modified adsorbents will be used to compare the results.
7. Determining the applicability of different adsorption isotherm models and estimating the parameters characterizing the performance of the batch and column processes through isotherm, thermodynamic, and breakthrough point calculations.

1.6 Scope of Work

1. A technique on use of modified biochar and modified bentonite in the removal of heavy metal from aqueous solution;
2. Laboratory batch kinetic and isotherm studies to evaluate the adsorption capacity of hydrochar, modified biochar, and unmodified and modified bentonite for Cr(VI), Ni(II), Zn(II);
3. Laboratory column study; and
4. Elution of metal ions from the adsorbents after adsorption.

2. LITERATURE REVIEW

In chapter two, the dissertation starts with a thorough literature review of the diverse wastewater technologies employed around the world today and also looks at adsorption, adsorbents, and adsorbents preparation techniques. It also gives a brief explanation of the adsorption and ion exchange concepts and their major role in wastewater treatment applications. This chapter also covers the characteristics and properties of hydrochar, biochar, and bentonite after and before modification and thoroughly discusses the different adsorbates being considered and their impact on aquatic life, human health, and the environment. Finally, the kinetics and adsorption modeling will be discussed for batch and continuous operations.

2.1 Adsorption

Adsorption is a widely used process in practice for removing substances from fluid phases. The general definition of adsorption is adhesion of chemical species from a fluid phase (adsorbate) on the surface of a liquid or a solid (adsorbent). However, the adsorption does not include both surface precipitation and polymerization (monomer molecules formed to polymer). These processes (e.g. adsorption, precipitation, and polymerization) are in term of sorption which involved in several mechanisms concerning both physical and chemical processes. Most commonly, the adsorption is described as an enrichment of chemical species on the surface of liquid or solid from a fluid phase. Adsorption in water treatment has been proved to be an efficient removal process for variant solutes. Here, ions or molecules are recovered onto a solid surface (adsorbents) from aqueous solution. The simple terms used in adsorption theory are displayed in Figure 2.1. The species that will be adsorbed are named adsorbate; the solid material that provides a surface for adsorption is called adsorbent. The adsorbed materials can be transferred back into the liquid phase after being released from the surface by doing a modification on the properties (e.g. temperature, concentration, pH). This reverse process is stated to as desorption.

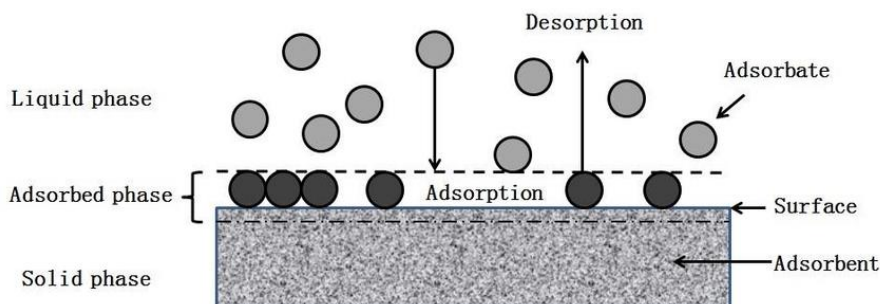


Figure 2. 1 Basic adsorption terms (Worch, 2012)

2.2 Adsorbents

In wastewater application various kinds of adsorbents being used or under investigation. Their performance or adsorption capacity (q_m) largely depends upon surface area, pore volume, porosity, surface functional groups, cation exchange capacity, ionic strength, etc. In order to provide with high sorptive capacity and strong surface morphology, adsorbents need to be further modified after preparation. The physical and chemical modifications have been considered by researchers to do the same. Chemical modification was identified to be worked well while using to recover heavy metals from wastewater. A small alteration in the surface ionic composition can make it perform well during ion exchange adsorption process.

2.2.1 Preparation of hydrochar and modified biochar adsorbents

2.2.1.1 Hydrothermal carbonization (HTC)

Hydrothermal carbonization (HTC) is a thermochemical process for the conversion of organic wastes and biomass at moderate pressure and temperature in the presence of water (Fig. 2.2).

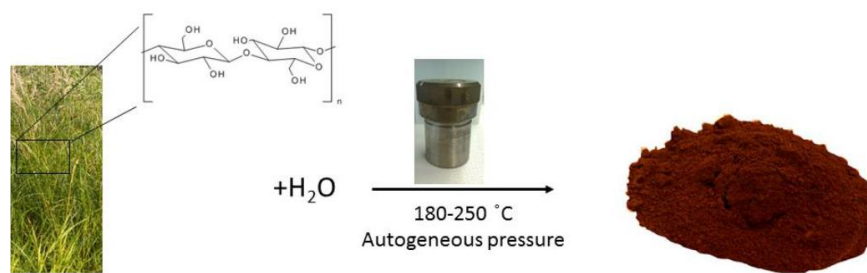


Figure 2. 2 Schematic diagram of the hydrothermal carbonization process showing from the starting material (plant derived) to the final carbon product

Because of the need for efficient biomass conversion technology and convenient way of transforming various feedstocks, HTC gets considerable interest in these days. The resulting products are gas and a coal-water slurry with different chemical and physical properties from the original feedstocks. From coal-water slurry, the solid coal like carbonaceous material is separated and further named as hydrochar. The produced carbonaceous materials are characterized by their extraordinary large specific surface area, well-developed porosity, and tuneable surface-containing functional groups, as a result, they can be used for several applications. Hydrochar gives amorphous aromatic/polyfuranic carbon complex with improved surface functional properties and significantly different from classically activated carbon. Their shape varies with the source of biomass such as from the carbohydrate-based materials the spherically shaped particles are obtained. The size and shape of these particles can also be altered by modifying operational conditions, which in the case of activated carbon is not possible. Simply monosaccharides *i.e.* fructose or glucose are applied as starting materials often but more productive and useful results were obtained successfully by performing HTC synthesis with starting materials such as cellulose, hemicellulose, and some biomass materials such as pinewood, cassava rhizome and corncob as well (Falco *et al.*, 2011; Hoekman *et al.*, 2011; Liu *et al.*, 2010; Nakason *et al.*, 2016; Zhang *et al.*, 2015). Typically, HC is dark brown powder like solid product with ~60-70 wt.% carbon content. These HCs are characteristically rich in oxygen surface functionalities (*e.g.* –OH, –C=O and –COOH) unlike coal but physically resemble natural coal. HCs does not generate a large amount of harmful gases unlike pyrolysis hydrothermal carbonization

and are not prone to auto-ignition due to the high amount of oxygen surface functional groups (Tekin, Karagöz, & Bekta, 2014). HTC of biomass gives a significant increase in energy density. The high heating value between 28.9-29.3 MJ/kg confirms its potential in the energetic application. On the other hand its ease of operation and inexpensive procedure make it feasible in the field of wastewater and gas adsorption process. Xue *et al.* (2012) hydrothermally-produced hydrochar by hydrothermal treatment by varying temperatures between (150-300 °C) from peanut hull and then treated with hydrogen peroxide (H₂O₂). They hypothesized after improved recovery of heavy metals from aqueous solution through batch and column experiments that enhancement of heavy metal removal was due to H₂O₂ treatment of the hydrochar could increase oxygen-containing functional groups on its surface. This research study shows that hydrochar received after the HTC process can be modified by improving its surface area and functional groups to enhance its ability in wastewater treatment applications.

In another work conducted by Ding *et al.* (2016), they converted rice husk (RH) into valuable HC with simple one-step HTC process (170-280 °C), and applied it for the efficient removal of hexavalent chromium Cr(VI) from aqueous solutions. According to the results, the optimum pretreatment conditions were found to be 240 °C and 1 h. Their results considered HC made from RH as a novel and promising adsorbent for Cr(VI) removal. HTC process not only produces hydrochar it also come up with two more products as liquid and gas. Gas in the form of energy can be utilized further and on the other hand, liquid may produce many other emended products after separation and minor post-treatment. Many researchers have worked on these products to make the HTC process more economical and productive.

Nakason *et al.* (2018) produced valuable products in the form of solid-liquid from cassava rhizome. They investigated the effect of process parameters including time, temperature, and biomass to water ratio (BTW) on HC characteristics and products from liquid fraction. The analyzed liquid fraction and identified various valuable chemical species including, furan compounds glucose, volatile fatty acid (succinic acid, formic acid, lactic acid, levulinic acid, acetic acid, (furfural, furfuryl alcohol, hydroxymethylfurfural), and propionic acid) with highest yields obtained (wt.% dry raw material) of 4.5, 18.5, and 24.3, respectively.

2.2.1.2 Modification of hydrochar

HC produced by HTC process has the surface area in the range (5- 70 m²/g), whereas most of the commercial adsorbents used for wastewater treatment have a very high surface area and porosity. The removal efficiency of heavy metals from wastewater was found low as compared to other adsorbents (Mihajlović *et al.*, 2016; J. L. Zhou, 2016; N. Zhou *et al.*, 2017). To increase the sorption capacity and removal efficiency of hydrochar, the modification was conducted inside furnace under slow pyrolysis process and in the presence of alkali and CO₂ or N₂ gas.

Sun *et al.* (2015), worked on the removal of heavy metals from water using modified hydrochars from different feedstock (corn stalk, sawdust, and wheat straw) via hydrothermal carbonization process and KOH modification processes. The results showed that hydrochars after modification with KOH have increased the cadmium sorption capacity from (13.92–14.52 mg/g) for unmodified HCs to (30.40–40.78 mg/g) for KOH-modified HCs, respectively. This might be reason due to increase to the oxygen-containing functional groups, and aromatics, such as carboxyl groups. Their findings also concluded that whether applied in a multi or single-metal system, the sorption capacity of heavy metals by modified hydrochars was found higher than that by unmodified ones and followed the order of Pb(II)>Cu(II)>Cd(II)>Zn(II).

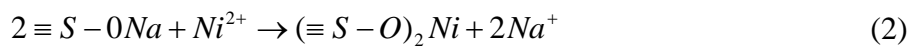
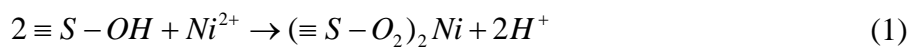
In another study by Huang *et al.* (2017), initially prepared hydrochar by hydrothermal carbonization of sawdust, further KOH-modified biochars were prepared under an oxygen-limited pyrolysis method inside a muffle furnace. Adsorption experiments were performed on the modified biochars for the removal of tetracycline (TC) from aqueous solution. The results showed an increase in maximum adsorption capacity ($q_{e,m}$) of TC onto KOH-modified biochar up to 21.17 mg/g relative to 4.30 mg/g in unmodified biochar of 300 °C.

2.2.2 Modification of natural bentonite

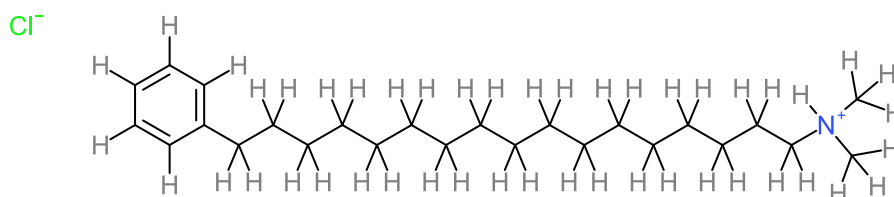
Clays have classic properties (high cation exchange capacity, large surface area, mechanical and chemical stability, and a layered structure) that predispose them to be good adsorbents. Bentonite belongs to the clay minerals group. The core component of bentonite is montmorillonite, consists of an octahedral shell of central alumina surrounded by units made up of two silica tetrahedral sheets. The net negative charge

on the clay surface result after isomorphous substitution in octahedral and tetrahedral sheets. The hydrated exchangeable cations (e.g. H^+ , Na^+ , and Ca^{2+}) after being adsorbed between the layers and their edges, may result the remaining negative charge to be balanced (Melichova & Hromada, 2013). This phenomenon was further validated by Tohdee *et al.* (2018), in which, they adsorbed Ni(II) and HA ions onto the modified bentonite in batch experiments. Their findings include the highest reductions of Ni (II) adsorption were 34.06% and 29.64% with NB and MB over the initial concentration range 50–800 mg/L, with an increase from 0 to 0.1 M in ionic strength, respectively. The results suggest possible ion exchange of sodium and hydrogen cations at the exchange sites (Pinskii, Minkina, Mandzhieva, Bauer, & Nevidomskaya, 2014).

The ion exchanges of Ni^{2+} with both $-Na$ and $-H$ are the main mechanisms of Ni (II) adsorption onto bentonite. The below two steps of the ion exchange mechanism reactions represent, in Eqs. (1) and (2).



According to (Tohdee *et al.*, 2018), the hydraulic conductivity of natural clay (bentonite) is severely reduced by swelling. Natural clay (bentonite) cannot effectively adsorb heavy metal ions from aqueous solution due to this reason. They worked on modification of natural bentonite using benzylhexadecyldimethyl ammonium chloride (BCDMACl) surfactant in order to improve its adsorption capacity. Their work remarkably reduced the swelling of MB up to zero levels, which further improved its adsorption efficiency. (Tohdee *et al.*, 2018) enhanced the removal of heavy metals Zn(II) and Cu(II) by using modified bentonite. They have shown the structure of unmodified and modified bentonite as shown below, which have a net negative charge due to the isomorphic replacement of Mg^{2+} with Al^{3+} in the octahedral layer at center. The lattice structure, such as Na^+ and Ca^{2+} located in the interlayer, can be used to balance the negative charge by exchangeable cations which can further improve the cationic adsorption of heavy metals.



BCDMACl surfactant mainly have two parts (hydrophilic head and hydrophobic tail), with ammonium cation $[R'-(CH_3)_2N^+R]$ being the head and a long chain forming the tail. The ammonium cation of BCDMACl micelles exchanges replaceable cations (Na^+ and Ca^{2+} and in interlayer) by being introduced into the interlayers for Al^{3+} and Mg^{2+} in the central octahedral layer, as shown in Figure 2.3 (Tohdee *et al.*, 2018). The NB and MB had silica and alumina as the major species, at 59.73% and 13.81%, and at 59.04% and 12.91% by weight, respectively. It was seen that Cl and Cs were present in MB at 3.86.

In a previous study conducted by (Díaz-Nava *et al.*, 2012), similar kind of surfactant hexadecyl trimethyl ammonium bromide (HDTMABr) and BCDMACl were used to modify bentonite and their efficiency was successfully tested for the removal of phenol from aqueous solution. Their results showed that the adsorption of phenol highly depends on the kind of surfactant used and the pH solutions. The adsorption was found higher for the bentonite modified with bencylcetyldimethylammonium chloride than hexadecyltrimethylammonium bromide.

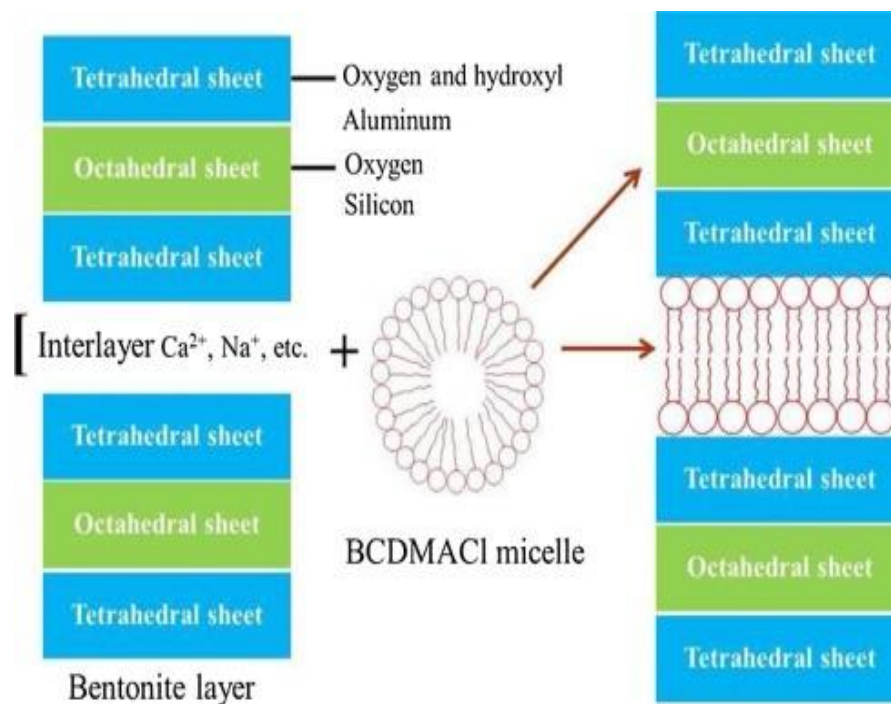


Figure 2. 3 Schematic graphic of BCDMACl (surfactant) modified bentonite (Tohdee *et al.*, 2018)

2.2.3 Binding of adsorbents

The use of a binder to make pallets, monolith, granules, and briquettes from different kind of adsorbents has been great attention by the researchers in the past. Their widely used applications are considered to be in the fields of energy generation, making of the capacitor and supercapacitor, soil amendments for long run fertilizers utilization, wastewater treatment etc. Currently, researchers are extending their works by searching cost-effective and efficient binders to let the adsorbent perform well in wastewater treatment without losing much its surface morphology and porosity. Various kinds of binders were tested to bind sorbents to increase their shelf life and physical properties for long run. Some of the widely used effective binders are discussed below.

a) Poly(vinylidene fluoride) (PVDF)

Polyvinylidene difluoride or Polyvinylidene fluoride is an extremely non-reactive thermoplastic semicrystalline fluoropolymer formed by the polymerization of vinylidene difluoride with melt viscosity = 18.7 kpoise, and specific gravity = 1.75, respectively. PVDF is a specialty plastic with applications in industries as resistance to solvents, hydrocarbons, and acids, as well as in applications requiring the highest purity. The chemical structure is shown in Figure 2.4 and the chemical formula is $-(C_2H_2F_2)_n-$.

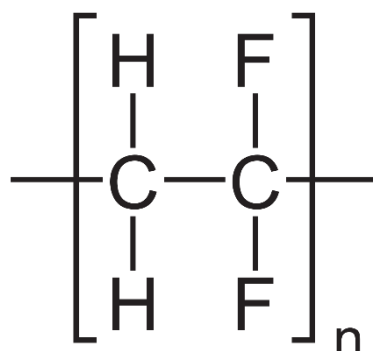


Figure 2. 4 Chemical structure of PVDF

(Z. Zhu *et al.*, 2016) used Nafion, poly(vinylidene difluoride) (PVDF), and poly(tetrafluoroethylene) (PTFE) and as a binder for preparation of supercapacitor and to check its performance. His findings suggest PVDF as the best suitable binder for supercapacitors with optimal content of 10 wt%. He also resulted in the PVDF conferred good mechanical properties. Water treatment is a major application area of poly(vinylidene fluoride) PVDF membranes nowadays. There have been several published articles reporting on the preparation, characterization, and applications of PVDF membranes in water treatment such as UF (ultrafiltration), MF (microfiltration), and MBR (membrane bioreactor), etc. (G. Kang & Cao, 2014). PVDF is nowadays in high demand to be used in membrane technology which makes it an important inorganic binder which retains the shape and structure of adsorbent material (G. Kang & Cao, 2014; Lin, Chang, Chen, & Cheng, 2002; Safarpour, Khataee, & Vatanpour, 2014). PVDF can also be used in repeated contact with food products, as it is FDA-compliant and completely non-toxic, good mechanical characteristics in tension as well as in torsion, deflection, and compression compared to other fluorinated polymers and will not alter or swell in a wet environment. The high bonding power of PVDF make it useful for binding adsorbents for longer use, also it is consumed in a very low amount

due to the high mechanical strength after binding. Besides the energy and supercapacitor PVDF binder may also be used to bind organic adsorbents for use in wastewater applications.

B) Methylcellulose (MC)

MC is produced synthetically by heating cellulose with a solution of sodium hydroxide or any caustic solution and further treating it with methyl chloride. In the replacement reaction that follows, the hydroxyl residues (-OH functional groups) are substituted by methoxide (-OCH₃ groups) (Fig. 2.5). The chemical formula is

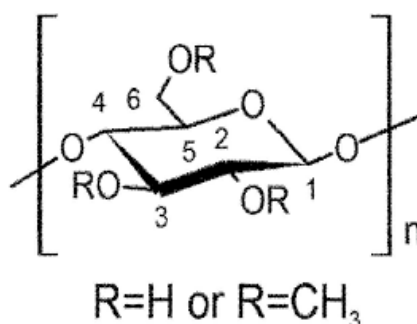


Figure 2. 5 Chemical structure of Methylcellulose

(Nasatto et al., 2015)

(Saeidi & Lotfollahi, 2015), prepared A well-shaped activated carbon monolith (ACM) with good adsorption capacity, high surface area, and proper mechanical strength using powdered activated carbon (PAC) was prepared. They used bentonite as a clay binder and methylcellulose as organic binder simultaneously and applied extrusion process to get ACM. Adsorption capacity was found by calculating the iodine number of ACM. The results showed that the adsorption capacity, mechanical strength (both compression and impact strength), the surface area of ACM significantly improved by rearranging and decreasing PAC size. They also identified that methylcellulose below 45 °C is completely soluble in water, which concluded that the methylcellulose has a gelation temperature (around 45 °C) and below this temperature, this material is completely soluble in water. Therefore its best utilized for the process above 45 °C in wastewater treatment. Besides being binder bentonite also act as an adsorbent which is enriched with alumina chemically and has magnesium or alumina sheet surrounded on either

side by a silica sheet. Bentonite with high porosity having a high surface area. They also mentioned that the properties of this activated carbon monolith is better than the previous work.

Apart from PVDF and MC many other naturally occurring organic binders were also investigated. (Amaya *et al.*, 2007) successfully used concentrated grape must as a binder to prepare activated carbon briquettes from rice husk and eucalyptus wood.

In a different study by (Rizhikovs *et al.*, altered grey alder (*Alnus incana* (L.) Moench) (GA) wood to prepared mechanically strong and dense granular activated carbon (GAC). The product was modified and palletized by direct carbonization and physical activation under a self-generated atmosphere with superheated steam. Hemicelluloses are degraded to produce a binder for the palletization process. They prepared a valuable sorbent from fast-growing cheap deciduous wood and its residues for an industrial application which is environmentally friendly and cost-effective. Due to strength, stability during high flowrate in continuous operation, swelling and wettability issues these organic binders were not applicable for industrial or large scale operations.

2.3 Properties and characteristics of adsorbents

2.3.1 Cation exchange capacity (CEC)

The CEC of an adsorbent represents the total amount of exchangeable cations that the adsorbent can adsorb. There is a vital role of CEC in adsorption of heavy metal from wastewater. For instance, (Zeng *et al.*, 2013) observed that the adsorption capacities of phosphate and ammonium largely increased by the metal-phosphate precipitation and the surface chemistry (negative surface charge) reactions than surface area. In different works conducted by (Mihajlović *et al.*, 2016; Xue *et al.*, 2012), Indicated that the hydrochars received at low HTC temperatures have better abundances of an oxygenated surface functional group such as carboxylate, hydroxyl, and carbonyl groups which yield a higher cation exchange capacity (CEC). The higher CEC is thus beneficial for the sorption of positively charged pollutants such as heavy metals and also for retention of nutrient in soils. The research study conducted by (Asadullah, Kaewsichan, & Tohdee, 2018) for the removal of Ni(II) from aqueous solution, the authors indicated

that improvement in heavy metal removal efficiency in their study is the reason due to the development of negative functional groups on the surface of HC and higher CEC value.

2.3.2 Surface functional groups

Surface functional groups have a vital role in the removal of heavy metals from wastewater. The variation in functional groups can be varied by varying procedure, biomass type and process condition during preparation and modification of hydrochar or biochar. The adsorption capacity of activated carbon highly depends upon adsorbate and hence oxygen-containing functional groups can either reduce or enhance the sorption capacity. Iqbal *et al.* (2009) through their worked validated that adsorption of Cd(II) and Pb(II) onto the biochar of mango peel waste was due to the acidic groups, in which, hydroxyl and carboxyl, were prominent contributors in metal ion uptake.

In the case of bentonite clay, the main functional groups are the siloxane surface groups. These functional groups associate with oxygen atoms bonded to the silica tetrahedral layer, and hydroxyl groups occurred at the edges of inorganic minerals (e.g. kaolinite and metal oxides, oxyhydroxides and hydroxides) (Goldberg, 1991).

2.4. Kinetics and modeling

2.4.1 Adsorption kinetics

Many factors are important component controlling the adsorption kinetics. These factors may include (1) mass transfer (solute) from the solution to the boundary interface surrounding the particle (bulk diffusion), (2) diffusion from the interface to the adsorbent surface (external diffusion), (3) diffusion from the adsorbent surface to the intra-particle sites (intra-particle diffusion) and (4) solute adsorption by several processes such as complexation, physicochemical adsorption and ion exchange. Bulk diffusion process can be ignored when sufficient agitation is allowable, avoiding particle and solute gradients. This can be assumed that the kinetic rate is not limited by mass transfer from the bulk liquid to the particle external surface, resulting in external diffusion might govern the adsorption process. The adsorption kinetic is a time-dependent process which is a good way to describe the adsorption behavior of heavy metals (e.g. chromium, zinc, and nickel etc.) by adsorbent produced from biological

sources. Amount of adsorbate adsorbed on a solid surface at a time (in mg of ion/g of adsorbent) can be determined from the following mass-balance equations:

$$q_e = \frac{v}{m}(C_o - C_e) \quad (1)$$

$$\% Removal = \frac{C_o - C_f}{C_o} \times 100 \quad (2)$$

Here q_e is the number of ions per unit weight of adsorbent in equilibrium (mg g^{-1}); m is the mass of adsorbent used (g); C_o is the initial metal ion concentration in the solution (mg L^{-1}); C_e is the equilibrium concentration of adsorbate (mg L^{-1}), C_f is the final chromium ion concentration (mg L^{-1}); and v is the volume of the solution (L).

a) Pseudo-first-order model

The adsorption kinetics can be accessed by using the differential rate equation fitting to the experimental data. A general form of rate expression of pseudo-first-order model proposed by Lagergren (Lagergren, 1898) is expressed as follows:

$$\frac{dq_t}{dt} = K_1(q_e - q_t) \quad (3)$$

$$\ln(q_e - q_t) = \ln q_e - \frac{K_1}{2.303}t \quad (4)$$

Equations 3 and 4 are the non-linear and the linearized form of the pseudo-first-order model. Where, q_t (mg g^{-1}) is the mass of adsorbate adsorbed per gram of adsorbent at time t (min); and K_1 is the rate constant (min^{-1}). A linear fit to $\ln(q_e - q_t)$ vs. t gives K_1 from the slope.

b) Pseudo-second-order model

The pseudo-second-order is the rate equation which most widely used for the sorption of a solute from a liquid phase. The pseudo-second-order model is generally applied where overall sorption kinetics is controlled by the adsorption/desorption balance. The model can also be employed to test the experimental data of adsorption.

The model was developed by Blanchard (Blanchard *et al.*, 1984) is expressed as follows: The commonly represented pseudo-second-order adsorption equation is:

$$\frac{dq_t}{dt} = K_2(q_e - q_t)^2 \quad (5)$$

$$\frac{t}{q_t} = \frac{1}{q_e^2 K_2} + \frac{t}{q_e} \quad (6)$$

Here K_2 ($\text{g mg}^{-1} \text{min}^{-1}$) is a rate parameter. The K_2 and q_e values can be obtained from the slope and the intercept of a linear fit to t/q_t vs. t , respectively.

2.4.2 Adsorption isotherm models

Adsorption isotherms provide significant information for determining the mechanisms of adsorption and for examining the metal ion interactions on the adsorbent surface. Different models were proposed from time to time to be used depending on the nature of adsorbate, adsorbent, and the process conditions etc. The following few widely used models are very common which covers a large area of adsorption complexity.

a) Langmuir isotherm

The Langmuir isotherm proposed by Irving Langmuir (Clarke & Irving Langmuir, 1916), was derived for monolayer adsorption on a homogenous surface and is expressed as:

Non-linear expression

$$q_e = \frac{q_m K_L C_e}{1 + K_L C_e} \quad (7)$$

Linearized form of Langmuir isotherm

$$\frac{C_e}{q_e} = \frac{1}{K_L \cdot q_m} + \frac{C_e}{q_m} \quad (8)$$

Here, q_m is the adsorption capacity (mg g^{-1}) and K_L (L mg^{-1}) is a constant related to the free energy of adsorption. The important characteristics of the Langmuir isotherm can be expressed by a dimensionless constant called the separation factor R_L .

$$R_L = \frac{1}{(1 + K_L C_o)} \quad (9)$$

R_L indicates unfavorable adsorption for $R_L > 1$, for $R_L = 1$ it's linear, favorable for $0 < R_L < 1$, and for $R_L = 0$ it's irreversible.

b) The Freundlich isotherm proposed initially by Herbert Freundlich (Freundlich, 1907), has been derived for adsorption on a heterogeneous surface. The following equations were derived to be used for identifying the adsorption mechanism.

Non-linear form

$$q_e = K_f C_e^{1/n} \quad (10)$$

and linearized form

$$\log q_e = \log K_f + \frac{1}{n} \log C_e \quad (11)$$

Here, K_f is the Freundlich constant linked to the bonding energy (L g^{-1}), and n is an empirical parameter that indicates the intensity of adsorption. According to the Freundlich assumptions, if $n < 1$ the adsorption is unfavorable, while the adsorption is favorable if $1 < n < 10$.

c) Temkin isotherm

A widely used two-parameter model proposed by (Temkin and Pyzhev 1940) was also tested for the complex solid–liquid adsorption system. The derivation of the Temkin isotherm is based on the assumption that the heat of sorption declines linearly with temperature rather than logarithmically, as in the Freundlich equation (Febrianto *et al.*, 2009). Eqs. (12) and (13) are the non-linear and linear forms of Temkin model.

$$q_e = \frac{RT}{b_T} \ln(K_T C_e) \quad (12)$$

$$q_e = \frac{RT}{b_T} \ln(K_T) + \frac{RT}{b_T} \ln(C_e) \quad (13)$$

Here, b_T is the heat of adsorption (kJ mol^{-1}) and K_T is the binding constant at equilibrium (L g^{-1}) corresponding to the maximum binding energy. Where b_T and K_T can be obtained from the slop and intercept of a linear fit between q_e vs. $\ln(C_e)$.

d) Dubinin-Radushkevich isotherm

D-R isotherm model presented by (Dubinin, 1960), relates to the apparent free energy of adsorption and characteristic porosity. The nonlinear (Eq. 14-15) and linear (Eq.16) forms of this model are:

$$q_e = q_m \exp(-K_{D-R} \varepsilon^2) \quad (14)$$

$$\varepsilon^2 = RT \ln\left(\frac{C}{C_e}\right) \quad (15)$$

$$\ln q_e = \ln q_m - K_{D-R} \varepsilon^2 \quad (16)$$

Here, K_{D-R} ($\text{mol}^2 \text{J}^{-2}$) is the mean free energy of adsorption constant; R ($\text{J mol}^{-1} \text{K}^{-1}$) is the gas constant ($8.314 \text{ J mol}^{-1} \text{K}^{-1}$); T (K) is the absolute temperature; and ε is the Polanyi potential ($\text{J}^2 \text{mol}^{-2}$). Furthermore, the roles of physical adsorption and

chemisorption can be evaluated from Eq.(17). If E_s value lies in the range between 8 and 16 kJ mol⁻¹ indicates chemisorption. Whereas, E_s below that range indicates that the dominant adsorption is physical.

$$E_s = \frac{1}{\sqrt{2K_{D-R}}} \quad (17)$$

2.4.3 Fixed bed Column breakthrough curve analysis and modeling

As one of the most predominant methods for purification and separation, fixed-bed adsorption has been broadly applied for its easy operation and high efficiency. The optimization of the operating conditions and the design of the dynamic adsorption column is obviously a significant issue. To determine the adsorption performance of a column under various conditions is typically time-consuming and expensive. Therefore, to predict the fixed-bed adsorption the development of mathematical model is necessary. An ideal model should be able to provide an exact estimation of the breakthrough behavior and should also be mathematically convenient, and can easily assess the effect of each variable on adsorption.

In adsorption process, the most popular option in practical application is considered to be the Fixed-bed or column adsorption, and due to lack of solid theory and complexity of column adsorption system, the mathematical modeling related to fixed-bed is more difficult and complicated than batch adsorption system. Convenience and accuracy should be considered simultaneously when choosing or developing a model (Xu, Cai, & Pan, 2013).

The model for dynamic adsorption study usually consists of an uptake rate equation(s), macroscopic mass conservation equation and isotherm. Considering the associated constituents of the adsorption systems (solvents, adsorbent, adsorbate), variable operating conditions and specific demands of calculative simplicity and accuracy, it is both challenging and important task to recommend a general use model, because maximum models derived from diverse assumptions are only appropriate for a limited condition but fail to describe others (Dichiara, Weinstein, & Rogers, 2015).

The fundamental equation initially needed to calculate important parameters of the process during operation. These function can further be utilized to calculate breakthrough points and the adsorption capacity.

Effluent volume (V_{eff}) can be calculated from Eq. (18);

$$V_{eff} = Qt_{total} \quad (18)$$

The total quantity of adsorbed heavy metal (maximum column capacity) can be found by using the area under the breakthrough curve (A), which was obtained by integrating the adsorbed concentration C_{ad} (mg/L) versus t (min). The total adsorbed metal capacity q_{total} (mg) in the column for a given flow rate (Q) and feed concentration and can be calculated from Eq. (19);

$$q_{total} = \frac{QA}{1000} = \frac{Q}{1000} \int_{t=0}^{t=t_{total}} C_{ad} dt \quad (19)$$

The total quantity of metal ions transmitted to the column M_{total} can be calculated using Eq. (20)

$$M_{total} = \frac{C_o Qt_{total}}{1000} \quad (20)$$

The total removal is calculated from Eq. (21);

$$Total\ removal\ (\%) = \frac{q_{total}}{M_{total}} \times 100 \quad (21)$$

The saturation capacity (q_{eq}) for the LABC-MB-monolith in these column studies was calculated by Eq. (22);

$$q_{eq} = \frac{q_{total}}{X} \quad (22)$$

Where, X= adsorbent (g)

Effective operation and design of the laboratory scale fixed bed adsorption column can be described by simple mathematical models. In this section, some widely used models are presented and discussed to select appropriate models when desirable.

a) Thomas model

The Thomas model is commonly applied to evaluate the adsorptive capacity of adsorbent and predict breakthrough curves, assuming the Langmuir isotherm and the second-order reversible reaction kinetics (Aksu & Gönen, 2004; Ghasemi, Reza, Dabbagh, & Safdari, 2011). Theoretically, it is appropriate to assess the adsorption process where internal and external diffusion resistances are exceptionally small (Aksu & Gönen, 2004). The Thomas model is given by

$$\ln\left(\frac{C_o}{C_t} - 1\right) = \frac{k_{TH}q_oW}{Q} - k_{TH}C_o t \quad (23)$$

where k_{TH} (mL/min mg) is the Thomas rate constant; q_o (mg/g) is the adsorbate uptake at equilibrium per g of the adsorbent; Q (mL/min) the flow rate; W (g) the mass of adsorbent; and t (min) the flow time.

b) Bohart-Adams model and bed depth service time (BDST) model

The Bohart-Adams (B-A) model was proposed Bohart and Adams (1920) when they progressed with their work of analyzing the distinctive chlorine-charcoal transmission curve. They postulated that the chlorine uptake rate is proportional to the concentration of the chlorine present in the bulk fluid and the residual adsorptive ability of charcoal, the basic form of the B-A model was obtained:

$$\ln \frac{C_t}{C_o} = k_{AB}C_o t - k_{AB}N_o \frac{Z}{F} \quad (24)$$

Hutchins (1973) presented a model, in which, the column performance and capacity is evaluated based on the necessary data obtained by three column tests. This is called the BDST approach and it is said to be the modified form of Bohart-Adams equation. It states that the service time, t and the bed depth, Z of a column allows a linear relationship. The adsorption rate is controlled by the surface reaction between adsorbate and the vacant capacity of the adsorbent. Constants from the model can be easily scaled up for different flow rates and concentrations without performing additional experiments. The linear relationship between bed depth and service time is given by Eq. (25)

$$t = \frac{NZ}{C_o v} - \frac{1}{K_\infty C_o} \ln\left[\left(\frac{C_o}{C}\right) - 1\right] \quad (25)$$

where C is the breakthrough adsorbate concentration (mg/L); Z is the column bed height (cm); N the bed adsorption capacity (mg/L); v is the linear flow velocity of adsorbate solution through the bed (ml/cm² h); and K_∞ the rate constant (L/mg h).

A simplified equation of the BDST model is given by Eq. (26)

$$t = aZ - b \quad (26)$$

Where, mx, the slope of the BDST line, used to identify the efficiency of the bed, with the change in the initial concentration, C₀, to update the value of solute concentration. The slope also represents the time required to travel a unit length through the adsorbent (Cloutier *et al.*, 1985). Where, a and b are the gradient and intercept, respectively, of the plot of t vs. Z.

As two commonly used models in exercise, the BDST and B-A models prospered in forecasting numerous breakthrough curves and optimizing the parameters, although it is comparatively rough (Ayoob *et al.*, 2007; Bhakat *et al.*, 2007; Maji *et al.*, 2007; Han *et al.*, 2008; Srivastava *et al.*, 2008). Moreover, at any bed height, the performance of fixed bed column can be predicted using above-said model.

c) Yoon-Nelson model

The Yoon-Nelson model is greatly summarized in form, the possibility of each adsorbate to get adsorbed is proportional to the prospect of its adsorption and breakthrough on the adsorbent (Yoon and James, 1984). The expression is represented by

$$\ln\left(\frac{C_o}{C_o - C_t}\right) = k_{YN}t - \tau k_{YN} \quad (29)$$

where k_{YN} (min⁻¹) is the Yoon-Nelson proportionality constant; and τ (min) the time required for retaining 50 % of the initial sorbate. As mentioned by (Mckay, 2011), the Yoon-Nelson model does not require fixed bed parameters or brief data regarding the characters of adsorbent or adsorbate. Indeed it has a more simple form than other

models. As restricted by its rough form, the Yoon-Nelson model is less convenient or valuable to acquire process variables and to identify adsorption under a variety of conditions.

3. MATERIALS AND METHODOLOGY

This chapter covers the detail of the materials (biomass, chemicals, reagents, equipment's) used in the current research study including their source. Hydrothermal carbonization (HTC) and slow pyrolysis methods are discussed in detail. Characterization of the materials before and after binding, before and after batch and continuous adsorption experiments are also given under this chapter.

3.1 Materials

3.1.1 Chemicals

All chemicals used in this study were analytical grade. Heavy metal salts, $Zn(NO_3)_2$ and $NiSO_4 \cdot 6H_2O$, $K_2Cr_2O_7$ purchased from Loba Chemie, and Ajax Finechem, respectively, were used to prepare the stock solutions of Cr (VI), Zn (II) and Ni (II). Modification of bentonite was conducted by a cationic surfactant (BCDMACl), obtained from Sigma Aldrich.

3.1.2 Biomass (*lepironia articulata*)

The main ingredient of this study was the biomass *lepironia articulata* (LA) obtained from the coastal belt of Thale Noi, Patthalung district, Thailand. LA was crushed into particle size range (2-5 cm) washed and dried until constant weight. Dried LA was kept into air tight bags for future use.

3.2 Methodology

This research study comprises a series of methodological steps to prepare targeted char products. In step 1, HC was prepared from the HTC process which was further taken to the tubular reactor for the pyrolysis process to get LABC. KOH was used as a chemical activating agent during the pyrolysis process. A schematic flow diagram of the same process along with process conditions is given in Figure 3.1. In step 2, natural bentonite was modified using BCDMACl surfactant. The detail steps of bentonite modification are given below. Furthermore, the properties of the adsorbents were tested by characterizing them before and after modification using proper instrumentation. The modified and unmodified adsorbents were further applied to identify their capacities

and efficiency to be used in the wastewater treatment applications to remove heavy metals from aqueous solution. Later on, the LABC and MB adsorbents were bound together using different binders. Their efficiencies were analyzed using fixed column packed bed study through breakthrough curve analysis. Different models were applied at the end to the search for the better fits and identify the type of adsorption process.

3.2.1 Preparation of HC

Hydrothermal carbonization technique was adopted to convert LA into HC.

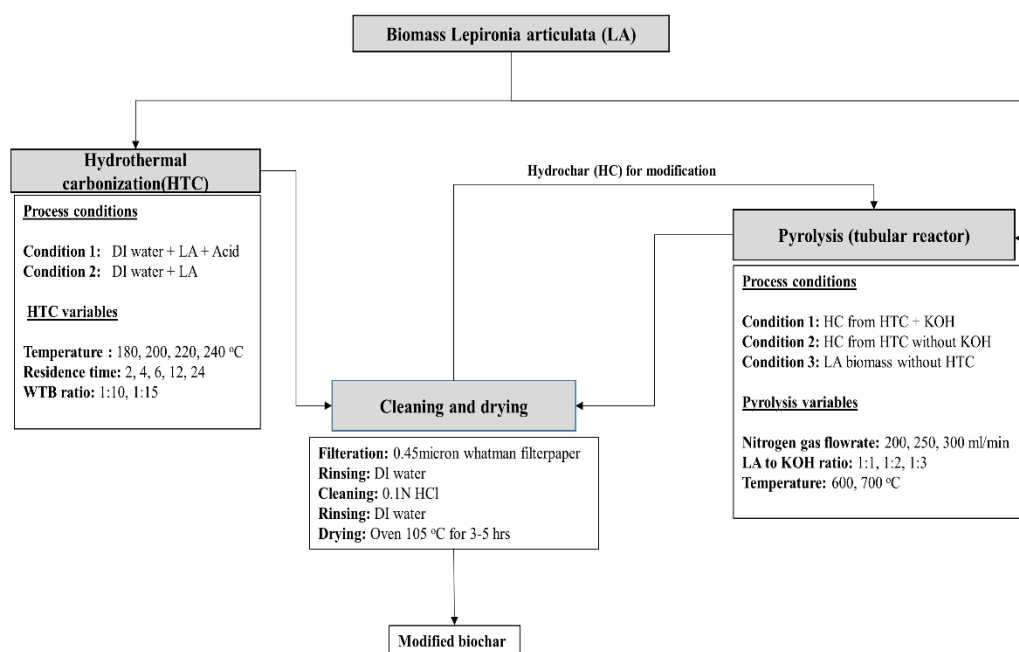


Figure 3. 1 Schematic flow diagram of the conversion of Lepironia articulata into hydrochar and modified biochar

Process conditions such as (temperature, WTB ratio, residence time etc.) were varied to get the HC in terms of high yield, surface area, developed functional groups etc. The biomass LA was treated in the hydrothermal and tubular reactor in order to get LAHC and modified biochar. The reactor was made of stainless steel with a heating coil in a jacketed shell surrounding the reactor. The inside temperature of the reactor was controlled by installing thermocouple attached with a PID temperature controller (Fig. 3.2). The reactor was equipped with a safety relief valve for inside reactor control.

Before doing HTC experiments on variable conditions the sample was treated with sulfuric acid to identify the impact of acid on HC yield and product quality.

Afterward, different samples of HCs were obtained based on varying process conditions (temperature, residence time, WTB ratio) and named as LAHC-2-180, LAHC-6-180, LAHC-8-180, LAHC-24-180, LAHC-2-200, LAHC-2-220, and LAHC-2-240. Where, 2, 6, 8 and 24 represents the number of hours and 180, 200, 220, and 240 represents the HTC temperatures in degree centigrade. The WTB ratio was set as 10:1 for all process conditions. Where in the above sample identification symbol, Centre numeric represents the residence time and the last one represents the temperature in degree Celsius. The detailed HC process is described in my published paper (Asadullah *et al.*, 2018). HCs produced at optimum conditions with maximum properties were selected as a precursor for the preparation of BC and later on modified biochar.

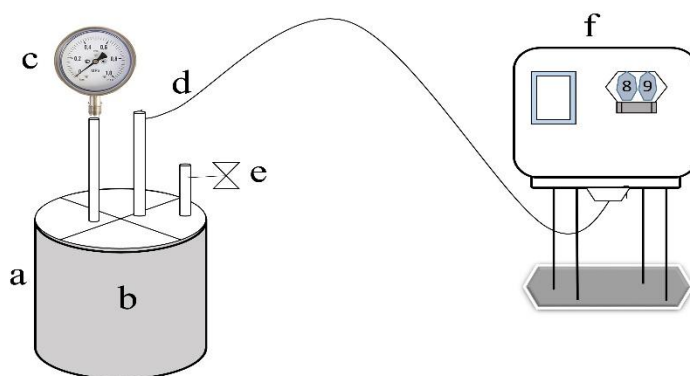


Figure 3. 2 Schematic diagram of HTC process a) hydrothermal reactor b) Heating coil jacket c) pressure gauge d) thermocouple e) safety pressure relieve valve f) Temperature controller

3.2.2 Pyrolysis of LAHC into modified biochar

HC sample obtained from hydrothermal treatment were further treated in a tubular reactor under controlled temperature. Other variables (KOH to HC ratio, N_2 flow rate) were also adjusted based on previous research experiments (Huang *et al.*, 2017; Mihajlović *et al.*, 2017; Sun *et al.*, 2015). The BC obtained from HTC process was kept into a tubular reactor for 2 hours under controlled temperature and N_2 flowrate. The temperature of the inside furnace was controlled using PID control panned attached with the furnace. The flowrate of the N_2 gas was controlled by Rota meter installed at

the outlet of N₂ cylinder. Figure 3.3. Shows the complete diagram of the tubular reactor along with temperature controller and heating system. The char component obtained at the end of the process was washed several times with DI water and 0.1N HCl solution and dried in an oven by keeping at 105 °C for 3-5 hrs or until moisture removed completely. The washed char was named as *lepironia articulata* biochar (LABC), and remaining products obtained at variable conditions were named accordingly as LABC-1-200, LABC-2-200, LABC-3-200, LABC-3-250, LABC-3-300, respectively. Where, 1, 2, and 3 represent the ratio of biomass to KOH, and 200, 250, and 300 represents the flow rate of N₂ gas to the reactor.



Figure 3. 3 Pyrolysis process a) tubular reactor b) heating box with coils c) Temperature controller (3 cycle)

3.2.3 Modification of bentonite using (BCDMCL) surfactant

Natural bentonite (NB) after being washed with DI water several times was converted into modified bentonite (MB) using BCDMCL as a cationic surfactant. Following steps were performed to modify NB.

The method for the preparation of MB was adopted from (Díaz-Nava *et al.*, 2012). The detailed procedure is given stepwise below.

1. Initially, NB bentonite was added into sodium acetate buffer solution at pH 5, which is allowed to react for 18 h.
2. Further reaction with 1 M potassium chloride solution at pH 7 was conducted by allowing them to react for 18 h.
3. The solid phase after separating was kept in 0.2 M cesium chloride solution for 6 h.
4. After again separating the solid-phase was kept in cesium chloride solution for 10 min.
5. The leftover solid from the previous step was then mixed into 8.40 mmol/L of BCDMACl.
6. The mixture was then shaken for 48 h at 303 K.
7. The solid was then separated from the solution using a centrifuge at 2500 rpm for 10 min and rinsed several times with distilled water eliminate excess surfactant. The washed solid clay was then dried by keeping in an oven for 24 h at 70 °C.

3.2.4 Analysis and instrumentation

a) Fourier transform infrared spectrophotometer (FTIR)

In this work the FTIR spectra for the detection of functional groups of LA, LAHC, LABC, NB, and the MB were analyzed from KBr pellets with a Fourier Transform Infrared Spectrometer, VERTEX 70, Bruker, Germany, provided by Scientific Equipment Center (SEC), Prince of Songkla University. Infrared spectra (4000 - 400 cm^{-1}) were attained based on the diamond attenuated total reflectance (ATR) method using an FT-IR Spectrometer (Bruker Vortex 70 spectrometer, Germany) at a resolution of 4 cm^{-1} by using 64 scans.

b) X-ray fluorescence spectrometer

The LA biomass, natural and modified bentonites were characterized with an X-ray fluorescence spectrometer, PW2400, PHILIPS, Netherlands, provided by Scientific Equipment Center (SEC), Prince of Songkla University. The detailed elemental composition is listed in table 1.2.

c) Brunauer, Emmett and Teller (BET) surface area

The BET surface areas and porosity of natural and modified bentonite were determined using BET-technique, ASAP2460, Micromeritics, USA, provided by Scientific Equipment Center (SEC), Prince of Songkla University.

d) Scanning electron microscopy (SEM) and energy-dispersive X-ray (EDX)

The morphology of samples HTC-180, HTC-230, and HTC-300 was analyzed using SEM SEM-EDX and nitrogen adsorption. For SEM, hydrochar samples were dispersed on a conductive pad and introduced into the SEM equipment (FEG Quanta 400), present in scientific equipment center, Prince of Songkla University, Hat Yai. The investigation was carried out by preparing samples by depositing about 50 mg of dry powdered Char samples on copper stud covered with carbon conduction tapes, and then to avoid charging throughout observation samples were coated with Au/Pt for 1 min using sputter coater. Samples were measured at (10000-30000) magnification level.

e) CNH and S

A CHN organic Elemental Analyzer (Macro FLASH 2000) was used to determine the carbon, Nitrogen, Sulphur and hydrogen contents of hydrochars. Oxygen content was then calculated by subtracting all these components from 100% of the sample material.

f) Swelling index

The swell index test method is used to determine the general swelling characteristics of bentonite clay. The Swell Index test has not been demonstrated to have a proportional correlation to hydraulic properties, a high swell is considered by most to be a good indicator of bentonite quality. Regardless, this test parameter can be used as a simple qualitative indicator of the base clay. The swelling characteristics of clay can be assessed in terms of the swelling index. The standard testing procedure followed was taken from (ASTM-D5890) which is briefly described in the following step:

1. A 2 g of ground and dried samples of both MB and NB were dispersed into a 100 mL graduated cylinder in 0.1g increments – see Fig. 3.4. To let the full hydration and the settlement of bentonite samples was left for 10 min after each 0.1 g increment until a complete 2 g of the sample has been added to the cylinder.

2. The sample was then protected from disturbances by covering for a period of 16 - 24 hours, afterward the level of the fully settled and swollen bentonite was recorded to the nearest 0.5 mL.

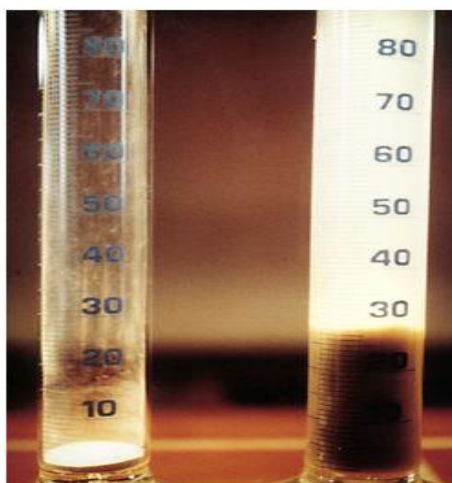


Figure 3. 4 Swelling of modified (left) and unmodified bentonite (right)

g) Wettability of adsorbent monoliths (Contact angle)

The contact angle measurement is a traditional method to describe the hydrophobic or hydrophilic behavior of a material. In principle, it provides information about the wettability of an ideal surface. In most cases, the intrinsic value of the contact angle is perturbed by surface porosity and roughness, heterogeneity, etc. Wettability studies usually involve the measurement of contact angles as the primary data, which indicates the degree of wetting when a solid and liquid interact. Small contact angles (90°) correspond to high wettability, while large contact angles (90°) correspond to low wettability (Glover, 2009).

The contact angle was measured using (OCA 15EC), an entry-level measuring device for professional contact angle measurements and drop shape analysis. The fast 6-fold zoom lens with manual focus and adjustable observation angle in combination with the USB camera ensures pin-sharp drop images and facilitates the effortless analysis with the SCA 20 software.

A simple procedure to calculate wettability parameters of the monolith was adopted. A drop of distilled water was added on the surface of adsorbent monolith placed on the sampling point through the needle to avoid access dispersion. SCA 20 software was used to calculate the contact angle of the adsorbent based on Young's equation. A clear image can show the closer look of the surface through a microscope on the computer screen. This can also show the exact contact angle of the material through drop dispersion analysis (Fig 3.5).

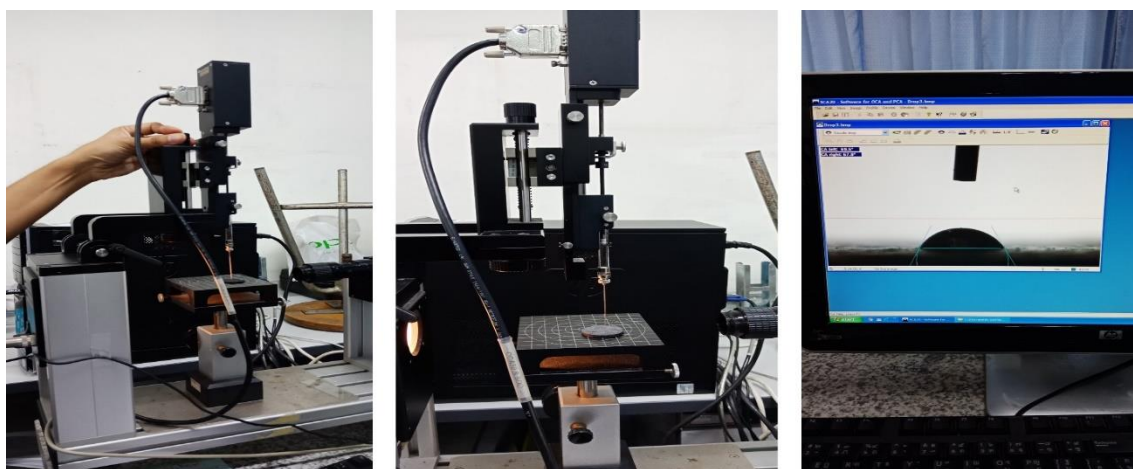


Figure 3. 5 Contact angle analysis using (OCA 15EC) contact angle analyser

h) Cation exchange capacity (CEC)

Based on the values obtained from the summation of exchangeable cations (Ca, Mg, Na, and K) and exchangeable Al, the CEC value of the clay can be obtained. The method followed in this study is the most widely applied neutral 1.00 M ammonium acetate (NH₄OAc) extraction method. This method is basically used to evaluate the soluble and quickly replaceable pools of alkali and alkaline elements present in soils. Following is the detailed procedure of this method in four steps:

Step 1. Cation replacement

- 1.1 5 g of air-dried sample was added into the centrifuge tube.
- 1.2 Sample was shaken for 30 min after adding 30 mL of 1 M NH₄OAc.
- 1.3 The sample was centrifuged at 2500 rpm for 10 min, further separated using filter paper number 5 only.

1.4 Repeated from step 1.2-1.3, by shaking with the hand instead of centrifuge for 1 min. After filtration volume was adjusted to 100 mL by 1 M NH₄OAc reach to 100 mL.

Step 2. Washing ammonium

2.1 The sample obtained from step 1.4 was mixed with 30 mL of 80% w/w ethanol and shaken for 1 min.

2.2 The sample was centrifuged using the same method as mentioned in order 1.3, only solid samples were collected.

2.3 Order 2.1-2.2 were repeated three times using the same sample.

3. Ejecting adsorbed ammonium

3.1 Sample collected from step no 2.3 was mixed with 30 mL of 10% w/v NaCl and shaken for 1 min.

3.2 The order 1.3 was followed and the sample was centrifuged, the solution was collected in a volumetric flask without filtration.

3.3 Order 3.1-3.2 were repeated 2 times for this sample and the volume of the solution was adjusted with NaCl to 100 mL.

4. Distillation of ammonium

4.1 20 mL of the solution from 3.3 was pipet out, adding 10 mL of magnesium oxide into it.

4.2 Ammonia Distilled in 5 mL boric acid into a 125 mL flask until the volume reaches to 30 mL using VAPODEST® - C. Gerhardt GmbH & Co. KG (Fig. 3.5).

4.3 Sample was titrated with 0.01M H₂SO₄.

4.4 NaCl (blank) was distilled later on following the same procedure discussed in 4.1-4.3.

Below is the mathematical equation to calculate CEC

$$CEC(\text{cmol}_c / \text{kg}) = 200AB \quad (30)$$

Where, A is the concentration of H_2SO_4 (mL) and B is the difference between blank and the titrant volume (mL).



Figure 3. 6 Gerhardts (Germany) ammonia distiller to calculate CEC

i) Lignocellulosic compositions

The acid detergent method is a widely used common method to calculate the lignocellulosic composition of any biomass or organic components. The method was adopted to calculate the rate of synthesis of lignin, cellulose, and hemicellulose with respect to the change in HTC temperature.

An updated van-Soest method using Pyrex® (Gooch) crucible was used to determine the contents of cellulose, hemicellulose, aqueous soluble compounds, and pseudo-lignin in the raw biomass (LA) and solid LAHC samples (Anyikude, 2016). The LA and LAHC samples were converted into the desired particle size (20-65 mesh) after crushing and sieving. Prior to the analysis, samples were dried at 105 °C for 24 h to remove any unnecessary moisture content if present. The contents of cellulose, lignin, and hemicellulose, were calculated from the difference of acid detergent fiber (ADF), neutral detergent fiber (NDF), acid detergent lignin (ADL), and ash from the following equations (Reza, Rottler, Herklotz, & Wirth, 2015):

$$\text{Extractives (\%)} = 100 - \text{NDF (\%)} \quad (31)$$

$$\text{Hemicellulose (\%)} = \text{NDF (\%)} - \text{ADF (\%)} \quad (32)$$

$$\text{Cellulose (\%)} = \text{ADF (\%)} - \text{ADL (\%)} \quad (33)$$

$$\text{Pseudo-lignin (\%)} = \text{ADL (\%)} - \text{Ash (\%)} \quad (34)$$

Higher heating value (HHV) was estimated according to the formula given in (Channiwala & Parikh, 2002)

$$HHV(MJ / kg) = 0.3491C + 1.1783H + 0.1005S - 0.1034O - 0.015N - 0.021A \quad (35)$$

Where, C, S, H, N, O and A symbolize carbon, sulfur, hydrogen, nitrogen, oxygen, and ash content (wt.% dry basis), respectively.

3.2.5 Batch adsorption experiments

Performance of adsorbents prepared from various methods has been identified through batch and continuous adsorption experiments. The effect of each parameter (temperature, initial adsorbate concentration, adsorbent dosage, pH, time) was calculated against the efficiency and capacity of adsorbents. A stock solution of 1000 mg/L of Zn(II), Ni(II), and Cr(VI) were prepared using appropriate amounts from standard salts. Batch experiments were performed initially for the removal of Zn(II), Ni(II), and Cr(VI) from aqueous solution as a whole and separately to identify optimum conditions of adsorption and capacity of adsorbent. These experiments were carried out in triplicate, utilizing 100-mL conical flasks. The volume of aqueous solution was fixed to 50 mL with appropriate amounts of the adsorbent for all the experiments. The incubator shaker (Daihan WIS-20 shaking incubator) (Fig 3.7), was used to shake samples at a certain controlled temperature and 150 rpm. To achieve the equilibrium for isotherm studies, samples were drawn every 5-20 min until a constant concentration

of adsorbate. The solution after obtaining from shaking incubator were filtered using disposable clear Nylon Syringe Filters, 0.45 μm and the filtrates were diluted where required to obtain adsorbate concentration levels corresponding to the linear range of calibration curves and were analyzed using a flame atomic absorption spectrometer



Figure 3. 7 Incubator shaker for batch adsorption experiments

(Perkin Elmer A Analyst 200), present in the department of chemical engineering, Prince of Songkla University, Hat Yai, Thailand. Batch adsorption data were analyzed using Eqs. (1) and (2) to obtain the adsorption capacity and the removal effectiveness of selected heavy metal ions.

3.2.6 Continuous adsorption experiments

Fixed-bed column adsorption experiments were carried out in a cylindrical glass column with an internal diameter of 2.5 cm and a height of 44 cm (Fig 3.8). The top and bottom of the column were covered with a 3-mm layer of glass beads and glass wool, respectively. The experiments conducted in batch experiments were repeated here by using appropriate amounts of adsorbent, meanwhile, the efficiency of the prepared adsorbent monolith was tested by treated with known concentrations of heavy metals in the continuous flow system. An aqueous solution containing heavy metals was pumped to the bottom of the column using a peristaltic pump to let the solution easily penetrate into the surface of the adsorbents. The removal was calculated based on changing one parameter while keeping others constant. The efficiency of adsorbent

was assessed by varying solution flow rate, and type of adsorbent. The flow rate was at a fixed flow rate (5–15 mL/min). To calculate the flow rate Rota meter was fixed before the inlet of the tube and controlled by adjusting the peristaltic pump inlet and outlet flow. All experiments were carried out at room temperature and had a pH of 2-3 (optimized in batch experiments). Samples from the outlet of the column were collected at specific intervals of time (10-20 min) to determine the metal ion concentration after the column was fully exhausted, the continuous adsorption experiments were stopped. After plotting the breakthrough curves (C_t/C_0 vs. time), the data obtained were analyzed through desired models using Equations (18-29).

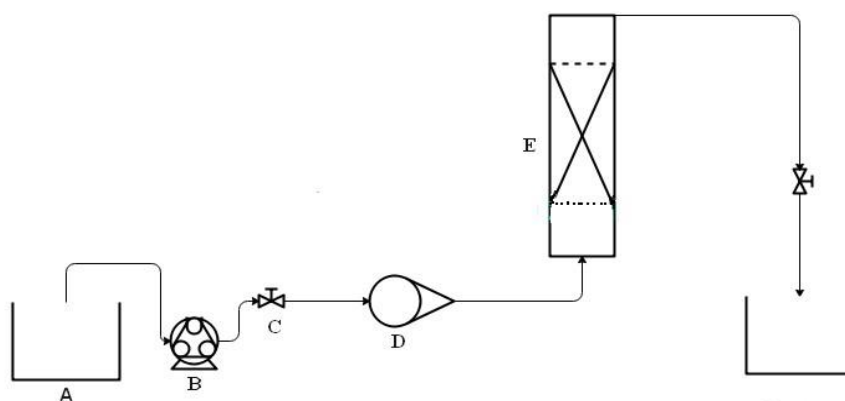


Figure 3. 8 Schematic diagram of fixed bed continuous adsorption process a) Liquid tank
b) Peristaltic pump c) control valve d) Rotameter e) fixed bed reactor

4. RESULTS AND DISCUSSION

4.1 Characterization of adsorbents

The detailed surface characterization results were conducted to identify the effectiveness of adsorbents and to adopt optimum conditions for the preparation and modification of adsorbents in the future.

4.1.1 Surface structure and morphology of adsorbents

The effect of process conditions were assessed on the porous structure and crystallinity of the adsorbent. Figure 4.1 shows the complete conversion images of LA into HC and MBio. In this image the highly porous structure build on the surface of MBio can be seen clearly, whereas the brown color image of HC indicates the complete synthesize of LA into the porous mass structure.



Figure 4. 1 Biomass LA converted into LAHC and LABC

Furthermore, in-depth morphological structures were assessed based on the below techniques:

a) SEM analysis

Surface structures of both LAHC and LABC were analyzed. In Figure 4.2A (LAHC), vesicles were formed through chemical decomposition and fragmentation of the LA matrix, taking into account the fact that hydrolysis is pre-dominant in biomass hydrothermal treatment (Sun *et al.*, 2015). The SEM image of LAHC shows less porous surface and more visible impurities (Fig. 4.2A). Because of the long residence time and

high temperature in the HTC process, the porous structure of hydrochar became partially blocked by re-polymerization recondensation of water-soluble compounds (Huang *et al.*, 2017). The LABC had irregular and highly porous surfaces (Fig. 4.2B). Since KOH has a cleaning effect on hydrochars, which possibly removes the impurities which block the pores (Sun *et al.*, 2015). The remarkable improvement in specific surface of LABC could be the result due to the removal of the components which were occupying the pores in LAHC.

b) BET Surface area, pore volume, and porosity analysis

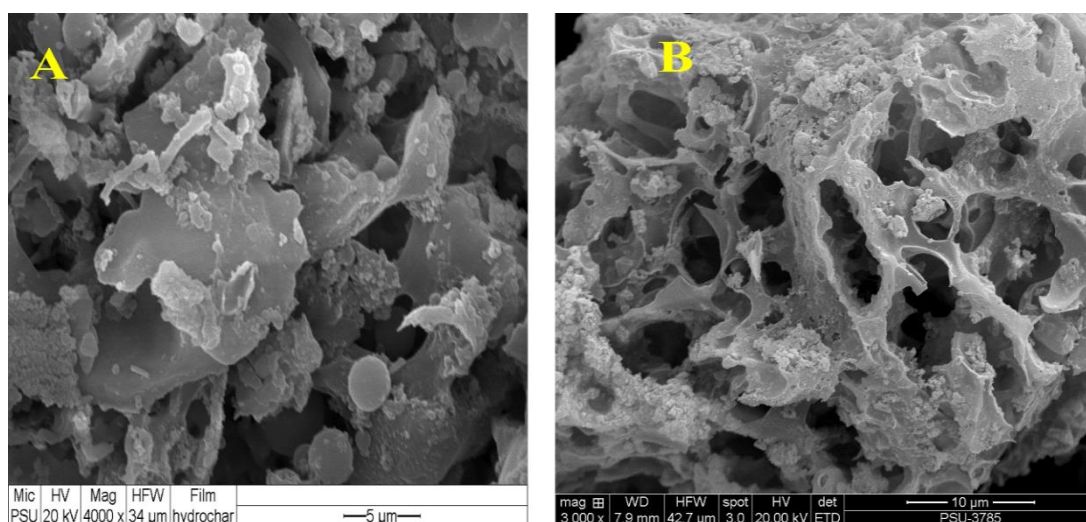


Figure 4. 2 SEM images of A) LAHC B) LABC

The surface area, porosity and pore volume of raw biomass LA, hydrochar LAHC, modified biochar (LABC), natural bentonite (NB), and modified bentonite (MB) were assessed to identify the effect of the modification on the said parameters during the preparation of adsorbents. The detail of BET results is shown in table 4.1. The results showed that the surface area of LAHC is very low as compared to LABC and ULABC, whereas the increment in surface area from ULABC to LABC is almost double. The reason for low surface area and pore volume of LAHC is largely due to the collapse of the pore wall as a result of melting and deformation. Also the fusion at high temperatures during HTC process, which typically take place at a lower temperature threshold for hydrochars than it does for dry pyrolysis chars, possibly because with an

increase in temperature the pressure during the HTC process increases (Fang, Gao, Chen, & Zimmerman, 2015). The BET surface area of LABC is almost double to that of ULABC. Adsorption of various heavy metals from contaminated water requires the large specific surface of adsorbent, so to further increase the specific surface of LAHC, slow pyrolysis was adopted. The specific surface area of LABC was increased to 820.54 $\text{m}^2 \text{g}^{-1}$ for LABC from 69.23 $\text{m}^2 \text{g}^{-1}$ and 416.72, for LAHC and unmodified biochar, respectively. The KOH to char ratio is critical for obtaining biochar with high porosity and large pore size. A number of previous studies confirm that higher KOH to char ratio results in higher porosity and surface area. In another study by Hanna F *et al.* (2015) (Fałtynowicz *et al.*, 2015), Observed a well-developed porous texture of activated carbons when KOH-to-char weight proportion was expanded from 2:1 to 3:1; however, additionally increment in the KOH-to-char proportion did not have a detectable effect. Therefore, the KOH to char ratio in this study was set at 3:1 for all the batches.

While calculating for bentonite, the BET result are shown in Table 4.1, where the specific surface area of NB and MB were calculated to be 44.60 and 15.57 m^2/g , respectively. The reason for the reduction in surface area of MB was by introducing the alkyl chains using a cationic surfactant, which ultimately had reduced the adsorbent pores.

Table 4. 1 Surface area, cation exchange capacity against the sample and process condition

Sample	Process condition	Modification/surfactant	BET surface area(m^2/g)	CEC(cmolc/kg)
LAHC	220 °C		69.23	40
ULABC	700 °C		416.72	64.2
LABC	700 °C	KOH	820.54	73.93
UB		BCDMACI	44.6	75.95
MB		BCDMACI	15.57	68.7
LABC-MB monolith		PVDF/MC	632.75	

4.1.2 Surface functional groups (SFG)

The Large surface area and well-built porosity are not only the indicators of the good ability of adsorbent for adsorption, besides the surface functional groups plays a vital role during the adsorption process. The results related to the FTIR for LAHC and LABC are given in Figure 4.3 and 4.4, respectively. In which Figure 4.3 shows the increments or decrease in peaks of FTIR spectra at different temperatures, which identifies the development or shift of new functional groups after varying HTC temperature. The performance of hydrochar was found improved in the variable application by introducing oxygenated functional groups such as OH, C-O, and COOH (Mihajlović *et al.*, 2017). Particularly, surface COOH and OH groups have greatly improved the adsorption capacity when LAHC was used as an adsorbent for the removal of heavy-metal aqueous solution. This is because such oxygenated functional groups interact with heavy metals via hydrogen bonding and complexation (Han *et al.*, 2017).

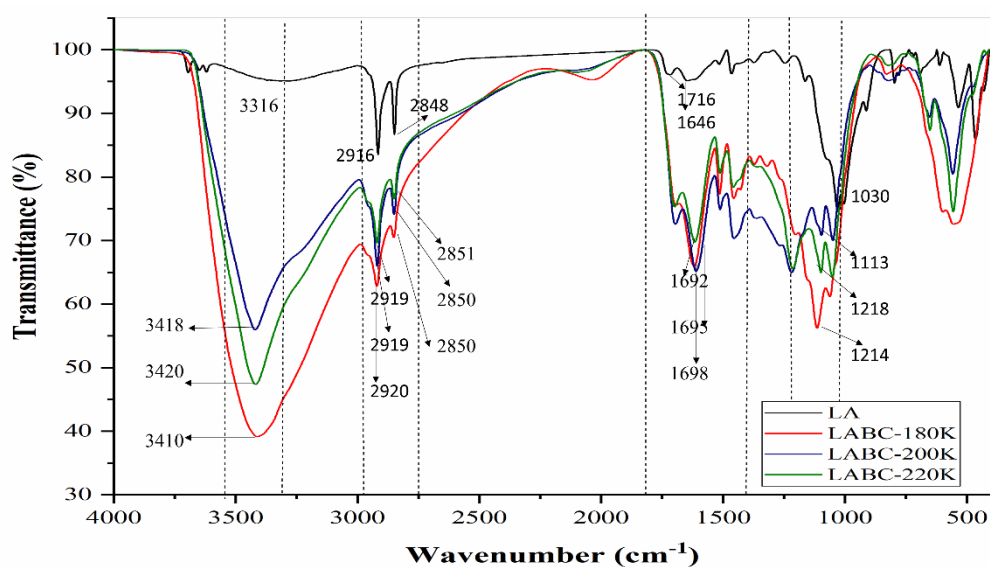


Figure 4. 3 FTIR spectrum of raw biomass lepironia articulata along with LAHCs prepared at different temperatures

The bands of unmodified hydrochar (LAHC) shows it was rich in surface functional groups. The peak assignments were made are: a wide strong band at 3420 cm^{-1} may be due to the stretching of O–H bonds and suggests the presence of hydroxyl (OH^-) groups (Coelho *et al.*, 2014), O-H and N-H stretching; 2903 cm^{-1} for C-H stretching; 1695 cm^{-1} for C=O stretching; 1610 cm^{-1} for asymmetrical stretching vibrations of COO^- ; 1512 cm^{-1} for in-plane bending vibrations of amide bond; 1455 cm^{-1} for C-H bending vibrations; and 1096 cm^{-1} for C-N stretching vibrations. The region $1280\text{--}1000\text{ cm}^{-1}$ has several peaks associated with C-O bonds, such as C-OH. Bands at 1361 cm^{-1} and 2919 refer to stretching of C–H bonds in aliphatic acid groups and alkane (Mihajlović *et al.*, 2017). A comparison between LAHC and LABC revealed some new peaks and the disappearance of a few old peaks. Si-O-Si vibrations are observed at 1096 cm^{-1} that mostly disappeared after treating with KOH. Alkali activation did not affect the groups around 1320 cm^{-1} (C-O stretching), 1161 cm^{-1} (-C-O-C- in cellulose) between 1060 and 1030 cm^{-1} (C-OH alcohol and/alkyl substituted ethers groups) and the bands between

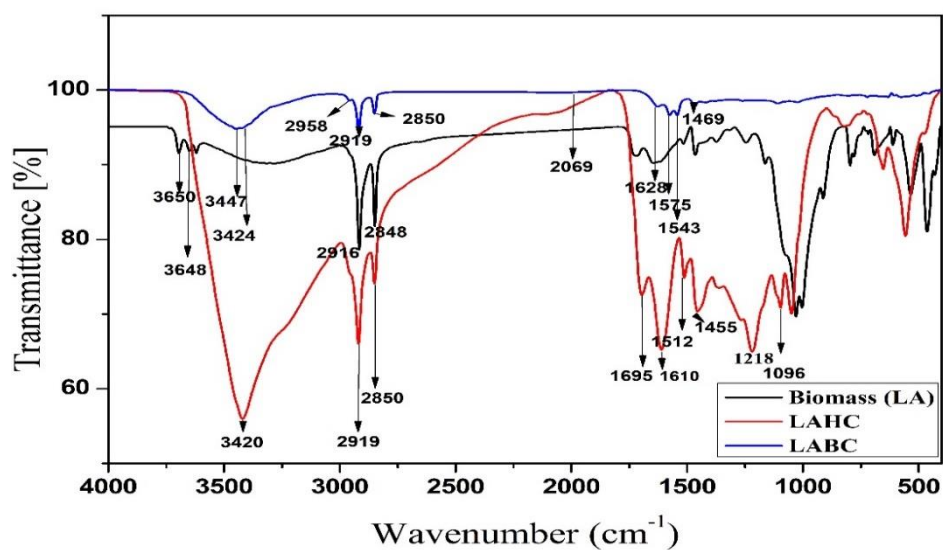


Figure 4. 4 FTIR spectra of biomass (LA), hydrochar (LAHC), and modified biochar (LABC)

720 and 590 cm^{-1} attributed to alcohol and -OH out-of-plane bending (Mihajlović *et al.*, 2017).

4.1.3 Hydrochar yield

The yield is another important factor to consider during designing optimum process condition for the production of hydrochar and biochar. All the yields and lignocellulosic composition of hydrochar at different temperature and process conditions are given in Table 4.2. It was noticed that the yield of hydrochar is maximum in the HC produced at 180 °C, whereas the lowest yield was obtained at 240 °C. The reason is because of the incomplete synthesis process at a lower temperature could lead to retain the composition without much losing the volatile or mineral components. The yields of HC obtained at 200 °C doesn't actually makes a big difference as compared to the yield at a lower temperature.

Table 4. 2 Lignocellulosic component and hydrochar yield by varying reaction parameters

Sample	Reaction Conditions		Hydrochar yield (wt % dry raw material)	Ash (wt% dry hydrochar)	Hemicellulose (wt% dry hydrochar)	Cellulose (wt% dry hydrochar)	Lignin (wt% dry hydrochar)
	Temperature (°C)	Time (h)					
Raw LA	--	--	--	14.3	30	36.7	19
LAHC-180-2		2	68.8	12.7	27.6	27.7	42.9
LAHC-180-4	180	4	67.6	12.05	26.54	27.22	42
LAHC-180-6		6	66.45	12.46	26	26.45	40.88
LAHC-200-2		2	64.85	12.7	13.4	12.4	52.24
LAHC-200-4	200	4	64	12	13.11	11.87	51.22
LAHC-200-6		6	63.12	11.89	13	11.69	51
LAHC-220-2		2	61.35	10.6	12.6	12.8	57.3
LAHC-220-4	220	4	60.56	10.22	12.65	12.08	57.22
LAHC-220-6		6	58.23	11.05	12.22	12.11	56.89
LAHC-240-2		2	56.725	8.87	9.84	10.24	61.55
LAHC-240-4	240	4	56	8.54	8.96	9.25	60.21
LAHC-240-6		6	55.2	7.21	8.25	9.11	59.65

4.1.4 Proximate and ultimate analysis

The effects of reaction temperature on compositions from ultimate and proximate analyses are summarized in Table 4.3. Increasing reaction temperature from 180 to 240 °C improved the carbon content, whilst decreased hydrogen and oxygen contents. This was attributed to the decarboxylation and dehydration reactions taken place during HTC (Nakason *et al.*, 2018), and this is corresponding to a decrease of hydrogen to carbon (H/C) ratio, and oxygen to carbon (O/C) ratio. This trend was predictable due to at a high temperature of some inorganics components were re-precipitation onto the hydrochar, as was also proposed earlier by (Reza *et al.*, 2013). A further calculation towards energy potential of the product revealed that an increase in the reaction temperature from 180 to 240 °C enhanced the HHV of LAHC samples from 22.25 to 24.95 MJ/kg.

Table 4. 3 Proximate and ultimate analysis of HC at different HTC temperature

		LA	LAHC-180-2	LAHC-200-2	LAHC-220-2	LAHC-240-2
Proximate analysis(wt.%,db)	Ash	14.7	12.7	10.6	8.8	7.24
	VM	64.9	61.5	57.07	55.27	51.21
	FC	20.4	25.8	32.33	35.93	41.55
Fuel ratio	FC/VM	0.314	0.420	0.566	0.650	0.811
Ultimate analysis(wt.%,db)	C	46.58	55.2	58.67	60.25	62.64
	H	5.44	5.36	5.21	4.96	4.68
	N	1.37	1.38	1.3	1.29	1.278
	S	0.86	0.86	0.86	0.86	0.86
	O	33.59	30.25	28.88	25.32	22.65
Atomic ratio	H/C	1.392	1.157	1.058	0.981	0.890
	O/C	0.541	0.411	0.370	0.315	0.271
HHV(MJ/kg)		18.955	22.257	23.479	24.142	24.955
HHV _{daf} (MJ/kg)		19.264	22.524	23.701	24.327	25.107

4.1.5 Contact angle and wettability

Wettability studies commonly include the measurement of contact angles as the primary data, which specifies the degree of wetting when a solid and liquid interact. Small contact angles (below 90°) correspond to high wettability and a term hydrophilic

is used, while large contact angles (above 90°) correspond to low wettability which indicates poor wettability and is termed hydrophobic. The contact angle the Θ value for all samples LABC-MB monolith were calculated to be well under 90° , therefore they are said to be hydrophilic in nature and the penetration of water molecules is highly admissible which lead to good homogenous adsorption process.

4.2 Chemical characterization of adsorbents

4.2.1 Cation exchange capacity (CEC)

CEC is one of the significant characteristics of adsorbent which identifies its capacity to hold exchangeable cations. The common ammonium acetate method was applied to determine the CEC values of LAHC and LABC, respectively. The CEC values were calculated to be 40 and 73.93 cmolc kg^{-1} for LAHC and LABC (Table 4.2), respectively. As CEC is said to be a function of surface functionality and the surface area, an increase in the CEC of LABC suggests either an improved surface functionality or by increasing porosity and surface area by unblocking of pores due to alkali modification. The CEC of NB and MB were calculated to be 75.95 (NB) to 68.70 cmolc/kg (MB), the reduction in CEC could be the cation from the surfactant was introduced in the clay and ultimately pushed other cations into solution, in that way significantly decreasing CEC (Akpomie *et al.*, 2016). The significant adsorption of the surfactant to the inner surface and micropores of the particles, decreasing the specific surface of MB (Tohdee *et al.*, 2018).

4.3 SEM-EDX after adsorption

EDX studies of LABC was carried out to determine the chemical composition of adsorbents (wt% of elements) before and after the adsorption process (Fig 4.5 and 4.6). Successful sorption of chromium on the surface of LABC was confirmed with EDX spectra of biosorbents. Generation of new spectra of Chromium and decrease of some contributing functional groups confirmed the uptake of chromium ions. Figure 4.6 shows the visible peaks of Ni(II) and Cr(VI) after adsorption onto LABC which is clearly indicative of heavy metal diffusion onto the modified sorbent.

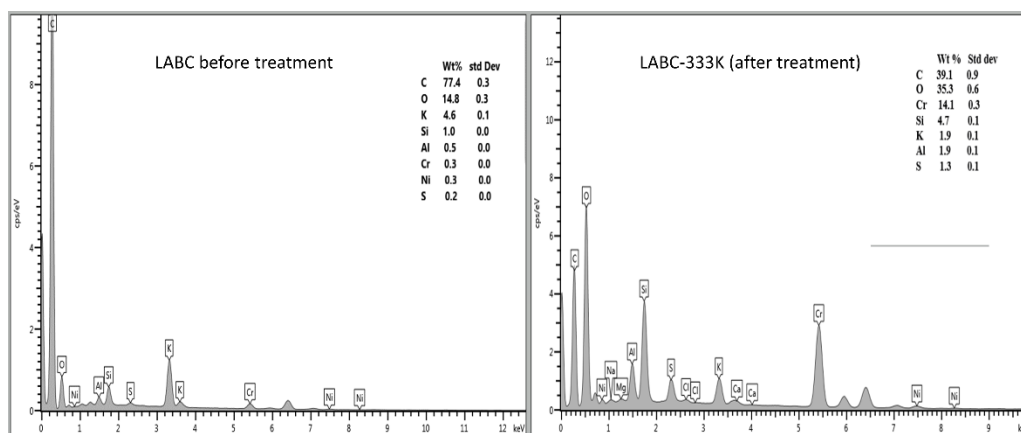


Figure 4. 5 SEM-EDX spectrum of LABC before and after adsorption of Cr at 333K , pH 2, Initial metal concentration of 50 mg L-1

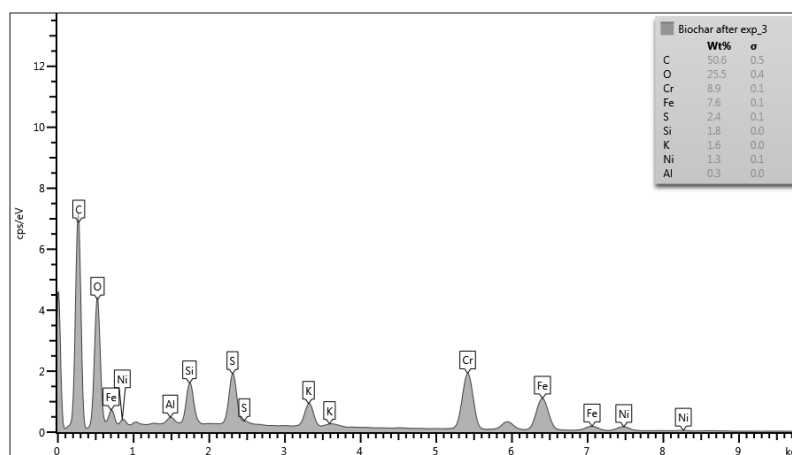


Figure 4. 6 SEM-EDX of Cr(VI) and Ni(II) in multi-system after adsorption using LABC

4.4 Batch adsorption experiments

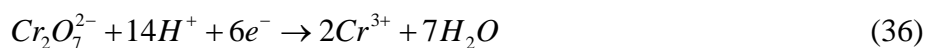
Experiments were conducted for the adsorption of Cr(VI), Ni(II), and Zn(II) onto LAHC and LABC. These experiments also suggested the effect of the modification on adsorbents. The effect of each parameter on the removal of heavy metals using LAHC and LABC were almost similar. The only improvement observed was the increase in the removal of contaminants and capacity of adsorption in case using LABC. Following

detail study on the effect of the individual parameter on the removal and capacity are given below.

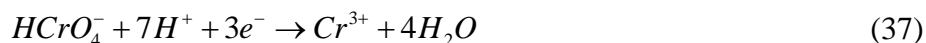
4.4.1 Effect of pH on the removal of heavy metals

Experiments were conducted to find the effect of pH on removal efficiency and capacity of adsorbents. When tested for individual components the removal efficiency of Cr(VI) was increased with the decrease in pH of the solution using LAHC and LABC, respectively (Fig 4.7). The optimum removal was achieved at a pH of 2. The improved removal of Cr at low pH is probably due to the reduction of hexavalent Cr to trivalent Cr (Verma, Chakraborty, & Basu, 2006).

Chromium at low pH



At moderate pH



At low pH, the diffusion of trivalent chromium through a negatively charged adsorbent surface is hindrance free due to the presence of a large number of H^+ ions. It is further predicted that the effect of pH on adsorption might be due to the expansion of an electrical double layer on the adsorbent. The polarity of the double layer at the adsorbent surface may be the changed from positive to negative as the H^+ -ion concentration changes from acidic to basic with the increase of pH. It was also noticed that at the lower pH the chromium adsorption percentage had increased with shorter time to attain equilibrium.

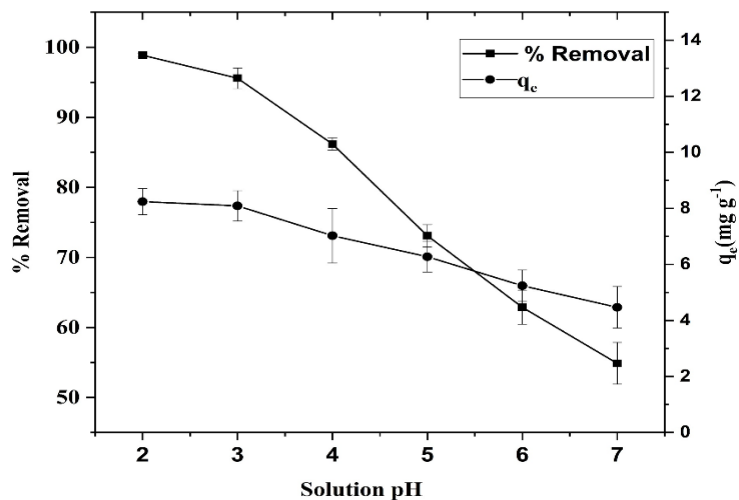


Figure 4. 7 Effect of pH on the removal of Cr(VI) and on the capacity q_e (mg g⁻¹) of LABC

Similarly when treating with Ni(II) and Zn(II) there was not a big difference in the removal with the increase or decrease in pH, However, the impact of pH was a little bit higher in case of Ni(II) as compared to Zn(II). The optimum removal of Ni (II) was achieved at pH level 6-7 (Fig. 4.8), and for Zn(II) between pH (3-5), respectively.

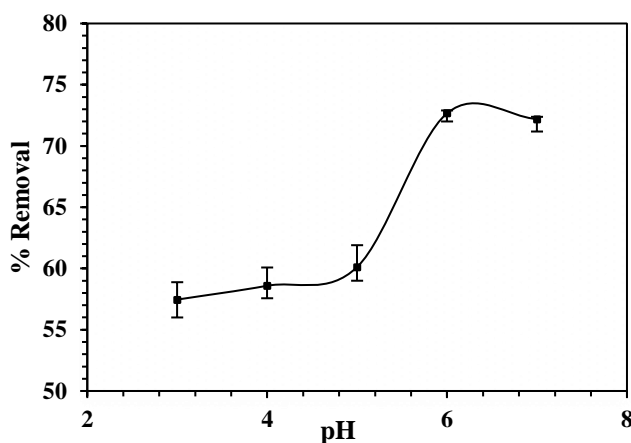


Figure 4. 8 The effect of pH on the percent removal of Ni(II) (initial metal concentration of 50 mg L⁻¹ and hydrochar dosage of 20 g L⁻¹)

(Olayinka, Oyedeji, & Oyeyiola, 2009), through their work on the removal of Ni(II) concluded that the optimum pH for the adsorbents could be between pHs 6 and 8. This could be due to an increased negative charge density on the adsorbent surface.

He also recorded that at pH above than 8, the removal of Ni(II) ions was generally due to precipitation and not by sorption. A similar result was obtained when sawdust was used as the adsorbent. When treating all the heavy metals together the pH of the solution was kept between 2-3, the reason is because the impact of pH on the removal of Cr(VI) was maximum which was less in the case of Ni(II) and Zn(II), therefore the overall effect of pH on removal efficiency was optimized at pH between (2-3) for multicomponent removal, which was further set as pH 6 for the removal of nickel and 5 for the removal of Zn(II), respectively. It was further observed that the pH impact on removal was consistent regardless of using any kind or dose of adsorbent.

Trivalent and hexavalent chromium speciation

The effect of pH on the removal of chromium was further investigated using ICP-MS and UV-Spectrophotometer to collect exact data that how much ions of the hexavalent and trivalent chromium adsorbed onto LABC at variable pH. The data collected shows the removal of the hexavalent chromium at pH 5-6 was 98% where as it was decreased to 1.6% at pH 2 and the rest was calculated to be trivalent chromium, the reason was discussed before to be the conversion of hexavalent chromium into trivalent chromium at lower pH. This has also enhanced the removal percentage at lower pH level.

4.4.2 Effect of initial metal concentration

Experiments were conducted to study the effect of initial metal concentration C_e (mg/g) on the removal efficiency and capacity of the adsorbents. Initially the effect of initial metal concentrations on the removal Ni(II) and q_e (mg/g) was conducted. Figure 4.9 & 4.10 shows the results indicating the removal and adsorption capacity were calculated to be 76% and 12.1 mg/g, respectively. The removal of Ni(II) decreased with increase in initial metal concentration whereas the adsorption capacity increased with increase in initial metal concentration.

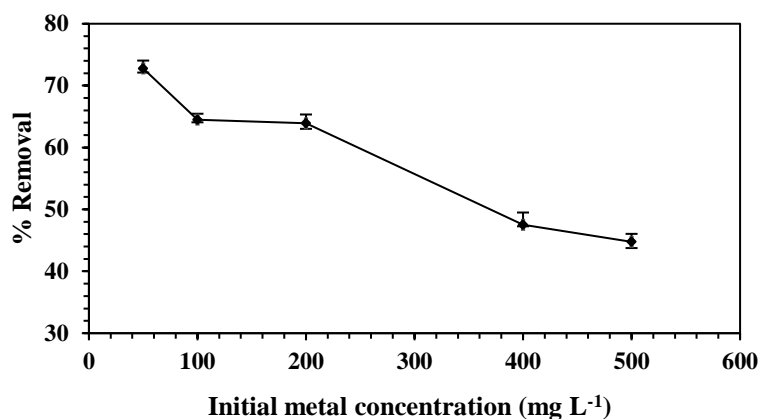


Figure 4. 9 Removal efficiency of Ni (II) with variable initial Concentration of adsorbate (mg L^{-1}) using LAHC

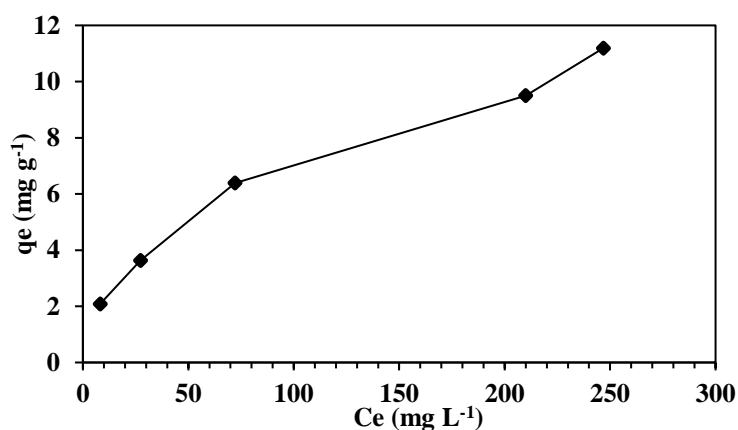


Figure 4. 10 Adsorption capacity q_e (mg g^{-1}) at different initial Ni(II) concentration C_e (mg L^{-1}) using hydrochar

Similarly while conducting experiment for the removal of Cr(VI) using LABC. The removal of chromium(VI) ions decreased with initial Cr(VI) concentration because a given mass of adsorbent has a restricted number of adsorption sites, and as the metal concentration increased these sites became saturated (Saravanan, Senthil Kumar, & Preetha, 2016). The maximum removal of Cr(VI) recorded using LAHC and LABC was 63.44 and 98.88 %, respectively, and the maximum capacity (q_{max}) was estimated to be 18.86 and 27.24 mg L^{-1} at constant pH 2 for the adsorbent dose 0.3 g/50 mL, respectively (Fig. 4.11).

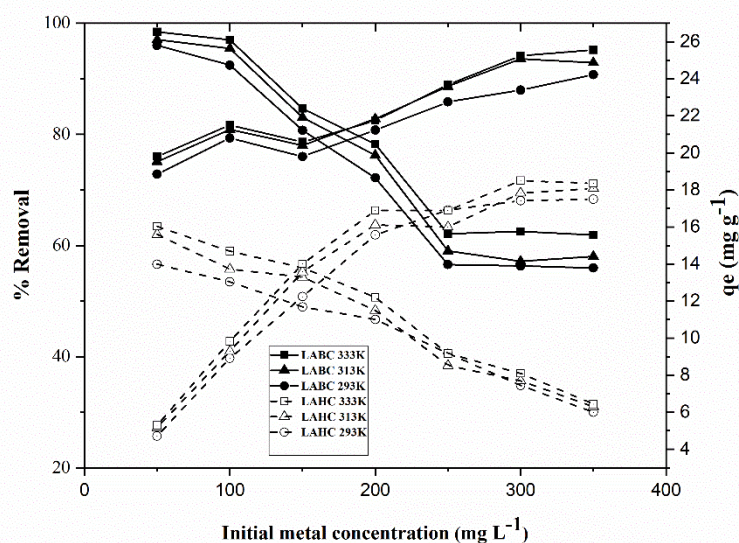


Figure 4. 11 Effects of initial metal concentration (mg L^{-1}) on the removal of Cr(VI) & q_e at pH 2 with adsorbent dose 0.3 g/50 mL of LABC and LAHC at selected temperatures

The effect of initial metal concentration on the removal of multi heavy metals in a single system was evaluated (Fig 4.12). It was noted that the removal of Ni(II) was almost similar for every initial metal concentration, there was a slight decrease in the removal

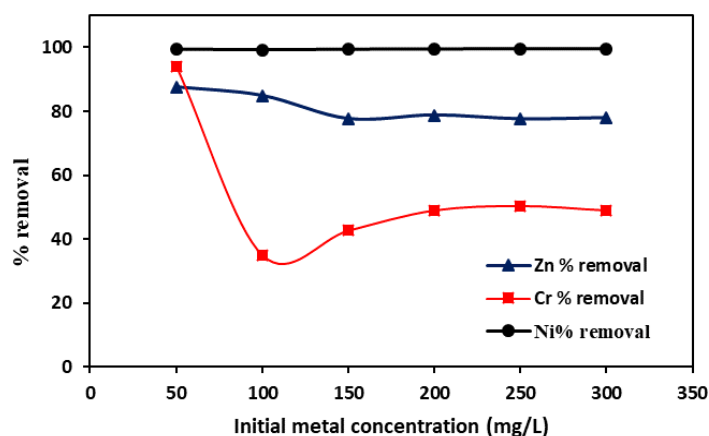


Figure 4. 12 Removal of Cr(VI), Ni(II), and Zn(II) at different initial metal concentration (mg/L) of Zn(II) at below 150 mg/L. There was a rapid decrease on the removal of Cr(VI) with an increase in initial metal concentration. This was due to larger ion molecules and interconversion of Cr(VI) to Cr(III) the pores were occupied by Ni(II) and Zn(II) ions earlier. However, there was an increase in adsorption capacity of LABC with the increase in initial metal concentration which was highest in the case of Ni(II) (Fig 4.13).

The percent removal of Ni(II) and Cr(VI) was also assessed against their initial concentrations using NB and MB. It is clearly shown in Figure 4.14 that removal of both metals decreased with increase in initial metal concentration. Importantly the removal percentage is higher using MB as compare with NB.

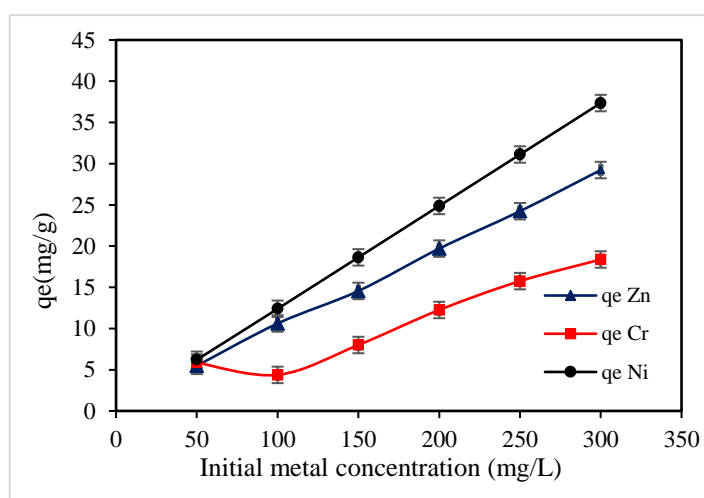


Figure 4. 13 The adsorption capacity of Ni(II), Cr(VI), and Zn(II) adsorption onto LABC-MB monolith

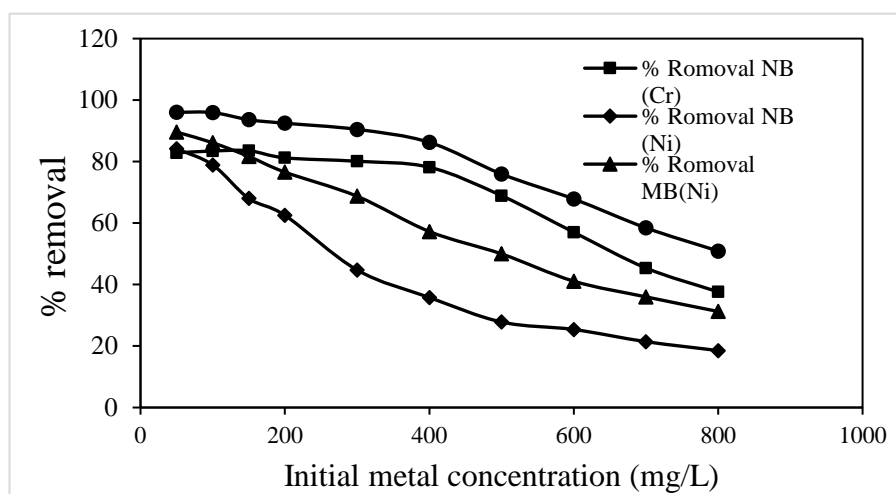


Figure 4. 14 Removal of Cr (VI), Ni (II) against the initial metal concentration (mg/L) using NB and MB

4.4.3 Effect of time

To calculate the kinetics of adsorption and equilibrium adsorption isotherm, the removal capacity of LABC was calculated based on the agitation time. Experiments were conducted to calculate the exact amount of heavy metal removed after every interval of time (10-20 min). It was noticed through analysis that the equilibrium time for Cr(VI) achieved after 2 hrs. (Fig. 4.14). Whereas the time to achieve equilibrium in the case of Ni(II) was achieved in 1.5 hrs. It was concluded from the above observations that the maximum removal of time required for the removal of Ni (II) was achieved in 120 min whereas the adsorption of Ni (II) took place immediately after 15 min of starting the process.

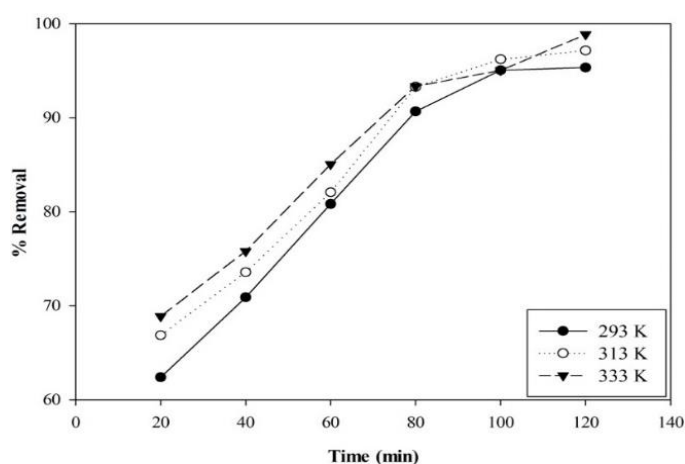


Figure 4. 15 Effects of contact time on the removal of Cr(VI) at selected adsorption Temperatures. The pH was held at 2, the dosage of adsorbent was 0.3g/50ml of the solution, and initial metal concentration was 50 mg L⁻¹

4.4.4 Effect of temperature

Temperature is a greatly significant parameter affecting adsorption. Experiments were performed at select temperatures (293, 313, and 333 K) with optimum pH and contact time for Cr(VI) removal. The initial metal concentration was also varied (50, 100, 150, 200, 250, 300 mg L⁻¹). It was observed that the adsorption increased from 95.98 to 98.44% for the hexavalent chromium ions as the temperature was increased from 293 to 333 K. It is evident from Figure 4.14 that adsorption of chromium increased with temperature because this adsorbent is not homogenous and the activation energies of adsorption sites vary. Therefore, at a low temperature, only the adsorption sites with low activation energy were occupied, while those with higher activation energy could

only be occupied as the temperature was increased. The improvement of adsorption capacity with temperature was effectively due to the increase in kinetic energy of adsorbent particles (Prasanthi, Jayasravanthi, & Nadh, 2016). Thus the collision frequency of adsorbent and adsorbate increased, which enhances adsorption onto the adsorbent. Secondly, at an elevated temperature bond ruptures in functional groups on the adsorbent surfaces increase active adsorption sites, which may also enhance adsorption (Tewari, Vasudevan, & Guha, 2005).

4.4.5 Batch adsorption kinetics

Kinetic data are vital for knowing the rate of adsorption can be limited by diffusion or the chemical reaction, which in turn is important in the design of an adsorption system that provides appropriate contact time: the dimensions of the system rely on such knowledge. In this study, non-linear pseudo-first-order and pseudo-second-order kinetic models were employed to examine the kinetics of adsorbing Cr(VI) ions on LABC. Therefore, the time profiles of concentration were fit with these models, and the associated parameters are collected in Table 4.4. As can be seen there, the equilibrium data were precisely fit by the pseudo-second-order kinetic model, with the better correlation coefficient of the two models. It should, however, be observed that for LABC the $q_{e,cal}$ determined from the pseudo-second-order model was closer to the $q_{e,exp}$ than the estimates from the pseudo-first-order model. Figure 4.16 shows the capacities of the adsorbent for various contact times. The pseudo-second-order kinetics match the experimental data very well. Therefore only the corresponding results are displayed in Figure 4.17. The diagnostics in Table 4.3 allow comparing the two kinetic models further

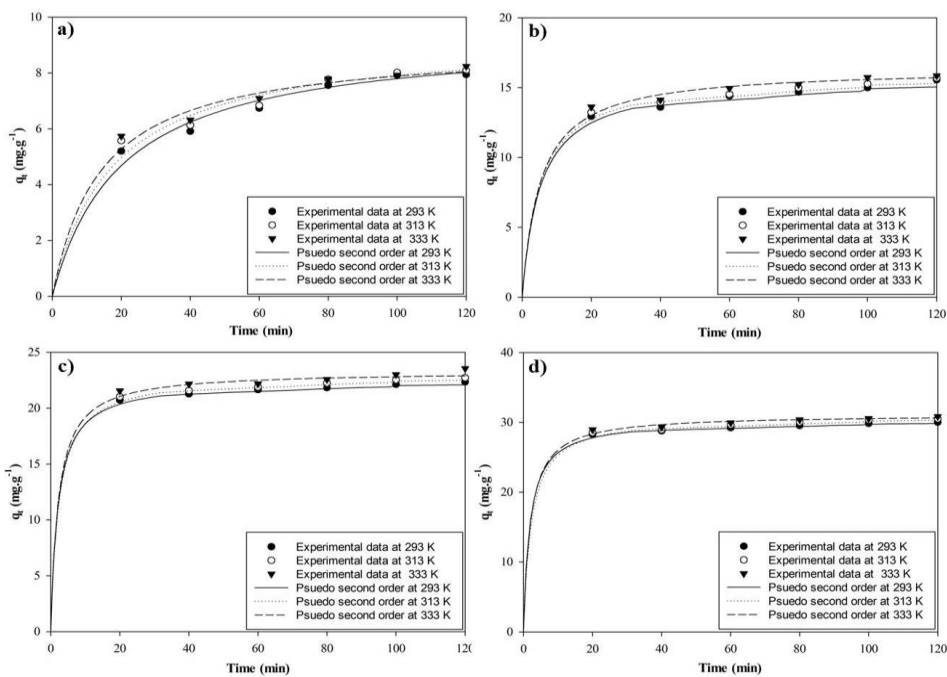


Figure 4. 16 Pseudo-second order model fit shown with experimental data at different temperatures and initial metal concentration a) 50 mg L^{-1} b) 100 mg L^{-1} c) 150 mg L^{-1} d) 200 mg L^{-1}

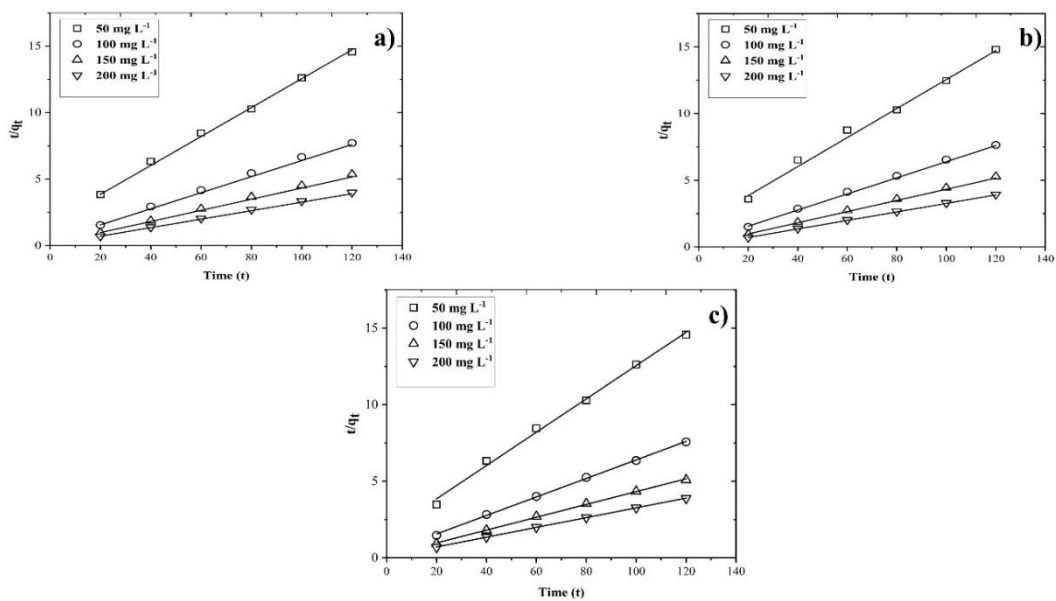


Figure 4. 17 Linearized pseudo-second-order kinetics plots for adsorption of Cr(VI) by LABC at different initial metal concentration (50 mg L^{-1} – 200 mg L^{-1}); different temperatures a) 293 K b) 313 K c) 333 K; at pH 2 and dosage $0.3 \text{ g}/50 \text{ mL}$

Table 4. 4 Collected parameters in the kinetic models

Temperature (T)	C _o (mg g ⁻¹)	Pseudo-first order				Pseudo-second order		
		q _{e,exp}	q _{e,cal}	K ₁	R ²	q _{e,cal}	K ₂	R ²
293 K	50	7.95	0.61	0.012	0.834	9.26	0.006	1.000
	100	15.56	0.25	0.013	0.972	16.18	0.009	0.998
	150	22.34	0.36	0.024	0.966	22.67	0.018	0.999
	200	30.02	0.28	0.028	0.946	30.48	0.016	0.999
313 K	50	8.09	0.10	0.044	0.906	9.28	0.006	0.993
	100	15.85	0.24	0.022	0.955	16.31	0.010	0.999
	150	23.54	0.31	0.026	0.958	23.15	0.016	0.999
	200	30.86	0.22	0.030	0.949	31.05	0.013	0.999
333 K	50	8.23	0.20	0.029	0.966	9.20	0.007	0.996
	100	15.85	0.16	0.035	0.878	16.39	0.114	0.998
	150	23.54	0.36	0.015	0.911	23.86	0.126	0.998
	200	30.86	0.28	0.025	0.978	31.34	0.014	0.999

4.4.6 Adsorption isotherm

The equilibrium data are important for the evaluation of adsorption mechanisms, which can help understand and improve efficiency. Therefore, assessing the adsorption capacity of LABC with various models facilitates process design and optimization of the operating protocols. In this work, equilibrium data were fit with Langmuir, Freundlich, D-R and Temkin models for the removal of Cr(VI), and two models were assessed in terms of removal of Ni(II). The results are shown in Figure. 4.17 for Ni(II) & 4.18a, 4.18b and 4.18c for Cr(VI), and the corresponding parameters are enlisted in Table 4.4 and 4.5. Comparison of the coefficients of determination R^2 for the fits to data collected at different temperatures and at pH 2, adsorbent dose 0.3 g/50 mL, and reaction time 120 min, reveals that the adsorption of Cr(VI) ions by LABC is consistent with the Langmuir model of isothermal adsorption with R^2 value of 0.9989, suggesting that the mechanism was monolayer adsorption. The R_L is between 0 and 1, which indicates favorable adsorption (Anbalagan *et al.*, 2015). The Dubinin–Radushkevich (D-R) and Temkin models are widely employed and represent adsorption with a Gaussian energy distribution of sites on a heterogeneous surface (Argun *et al.*, 2007). The mean adsorption free energy (E_s) estimate from the D–R isotherm provides such important information (Bering, Dubinin, & Serpinsky, 1972). The D-R is typically applied to

differentiate between chemical and physical adsorption of metal ions by E_s values (El-latif & Elkady, 2010). The average $E_s < 8 \text{ kJ mol}^{-1}$ in the current study suggests physisorption as the dominant sorption mechanism. In Temkin isotherm the heat of adsorption is presumed to be in a layer decreases linearly rather than logarithmically with coverage, due to adsorbate-adsorbent interfaces, disregarding extremely low or high concentrations. Numerous constants and parameters can be estimated from the above models fitted to experimental values. The high value of b_T shows fast sorption of adsorbate in the initial stage. Correspondingly, low K_T identifies weak bonding of the adsorbate onto the medium (Sepehr, Amrane, Karimaian, Zarrabi, & Ghaffari, 2014). The Freundlich model was declared to be the best fit model with the data obtained for the removal of Ni(II). As can be seen, LABC after the modification was among the most efficient adsorbents, and hence appears highly promising when compared with the other adsorbents for the application targeted in this study (Table. 4.7). The maximum adsorbent capacity obtained was 27.24 mg g^{-1} at 313 K and pH 2.

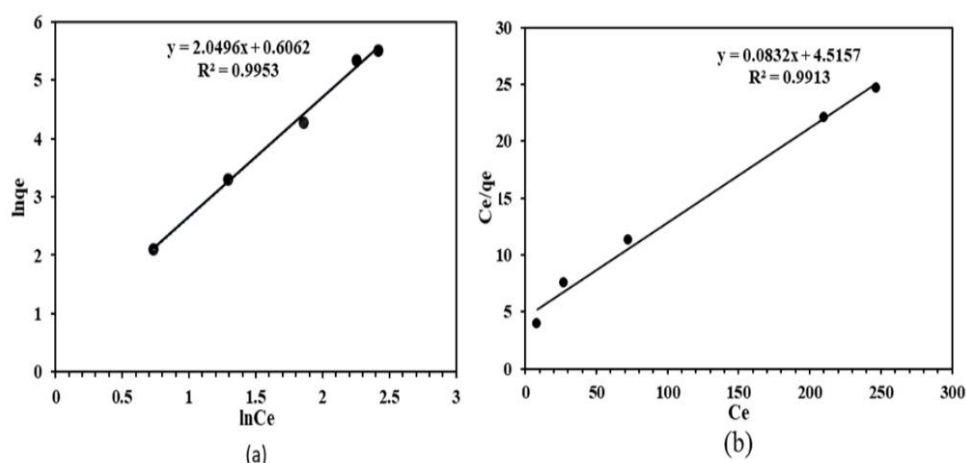


Figure 4. 18 Freundlich adsorption (a) and Langmuir adsorption isotherm (b) for removal of Ni(II) using LAHC

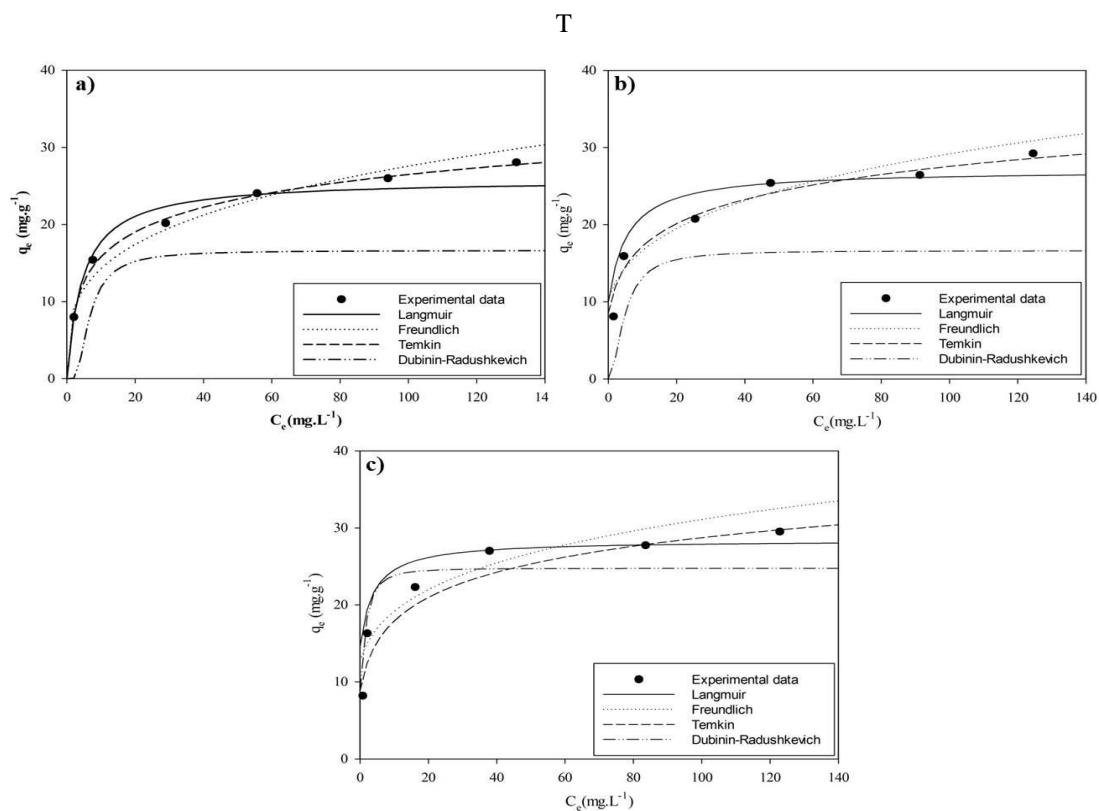


Figure 4. 19 The fitted adsorption isotherms are shown with experimental data for selected temperatures and different initial metal concentration (C_0) a) 50 mg L⁻¹ b) 100 mg L⁻¹ c) 150 mg L⁻¹ d) 200 mg L⁻¹

Table 4. 5 Langmuir and Freundlich isotherm parameters for the sorption of Ni(II) ions onto hydrochar

Isotherm	Parameter	value
Langmuir	q_m (mg g ⁻¹)	12.1
	K_L	0.0183
	R^2	0.9913
Freundlich	n	2.06
	K_f	1.33
	R^2	0.9953

Table 4. 6 Collected parameters for the fitted isotherm models

T (K)	Langmuir's constants				Freundlich's constants			D-R parameters			Temkin parameters		
	K_L (L mg ⁻¹)	q_{max} (mg g ⁻¹)	R_L	R^2	K_f (L g ⁻¹)	n (g L ⁻¹)	R^2	q_{max} (mg g ⁻¹)	E_s (kJ mol ⁻¹)	R^2	K_T (L g ⁻¹)	bT (kJ mol ⁻¹)	R^2
293	0.225	25.2	0.083	0.99	7.473	0.26	0.94	22.5	0.70	0.84	3.14	4.63	0.96
313	0.286	27.2	0.064	0.99	8.605	0.27	0.94	23.8	0.54	0.84	2.67	4.84	0.96
333	0.565	27.1	0.036	0.98	8.659	0.26	0.93	24.6	0.28	0.83	2.41	5.05	0.96

Table 4. 7 Maximum sorption capacities of some adsorbents of hexavalent chromium

Adsorbent	q_{max} (mg g ⁻¹)	Reference
Activated carbon	186	(Khezami & Capart, 2009)
Bagasse	0.57	(Bhatt, Sreedhar, & Padmaja, 2015)
Sorghum stem powder	7.9	(Prasanthi <i>et al.</i> , 2016)
Modified groundnut hull	131	(Owalude & Tella, 2016)
Activated carbon from agriculture waste material	22.29	(Mohan <i>et al.</i> , 2005)
Rubberwood saw dust	4.87	(Suratman <i>et al.</i> , 2009)
methylated biomass of <i>Spirulina platensis</i>	16.70	(Finocchio <i>et al.</i> , 2010)
Sulphuric acid modified waste activated carbons	7.84	(Ghosh, 2009)
Nitric acid modified waste activated carbons	10.92	(Ghosh, 2009)
Montmorillonite-supported magnetite nanoparticles	10.6	(Yuan <i>et al.</i> , 2009)
Lepironia articulata biochar)LABC(27.24	Present study
Lepironia articulata hydrochar (LAHC)	18.86	Present study

4.4.7 Adsorption thermodynamics

To identify the effectiveness of temperature on the removal of heavy metals which was discussed previously, Cr(VI) was selected to go further in-depth energy calculations. The thermodynamics of Cr(VI) adsorption on LABC was investigated based on temperature profile with adsorption kinetics calculated before. When the quantity of adsorbate in the aqueous solution is constant or in an equilibrium state, the change in standard adsorption energy can be obtained by below Eq. (18):

$$\Delta G^{\circ} = -RT \ln K_c \quad (36)$$

The relationship of ΔG° to ΔS° and ΔH° is:

$$\Delta G^{\circ} = \Delta H^{\circ} - T\Delta S^{\circ} \quad (37)$$

By substituting Eq. (36) into Eq. (37), a familiar van't Hoff equation is obtained

$$\ln K_c = \frac{\Delta S^{\circ}}{R} - \frac{\Delta H^{\circ}}{RT} \quad (38)$$

Here, K_c ($L\ g^{-1}$) is an equilibrium constant for two phases. The values of ΔH° and ΔS° are estimated from slope and intercept of a linear fit to $\ln K_c$ vs $1/T$.

The Gibbs free energy change (ΔG°) indicates whether a chemical reaction would take place spontaneously, and therefore is an important piece of information. Negative ΔG° confirms spontaneous adsorption, positive prohibits it. ΔH° (enthalpy change) is the amount of energy released (exothermic process) or consumed (endothermic process) by adsorption. ΔS° (change in entropy), the positive value shows increased randomness whereas the negative value shows decreased during adsorption. A positive ΔS° also specifies that the adsorption comprises a dissociative mechanism, while positive ΔS° corresponds to an associative mechanism (Tran *et al.*, 2016). It is prescribed that the equilibrium constant (K_c) must be dimensionless. In fact, the

common units of ΔG^0 , temperature and, the gas constant are J mol^{-1} , K, $\text{J mol}^{-1} \cdot \text{K}$, and making the K_c in Eq. (36) dimensionless. Various studies have investigated which method provides accurate K_c values for further energy calculations. In this study, to estimate the thermodynamic parameters we applied the Langmuir constant (K_L). The dimensionless K_c can be easily calculated by simply multiplying K_L with the molecular weight of adsorbate (i.e., $51.996 \text{ g mol}^{-1}$ for chromium), 1000, and then 55.5 (moles in one litre of pure water). The above method is briefly explained by Milonji *et al.* (Milonjić, 2007), and Zhou and Zhou (X. Zhou & Zhou, 2014), and has been later on recommended by Tran *et al.* (Tran, Lee, Vu, & Chao, 2017; Tran *et al.*, 2016) in various studies. The summary of estimated thermodynamic parameters from Eqs. (36-38) are listed in Table 4.5. The negative values of ΔG^0 at all temperatures tested confirm that the adsorption of Cr(VI) ions onto LABC was spontaneous. The positive value of ΔS^0 indicates increased disorder at the adsorbent/solution interface from the adsorption of Cr(VI) ions onto LABC. Furthermore, the $-\Delta S^0$ value also indicates that the current adsorption process is entropy-dominated rather than enthalpy-dominated. Meanwhile, the positive ΔH^0 replicates the endothermic nature of the adsorption process, which matches increasing trends of equilibrium constant (Table 4.8) adsorption capacity (Fig. 4.5) with temperature: a higher temperature makes adsorption easier. According to a study by Schneider *et al.*, (2007) endothermic adsorption may be caused by the energy required in a diffusion of ions from the bulk solution to the adsorbent interface, to overcome interactions with dissolved ions and solvated molecules. However, adsorption is expected to occur spontaneously at ambient and elevated temperatures, because ΔH^0 and ΔS^0 are larger than 0 (Schneider *et al.*, 2007).

Table 4. 8 Thermodynamic parameters of the adsorption of Cr(VI) onto Lepironia articulata-derived biochar (LABC) estimated from KL of Langmuir fits equilibrium data

Adsorbate	Temperature (K)	K_c	ΔG° (KJ mol ⁻¹)	ΔH° (KJ mol ⁻¹)	ΔS° (J mol ⁻¹ K ⁻¹)
Cr(VI)	303	651897	-33.73	11.06	114.95
	313	825910	-35.45		
	333	1630465	-39.60		

4.5 Continuous adsorption experiments using fixed-bed column

The efficiency of the adsorbent monolith was tested on a fixed bed adsorption column. A mixture of the aqueous solution was prepared using appropriate amounts of each heavy metals Cr(VI), Ni(II), and Zn(II). The effects of the flowrate (5, 10, and 15 mL/min) and bed height (2, 3, 4 cm) were investigated by keeping other parameters constant. The pH level for all the experiments was kept between 2-3, because of the reason that this is the optimum pH obtained with the highest removal efficiency during batch adsorption experiments. The aqueous solution prepared of 100 mg/L was prepared by mixing the appropriate amount of each heavy metal (Cr(VI), Ni(II), and Zn(II)) from the stock solution. Figure 4.20 shows the breakthrough profiles of metal sorption at different bed heights. It was observed that with the increase in the bed height the breakthrough time (t_b) and exhaustion time (t_e) were also increased (Table 4.8). This may be due to an increase in the surface area of the LABC-MB monolith.

4.5.1 Effect of flow rate

The effect of flow rate on Cr(VI), Ni(II), and Zn(II) sorption was studied by varying the flow rate from 5 to 15 mL/ min, while the bed height and initial metal concentration were held constant at 2cm and 50 mg /L, respectively. Figure 4.19 & 4.20 depicts the breakthrough profile of heavy metals sorption at diverse flow rates, and the results of the breakthrough curve analysis are given in Table 4.8. As estimated, the breakthrough curves became sharper and the breakthrough time decreased with the increase in flow rate. The metal uptake was strongly influenced by increasing the flow rate (from 5 to 15 mL/min), so that, its value increased from 168.43 to 315.43 mg g⁻¹.

In addition, the results showed that in the range of higher flow rates (lower residence times), the overall rate of metal sorption by LABC-MB-monolith was controlled by diffusion limitations of the solute into the pores of sorbent. When the flow rate increased from 5 to 15 mL/min, the liquid residence time in the column decreased, resulting in a lesser sorption of metal ions, and hence, the metal uptake decreased from 315.43 to 308.07 mg/g. A similar observation was reported by Vijayaraghavan *et al.*, 2014, using marine green algae *Ulva reticulata* for biosorption of cobalt, copper and nickel ions in a packed column. All other related regression data obtained from breakthrough models and listed in table 4.8.

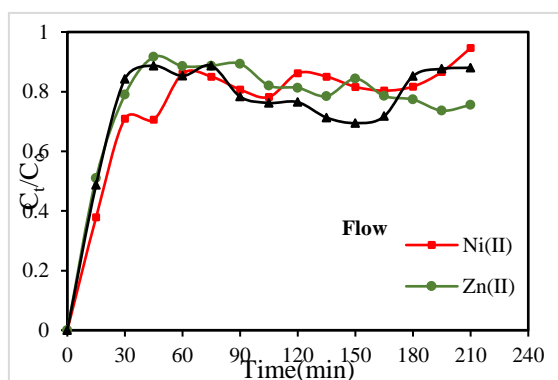


Figure 4. 21 Breakthrough curves for heavy metal adsorption on the LABC-MB monolith at 15 mL/min flow rate at constant inlet metal concentration of 100 (mg/L) and a bed height of 2 cm

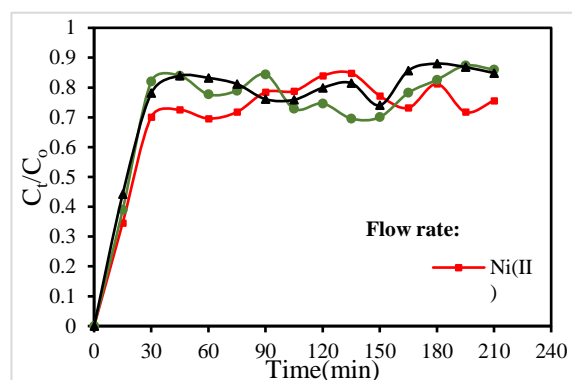


Figure 4. 20 Breakthrough curves for heavy metal adsorption on the LABC-MB monolith at 5 mL/min flow rate at constant inlet metal concentration of 100 (mg/L) and a bed height of 2 cm

4.5.2 Effect of bed height

The sorption performance of LABC-MB monolith was tested at various bed heights at 5 ml /min flow rate and 50 mg/L initial Cr(VI), Ni(II) and Zn(II) concentrations. In order to yield different bed heights, 3, 4 and 6 g of the LABC-MB monolith adsorbent were added to produce bed heights of 2, 3 and 4 cm, respectively. Fig. 4.22 & 4.23 shows the breakthrough profiles of heavy metals sorption at different bed heights. The influence of the bed height was prominent in terms of breakthrough time (t_b) and exhaustion time (t_e), as they both increased with increasing the bed height (Table 4.9). This may be due to an increase in the surface area of the monolith, as the number of adsorbents in monolith increased which was ultimately grown the packed bed in the column, which increased the residence time of the solute in the column,

which tends the solutions containing metal to leave the column before equilibrium is achieved. The second observations is that at the low flow rates range (high residence times), the removal of metal ions in the packed column was controlled by external mass transfer limitations.

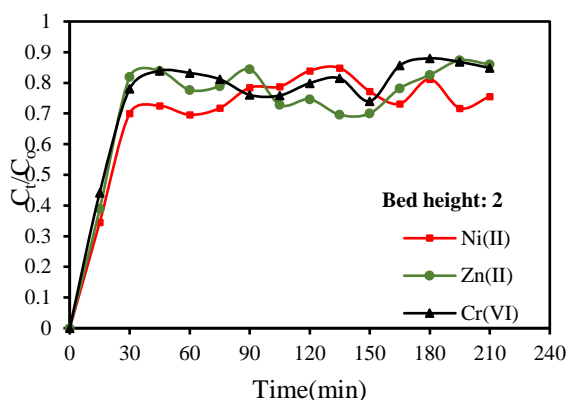


Figure 4. 23 Breakthrough curves for heavy metal adsorption on the LABC-MB monolith at 2 cm bed height and at constant inlet metal concentration of 100 (mg/L) and flow rate 5 mL/min

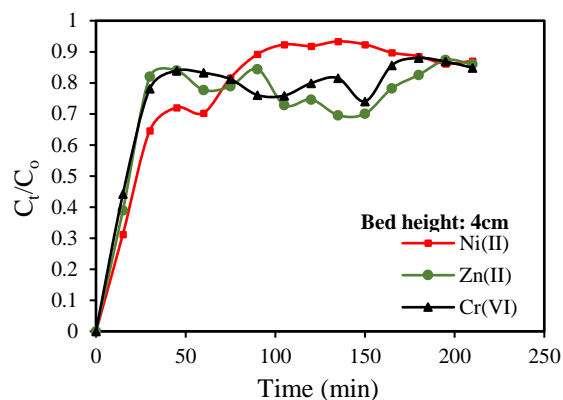


Figure 4. 22 Breakthrough curves for heavy metal adsorption on the LABC-MB monolith at 4 cm bed height and at constant inlet metal concentration of 100 (mg/L) and flow rate 5 mL/min

4.5.3 Breakthrough curve calculations and modeling

a) The bed depth service time (BDST) model

The plot of bed depth versus service time of BDST model was linear at a flow rate of 5 mL/min is linear. A very high correlation coefficient value R^2 of 0.9959 is indicating that the validity of the model is very good. The calculated values of the model parameters (N) and ($K\alpha$) are 393.75 (mg/L) and 0.037 (L/mg h), respectively. Due to smaller ($K\alpha$) value in current study, a progressively deeper bed is required to avoid breakthrough. Whereas, with the larger value of ($K\alpha$), a shorter bed is sufficient to avoid breakthrough.

b) The Adams-Bohart model

The Adams-Bohart model was applied to the experimental data, and the values are presented in the Table 4.8. The correlation coefficients R^2 was obtained in the range of (0.9282 to 0.9788). The effect of flow rate was observed first which indicated the increase in (N_0) with an increase in the flow rate of heavy metals, whereas the (k_{AB})

was decreased, indicating that the adsorption kinetics were controlled by external mass transfer at the start of the adsorption in the packed column. While in case of bed height parameter, there was increase in (N_0) was observed with increase in the bed height, whereas (k_{AB}) value decreased. According to this model, the sorption rate of heavy metals on LABC-MB monolith at equilibrium is not instantaneous, and is proportional to the fraction of sorption capacity (Kizito, Wu, Mondono, Guo, & Dong, 2016).

c) The Thomas model

The experimental data were fitted to the Thomas model. The parameters k_{Th} , q_0 , and the correlation R^2 (obtained in the range of 0.8939 to 0.9838) are calculated and listed in Table 4.9. It can be seen that with the increase in flowrate and decrease in bed height the value of q_0 decreased. The increase in q_0 with bed height was due to the availability of more adsorption sites were available. Whereas, at lower flow rates, the contact time between adsorbate and adsorbent was longer with a higher rate constant, signifying that the adsorption capacity will achieve the equilibrium value quicker (Amin, Alazba, & Shafiq, 2017; Bino, 1990; Chowdhury *et al.*, 2013; Hasan, Ranjan, & Talat, 2010; Kulkarni & Kaware, 2014; Kundu & Gupta, 2005; Papa, 2017).

d) The Yoon-Nelson mode

Finally the Yoon-Nelson model was applied to the obtained experimental data. To retain the 50 % (τ) the time required was obtained for all the data of the breakthrough curves including the corresponding correlation coefficient are shown in Table 4.9. The value of R^2 0.9904 through this model suggest a better fit than the Thomas and Adams-Bohart models, but not the BDST model. There was an increase in the rate constant with an increase in flow rate. In the case of high flow rate, the number of heavy metal ions passing through a particular monolith adsorbent was more, which increases the rate. Whereas a decreases in rate constant was noted with an increase in bed height. Because at higher bed height, the heavy metal molecules had more time to migrate through the column which ultimately results in the decrease in adsorption rate (Amin *et al.*, 2017; Chowdhury *et al.*, 2013; Kulkarni & Kaware, 2014; Kundu & Gupta, 2005).

Table 4. 9 Adams-Bohart, Thomas, and Yoon-Nelson model results from linear regression analysis

Variable Parameters	Initial metal concentration(mg/L)	Adams-Bohart model			Thomas model			Yoon-Nelson model			
		$K_{ab}(L/mg \cdot min)$	N_o (mg/L)	R^2	k_{TH} (L/mg.min)	q_o (mg/g)	R^2	k_{YN} (L/mg.min)	τ (min)	R^2	
Flow rate (mL/min)	5	100	0.0031	296.25	0.92	0.003	7235.8	0.92	0.018	212.3	0.96
	10	100	0.0002	839.65	0.92	0.005	9213.2	0.97	0.012	192.3	0.98
	15	100	0.0002	966.23	0.94	0.0006	9862.21	0.97	0.017	68.4	0.97
Bed height (cm)	2	100	0.0002	789.63	0.95	0.0005	9963.41	0.92	0.012	198.6	0.98
	3	100	0.0001	953.14	0.95	0.002	9786.85	0.89	0.014	188.2	0.98
	4	100	0.0004	1025.78	0.92	0.0005	9218.3	0.97	0.01	59.81	0.99

4.6 Desorption and recycling

This result is significant because the reuse of adsorbent not only can boost its efficiency but also increase its cost-effectiveness. The high percentage desorption of both metal ions indicates the suitability of LABC as a good potential adsorbent. Therefore, the effectiveness of adsorbents was further investigated after conducted desorption experiments using 0.1M NaOH solution. The method followed a three cycle desorption process based on the method obtained from (Ghasemi *et al.*, 2011):

1. 0.1 M solution of NaOH was prepared using 1-liter volumetric flask.
2. 20 mL of 0.1 M NaOH solution was agitated with 0.4g of LABC for 3 hrs.
3. The solution obtained from the last step was filtered and washed several time using DI water.
4. The adsorbent was recycled and used again for the same adsorption process to identify how much effect it works still.

The adsorbent was recycled three times and its efficiency was a measure for the removal of heavy metals, particularly chromium. It was found that the efficiency of adsorbent was little decreased to 96, 88, and 86 % for the first, second and third cycle, respectively. The desorption process was also necessary to calculate the species of

Cr(VI) and Cr(III) individually which is important to identify the adsorption of each element individually.

5. CONCLUSION AND RECOMMENDATIONS

5.1 Conclusion

In the recent development, working on a new biomass material with its effective potential application is utmost important. Keeping in view and utilizing an alternate biomass *Lepironia articulata* (LA) as potential biomass was successfully converted into a variety of products i.e., hydrochar, biochar, liquid, and gas fractions through HTC process. Further modification using KOH as activation agent made the char material more porous, crystallinity and developed the high specific surface area. The following conclusions were made based on characteristics behavior, application, and recycling.

1. The surface morphological structure of the LAHC was much more developed than raw LA. Modification of LAHC into LABC increased its surface area to $820.54 \text{ m}^2 \text{ g}^{-1}$ for LABC from $69.23 \text{ m}^2 \text{ g}^{-1}$ for LAHC.
2. The recovery of heavy metals from aqueous solution was brilliantly improved when applied in a single and mixed heavy metal solution in the batch adsorption experiments. The removal of heavy metals was calculated to be Ni(II) 76 %, Cr(VI) 68%, and Zn(II) 72% when using LAHC, which was improved to be 99.96, 96.56, and 99 % when LABC was introduced as an adsorbent. Similarly, the same trend of increment was calculated in terms of adsorption capacity, which were calculated to be 12.1, 11, and 10 mg/g when using LAHC and increased to 37, 29, and 27 mg/g for Ni(II), Zn(II), and Cr(VI), respectively, when using LABC.
3. The results also concluded that the removal of Cr(VI) was highest at pH 2 which is highest at pH 6 in case of Ni(II) and there was no remarkable change was observed in case of Zn at any pH between 2-7, respectively.
4. The removal of heavy metals was decreased with increase in initial metal concentration, which was calculated to be increased in the case of adsorption capacity.
5. The removal of heavy metals increased with increase in temperature during batch adsorption experiments, the impact of temperature was more while recovering Cr(VI) as compared to Ni(II) and Zn(II).
6. A mixture of cationic surfactant modified bentonite MB and LABC were used to prepare a monolith adsorbent. The unique binders were introduced to sustain its

durability, resistance, and strength. The characteristic behavior of the monolith was very much improved once applied in a fixed bed column study.

7. The removal of heavy metals in a fixed bed column was achieved in 90 minutes with almost 99.9% removal of heavy metals at flowrate 5 mL/min and 50 mg/L initial metal concentration. It was noticed that monolith was strong enough to retain its shape and structure. The waste generation was almost zero due to the non-dispersion of the adsorbent monolith.

8. Desorption cycle of both powdered LABC and monolith was performed to recover back 95 % of the heavy metals that were being absorbed. The monolith was used again for the next batch of experiment and gave almost above 95 % efficiency to remove heavy metals.

5.2 Future recommendation

Several secondary products obtained during HTC treatment can be furthered post-processed to get more valuable products in terms of liquid, solid and gas. Following recommendations are made based on the importance of HTC treatment and the new monolith adsorbent.

1. Once using acid i.e. sulphuric acid during the HTC process may generate more sulphur contents on the char product as well as increase the acidity of the liquid solution. Neglecting the use of acid perhaps need to increase the temperature to synthesize the material well but may give benefit to avoid access washing, removing unwanted sulfur contents, saving the cost of acid, recycling of the liquid product will be easier.

2. The efficiency of LABC can be assessed for the removal of any other contaminants present particularly in industrial and municipal wastewater.

3. Adsorbent monolith could be used as a carbon membrane once designed and re-structured based on its shape, thickness, and content of materials.

4. The adsorbent can be applied in dual applications i.e. 50 % of the adsorption capacity can be attained during heavy metal removal rest of the 50 % can be achieved in soil modification in a future work.

REFERENCES

- Ajaykumar, A. V., Darwish, N. a, & Hilal, N. (2009). Study of various parameters in the biosorption of heavy metals on activated sludge. *World Applied Sciences Journal* 5, 5(2), 32–40.
- Akmar Zakaria, Z., Suratman, M., Mohammed, N., & Azlina Ahmad, W. (2009). Chromium(VI) removal from aqueous solution by untreated rubber wood sawdust. *Desalination*, 244(1–3), 109–121. <https://doi.org/10.1016/j.desal.2008.05.018>
- Aksu, Z., & Gönen, F. (2004). Biosorption of phenol by immobilized activated sludge in a continuous packed bed : prediction of breakthrough curves, 39, 599–613. [https://doi.org/10.1016/S0032-9592\(03\)00132-8](https://doi.org/10.1016/S0032-9592(03)00132-8)
- Al-Shahrani, S. S. (2014). Treatment of wastewater contaminated with cobalt using Saudi activated bentonite. *Alexandria Engineering Journal*, 53(1), 205–211. <https://doi.org/10.1016/j.aej.2013.10.006>
- Aljlil, S. A., & Alsewailem, F. D. (2014). Adsorption of Cu & Ni on bentonite clay from wastewater. *Athens Journal of Natural & Formal Sciences*, 1(March), 21–30.
- Amaya, A., Medero, N., Tancredi, N., Silva, H., & Deiana, C. (2007). Activated carbon briquettes from biomass materials. *Bioresource Technology*, 98(8), 1635–1641. <https://doi.org/10.1016/j.biortech.2006.05.049>
- Amin, M. T., Alazba, A. A., & Shafiq, M. (2017). Batch and fixed-bed column studies for the biosorption of Cu(II) and Pb(II) by raw and treated date palm leaves and orange peel. *Global Nest Journal*, 19(3), 464–478.
- Anbalagan, K., Senthil Kumar, P., Sangita Gayatri, K., Shahul Hameed, S., Sindhuja, M., Prabhakaran, C., & Karthikeyan, R. (2015). Removal and recovery of Ni(II) ions from synthetic wastewater using surface modified *Strychnos potatorum* seeds: experimental optimization and mechanism. *Desalination and Water Treatment*, 53(1), 171–182. <https://doi.org/10.1080/19443994.2013.837008>
- Anyikude, K. U. (2016). Analysis of pollutants in biochars and hydrochars produced by pyrolysis and hydrothermal carbonization of waste biomass.
- Argun, M. E., Dursun, S., Ozdemir, C., & Karatas, M. (2007). Heavy metal adsorption by modified oak sawdust: Thermodynamics and kinetics. *Journal of Hazardous Materials*, 141(1), 77–85. <https://doi.org/10.1016/j.jhazmat.2006.06.095>
- Asadullah; Kaewsichan, Lupong; Tohdee, K. (2018). Potential of BCDMACl modified bentonite in simultaneous adsorption of heavy metal Ni (II) and humic acid. *Journal of Environmental Chemical Engineering*, 6(4), 5616–5624. <https://doi.org/10.1016/j.jece.2018.08.051>
- Asadullah, Kaewsichan, L., & Tohdee, K. (2018). Prospective sorption evaluation of hydrothermally carbonized lepironia articulata (grey sedge) for the removal of Ni (II) from aqueous solution. *Chiang Mai J. Sci*, 45(5), 2220–2231. Retrieved from

http://it.science.cmu.ac.th/ejournal/journalDetail.php?journal_id=9415

- Bering, B. P., Dubinin, M. M., & Serpinsky, V. V. (1972). On thermodynamics of adsorption in micropores. *Journal of Colloid And Interface Science*, 38(1), 185–194. [https://doi.org/10.1016/0021-9797\(72\)90233-0](https://doi.org/10.1016/0021-9797(72)90233-0)
- Bhatt, R., Sreedhar, B., & Padmaja, P. (2015). Adsorption of chromium from aqueous solutions using crosslinked chitosan-diethylenetriaminepentaacetic acid. *International Journal of Biological Macromolecules*, 74, 458–466. <https://doi.org/10.1016/j.ijbiomac.2014.12.041>
- Bino, M. J. (1990). Fixed Bed Adsorption for the Removal of Pollutants from Water. *Water Science and Technology*, 22(1), 33–53.
- Cai, J., Li, B., Chen, C., Wang, J., Zhao, M., & Zhang, K. (2016). Hydrothermal carbonization of tobacco stalk for fuel application. *Bioresource Technology*, 220, 305–311. <https://doi.org/10.1016/j.biortech.2016.08.098>
- Channiwala, S. A., & Parikh, P. P. (2002). A unified correlation for estimating HHV of solid, liquid and gaseous fuels. *Fuel*, 81(8), 1051–1063. [https://doi.org/10.1016/S0016-2361\(01\)00131-4](https://doi.org/10.1016/S0016-2361(01)00131-4)
- Chen, X., Lin, Q., He, R., Zhao, X., & Li, G. (2017). Hydrochar production from watermelon peel by hydrothermal carbonization. *Bioresource Technology*, 241, 236–243. <https://doi.org/10.1016/j.biortech.2017.04.012>
- Chowdhury, Z. Z., Zain, S. M., Rashid, A. K., Ra, R., & Khalid, K. (2013). Breakthrough Curve Analysis for Column Dynamics Sorption of Mn (II) Ions from Wastewater by Using Mangostana garcinia Peel-Based Granular-Activated Carbon, 2013(Ii).
- Clarke, F. W., & Irving Langmuir, B. (1916). Constitution of solids and liquids. *J. Am. Chem. Soc.*, 38(11), 2221–2295. <https://doi.org/10.1021/ja02268a002>
- Coelho, G. F., Gonçalves, A. C., Tarley, C. R. T., Casarin, J., Nacke, H., & Francziskowski, M. A. (2014). Removal of metal ions Cd (II), Pb (II), and Cr (III) from water by the cashew nut shell *Anacardium occidentale* L. *Ecological Engineering*, 73, 514–525. <https://doi.org/10.1016/j.ecoleng.2014.09.103>
- Díaz-Nava, M. C., Olguín, M. T., & Solache-Ríos, M. (2012). Adsorption of phenol onto surfactants modified bentonite. *Journal of Inclusion Phenomena and Macrocyclic Chemistry*, 74(1–4), 67–75. <https://doi.org/10.1007/s10847-011-0084-6>
- Dichiara, A. B., Weinstein, S., & Rogers, R. E. (2015). On the choice of batch or fixed-bed adsorption processes for wastewater treatment. <https://doi.org/10.1021/acs.iecr.5b02350>
- Ding, D., Ma, X., Shi, W., Lei, Z., & Zhang, Z. (2016). Insights into mechanisms of hexavalent chromium removal from aqueous solution by using rice husk pretreated using hydrothermal carbonization technology. *RSC Adv.*, 6(78), 74675–74682. <https://doi.org/10.1039/C6RA17707G>

- Dubinin, M. . (1960). The potential theory of adsorption of gases and vapors. *Adsorption Journal Of The International Adsorption Society*, (13).
- El-latif, M. M. A., & Elkady, M. F. (2010). Equilibrium isotherms for harmful ions sorption using nano zirconium vanadate ion exchanger. *DES*, 255(1–3), 21–43. <https://doi.org/10.1016/j.desal.2010.01.020>
- Falco, C., Baccile, N., & Titirici, M. M. (2011). Morphological and structural differences between glucose, cellulose and lignocellulosic biomass derived hydrothermal carbons. *Green Chemistry*, 13(11), 3273–3281. <https://doi.org/10.1039/c1gc15742f>
- Fałtynowicz, H., Kaczmarczyk, J., & Kułazyński, M. (2015). Preparation and characterization of activated carbons from biomass material - Giant knotweed (*Reynoutria sachalinensis*). *Open Chemistry*, 13(1), 1150–1156. <https://doi.org/10.1515/chem-2015-0128>
- Fang, J., Gao, B., Chen, J., & Zimmerman, A. R. (2015). Hydrochars derived from plant biomass under various conditions: Characterization and potential applications and impacts. *Chemical Engineering Journal*, 267, 253–259. <https://doi.org/10.1016/j.cej.2015.01.026>
- Febrianto, J., Kosasih, A. N., Sunarso, J., Ju, Y. H., Indraswati, N., & Ismadji, S. (2009). Equilibrium and kinetic studies in adsorption of heavy metals using biosorbent: A summary of recent studies. *Journal of Hazardous Materials*, 162(2–3), 616–645. <https://doi.org/10.1016/j.jhazmat.2008.06.042>
- Finocchio, E., Lodi, A., Solisio, C., & Converti, A. (2010). Chromium (VI) removal by methylated biomass of *Spirulina platensis*: The effect of methylation process. *Chemical Engineering Journal*, 156(2), 264–269. <https://doi.org/10.1016/j.cej.2009.10.015>
- Freundlich, H. (1907). Über die Adsorption in Lösungen. *Zeitschrift Für Physikalische Chemie*, 57U(1). <https://doi.org/10.1515/zpch-1907-5723>
- Ghasemi, M., Reza, A., Dabbagh, R., & Safdari, S. J. (2011). Biosorption of uranium (VI) from aqueous solutions by Ca-pretreated *Cystoseira indica alga*: Breakthrough curves studies and modeling. *Journal of Hazardous Materials*, 189(1–2), 141–149. <https://doi.org/10.1016/j.jhazmat.2011.02.011>
- Ghosh, P. K. (2009). Hexavalent chromium [Cr(VI)] removal by acid modified waste activated carbons. *Journal of Hazardous Materials*, 171(1–3), 116–122. <https://doi.org/10.1016/j.jhazmat.2009.05.121>
- Glover, P. (2009). Chapter 1: Introduction. *Advances in Cancer Research*, 104(xiii), 1–8. [https://doi.org/10.1016/S0065-230X\(09\)04001-9](https://doi.org/10.1016/S0065-230X(09)04001-9)
- Goldberg, S. (1991). Sensitivity of surface complexation modeling to the surface site density parameter. *Journal of Colloid And Interface Science*, 145(1), 1–9. [https://doi.org/10.1016/0021-9797\(91\)90095-P](https://doi.org/10.1016/0021-9797(91)90095-P)
- Han, L., Sun, H., Ro, K. S., Sun, K., Libra, J. A., & Xing, B. (2017). Removal of antimony (III) and cadmium (II) from aqueous solution using animal manure-

- derived hydrochars and pyrochars. *Bioresource Technology*, 234, 77–85. <https://doi.org/10.1016/j.biortech.2017.02.130>
- Harper, T. R., & Kingham, N. W. (1992). Removal of arsenic from wastewater using chemical precipitation methods. *Water Environment Research*, 64(3), 200–203. <https://doi.org/10.2175/WER.64.3.2>
- Hasan, S. H., Ranjan, D., & Talat, M. (2010). Agro-industrial waste “wheat bran” for the biosorptive remediation of selenium through continuous up-flow fixed-bed column. *Journal of Hazardous Materials*, 181(1–3), 1134–1142. <https://doi.org/10.1016/j.jhazmat.2010.05.133>
- Hoekman, S. K., Broch, A., & Robbins, C. (2011). Hydrothermal carbonization (HTC) of lignocellulosic biomass. *Energy and Fuels*, 25(4), 1802–1810. <https://doi.org/10.1021/ef101745n>
- Huang, H., Tang, J., Gao, K., He, R., Zhao, H., & Werner, D. (2017). Characterization of KOH modified biochars from different pyrolysis temperatures and enhanced adsorption of antibiotics. *RSC Adv.*, 7(24), 14640–14648. <https://doi.org/10.1039/C6RA27881G>
- Iqbal, M., Saeed, A., & Zafar, S. I. (2009). FTIR spectrophotometry, kinetics and adsorption isotherms modeling, ion exchange, and EDX analysis for understanding the mechanism of Cd²⁺ and Pb²⁺ removal by mango peel waste. *Journal of Hazardous Materials*, 164(1), 161–171. <https://doi.org/10.1016/j.jhazmat.2008.07.141>
- Järup, L. (2003). Hazards of heavy metal contamination. *British Medical Bulletin*, 68, 167–182. <https://doi.org/10.1093/bmb/ldg032>
- Kang, G., & Cao, Y. (2014). Application and modification of poly(vinylidene fluoride) (PVDF) membranes – A review, 463, 145–165. <https://doi.org/10.1016/j.memsci.2014.03.055>
- Kang, S., Li, X., Fan, J., & Chang, J. (2012). Characterization of hydrochars produced by hydrothermal carbonization of lignin, cellulose, d-xylose, and wood meal. *Industrial and engineering chemistry research*, 51(26), 9023–9031. <https://doi.org/10.1021/ie300565d>
- Kang, S., Li, X., Fan, J., & Chang, J. (2016). A direct synthesis of adsorbable hydrochar by hydrothermal conversion of lignin. *Energy Sources, Part A: Recovery, utilization, and environmental effects*, 38(9), 1255–1261. <https://doi.org/10.1080/15567036.2011.631970>
- Kannan, S., Garipey, Y., & Raghavan, G. S. V. (2017). Optimization and characterization of hydrochar derived from shrimp waste. *Energy and Fuels*, 31(4), 4068–4077. <https://doi.org/10.1021/acs.energyfuels.7b00093>
- Khezami, L., & Capart, R. (2005). Removal of chromium(VI) from aqueous solution by activated carbons: Kinetic and equilibrium studies. *Journal of Hazardous Materials*, 123(1–3), 223–231. <https://doi.org/10.1016/j.jhazmat.2005.04.012>
- Kizito, S., Wu, S., Mondono, S., Guo, L., & Dong, R. (2016). Science of the Total

- Environment Evaluation of ammonium adsorption in biochar- fixed beds for treatment of anaerobically digested swine slurry : Experimental optimization and modeling. *Science of the Total Environment*. <https://doi.org/10.1016/j.scitotenv.2016.05.149>
- Kulkarni, S. J., & Kaware, J. P. (2014). Fixed Bed Removal of Heavy Metal- a Review, (6), 861–871.
- Kundu, S., & Gupta, A. K. (2005). Analysis and modeling of fixed bed column operations on As(V) removal by adsorption onto iron oxide-coated cement (IOCC). *Journal of Colloid and Interface Science*, 290(1), 52–60. <https://doi.org/10.1016/j.jcis.2005.04.006>
- Lin, D., Chang, C., Chen, T., & Cheng, L. (2002). Microporous PVDF membrane formation by immersion precipitation from water / TEP / PVDF system, 145, 25–29.
- Liu, Z., Zhang, F. S., & Wu, J. (2010). Characterization and application of chars produced from pinewood pyrolysis and hydrothermal treatment. *Fuel*, 89(2), 510–514. <https://doi.org/10.1016/j.fuel.2009.08.042>
- Mckay, G. (2011). Simplified fixed bed design models for the adsorption of acid dyes on novel pine cone derived activated carbon simplified fixed bed design models for the adsorption of acid dyes on novel pine cone derived activated carbon, (June). <https://doi.org/10.1007/s11270-010-0635-2>
- Melichova, Z., & Hromada, L. (2013). Adsorption of Pb^{2+} and Cu^{2+} Ions from aqueous solutions on natural bentonite. *Polish Journal of Environmental Studies*, 22(2), 457–464.
- Mihajlović, M., Petrović, J., Kragović, M., Stojanović, M., Milojković, J., Lopičić, Z., & Koprivica, M. (2017). Effect of KOH activation on hydrochars surface: FT-IR analysis. *RAD Association Journal*, 2(1), 65–67. <https://doi.org/10.21175/RadJ.2017.01.014>
- Mihajlović, M., Petrović, J., Stojanović, M., Milojković, J., Lopičić, Z., Koprivica, M., & Lačnjevac, Č. (2016). Hydrochars, perspective adsorbents of heavy metals: A review of the current state of studies. *Zastita Materijala*, 57(3), 488–495. <https://doi.org/10.5937/ZasMat1603488M>
- Milonjić, S. K. (2007). A consideration of the correct calculation of thermodynamic parameters of adsorption. *Journal of the Serbian Chemical Society*, 72(12), 1363–1367. <https://doi.org/10.2298/JSC0712363M>
- Mohan, D., Singh, K. P., & Singh, V. K. (2005). Removal of hexavalent chromium from aqueous solution using low-cost activated carbons derived from agricultural waste materials and activated carbon fabric cloth. *Industrial and Engineering Chemistry Research*, 44(4), 1027–1042. <https://doi.org/10.1021/ie0400898>
- Nakason, K., Panyapinyopol, B., Kanokkantapong, V., Viriya-empikul, N., Kraithong, W., & Pavasant, P. (2016). Characteristics of hydrochar and liquid fraction from hydrothermal carbonization of cassava rhizome. *Journal of the Energy Institute*.

<https://doi.org/10.1016/j.joei.2017.01.002>

- Nakason, K., Panyapinyopol, B., Kanokkantung, V., Viriya-empikul, N., Kraithong, W., & Pavasant, P. (2018). Characteristics of hydrochar and liquid fraction from hydrothermal carbonization of cassava rhizome. *Journal of the Energy Institute*, *91*(2), 184–193. <https://doi.org/10.1016/j.joei.2017.01.002>
- Nasatto, P. L., Pignon, F., Silveira, J. L. M., Duarte, M. E. R., Nosedá, M. D., & Rinaudo, M. (2015). Methylcellulose, a cellulose derivative with original physical properties and extended applications. *Polymers*, *7*(5), 777–803. <https://doi.org/10.3390/polym7050777>
- Olayinka, O. K., Oyedéji, O. A., & Oyeyiola, O. A. (2009). Removal of chromium and nickel ions from aqueous solution by adsorption on modified coconut husk. *Science And Technology*, *3*(10), 286–293. <https://doi.org/10.5897/AJEST09.053>
- Owalude, S. O., & Tella, A. C. (2016). Removal of hexavalent chromium from aqueous solutions by adsorption on modified groundnut hull. *Beni-Suef University Journal of Basic and Applied Sciences*, *5*(4), 377–388. <https://doi.org/10.1016/j.bjbas.2016.11.005>
- Papa, E. F. (2017). Batch and fixed bed column studies on cadmium (II) and lead (II) adsorption from aqueous solution by coffee pulp biochar. *5th International conference on civil, architecture, environment and waste management (CAEWM-17)*, (ii), 284–289.
- Pinskii, D. L., Minkina, T. M., Mandzhieva, S. S., Bauer, T. V., & Nevidomskaya, D. G. (2014). Adsorption features of Cu (II), Pb (II), and Zn (II) by an ordinary chernozem from nitrate, chloride, acetate, and sulfate solutions, *47*(1), 22–29. <https://doi.org/10.1134/S1064229313110069>
- Prasanthi, M. R., Jayasravanthi, M., & Nadh, R. V. (2016). Kinetic, thermodynamic and equilibrium studies on removal of hexavalent chromium from aqueous solutions using agro-waste biomaterials, casuarina equisetifolia L. and sorghum bicolor, *33*(8), 2374–2383. <https://doi.org/10.1007/s11814-016-0078-6>
- Puccini, M., Stefanelli, E., Hiltz, M., & Seggiani, M. (2017). Activated carbon from hydrochar produced by hydrothermal carbonization of wastes. *Chemical Engineering Transactions*, *57*, 169–174. <https://doi.org/10.3303/CET1757029>
- Reza, M. T., Lynam, J. G., Uddin, M. H., & Coronella, C. J. (2013). Hydrothermal carbonization: Fate of inorganics. *Biomass and Bioenergy*, *49*, 86–94. <https://doi.org/10.1016/j.biombioe.2012.12.004>
- Reza, M. T., Rottler, E., Herklotz, L., & Wirth, B. (2015). Hydrothermal carbonization (HTC) of wheat straw: Influence of feedwater pH prepared by acetic acid and potassium hydroxide. *Bioresource Technology*, *182*, 336–344. <https://doi.org/10.1016/j.biortech.2015.02.024>
- Rizhikovs, J., Zandersons, J., Spince, B., Dobeles, G., & Jakab, E. (2012). Preparation of granular activated carbon from hydrothermally treated and pelletized deciduous wood. *Journal of Analytical and Applied Pyrolysis*, *93*, 68–76.

<https://doi.org/10.1016/j.jaap.2011.09.009>

- Saeidi, N., & Lotfollahi, M. N. (2015). Effects of powder activated carbon particle size on activated carbon monoliths properties, *6914*(December). <https://doi.org/10.1080/10426914.2015.1117630>
- Safarpour, M., Khataee, A., & Vatanpour, V. (2014). Preparation of a novel PVDF ultrafiltration membrane modified with reduced graphene oxide / TiO₂ nanocomposite with enhanced hydrophilicity and antifouling properties. <https://doi.org/10.1021/ie502407g>
- Saravanan, A., Senthil Kumar, P., & Preetha, B. (2016). Optimization of process parameters for the removal of chromium(VI) and nickel(II) from aqueous solutions by mixed biosorbents (custard apple seeds and *Aspergillus niger*) using response surface methodology. *Desalination and Water Treatment*, *57*(31), 14530–14543. <https://doi.org/10.1080/19443994.2015.1064034>
- Schneider, R. M., Cavalin, C. F., Barros, M. A. S. D., & Tavares, C. R. G. (2007). Adsorption of chromium ions in activated carbon. *Chemical Engineering Journal*, *132*(1–3), 355–362. <https://doi.org/10.1016/j.cej.2007.01.031>
- Seki, K., Saito, N., & Aoyama, M. (1997). Removal of heavy metal ions from solutions by coniferous barks. *Wood Sci. Technol.*, *31*(6), 441–447.
- Sepehr, M. N., Amrane, A., Karimaian, K. A., Zarrabi, M., & Ghaffari, H. R. (2014). Potential of waste pumice and surface modified pumice for hexavalent chromium removal: Characterization, equilibrium, thermodynamic and kinetic study. *Journal of the Taiwan Institute of Chemical Engineers*, *45*(2), 635–647. <https://doi.org/10.1016/j.jtice.2013.07.005>
- Sun, K., Tang, J., Gong, Y., & Zhang, H. (2015). Characterization of potassium hydroxide (KOH) modified hydrochars from different feedstocks for enhanced removal of heavy metals from water. *Environmental Science and Pollution Research*, *22*(21), 16640–16651. <https://doi.org/10.1007/s11356-015-4849-0>
- Syafalni, R., Abdullah, I., Abustan, A. N. M. I. (2013). Wastewater treatment using bentonite, the combinations of bentonite-zeolite, bentonite-alum, and bentonite-limestone as adsorbent and coagulant. *International Journal of Environmental Sciences*, *4*(3), 379–391. <https://doi.org/10.6088/ijes.2013040300014>
- Tekin, K., Karagöz, S., & Bekta, S. (2014). A review of hydrothermal biomass processing, *40*, 673–687. <https://doi.org/10.1016/j.rser.2014.07.216>
- Tewari, N., Vasudevan, P., & Guha, B. K. (2005). Study on biosorption of Cr(VI) by *Mucor hiemalis*. *Biochemical Engineering Journal*, *23*(2), 185–192. <https://doi.org/10.1016/j.bej.2005.01.011>
- Tohdee, K., Kaewsichan, L., & Asadullah. (2018). Enhancement of adsorption efficiency of heavy metal Cu(II) and Zn(II) onto cationic surfactant modified bentonite. *Journal of Environmental Chemical Engineering*, *6*(2), 2821–2828. <https://doi.org/10.1016/j.jece.2018.04.030>
- Tran, H. N., Lee, C. K., Vu, M. T., & Chao, H. P. (2017). Removal of Copper, Lead,

- Methylene Green 5, and Acid Red 1 by Saccharide-Derived Spherical Biochar Prepared at Low Calcination Temperatures: Adsorption Kinetics, Isotherms, and Thermodynamics. *Water, Air, and Soil Pollution*, 228(10). <https://doi.org/10.1007/s11270-017-3582-3>
- Tran, H. N., You, S. J., & Chao, H. P. (2016). Thermodynamic parameters of cadmium adsorption onto orange peel calculated from various methods: A comparison study. *Journal of Environmental Chemical Engineering*, 4(3), 2671–2682. <https://doi.org/10.1016/j.jece.2016.05.009>
- Tripathi, A., & Rawat Ranjan, M. (2015). Heavy metal removal from wastewater using low cost adsorbents. *Journal of Bioremediation & Biodegradation*, 06(06). <https://doi.org/10.4172/2155-6199.1000315>
- Verma, A., Chakraborty, S., & Basu, J. K. (2006). Adsorption study of hexavalent chromium using tamarind hull-based adsorbents. *Separation and Purification Technology*, 50(3), 336–341. <https://doi.org/10.1016/j.seppur.2005.12.007>
- Worch, E. (2012). *Adsorption technology in water treatment: Fundamentals, Processes, and Modeling*. <https://doi.org/10.1515/9783110240238>
- Xu, Z., Cai, J.-G., & Pan, B.-C. (2013). Mathematically modeling fixed-bed adsorption in aqueous systems. *Journal of Zhejiang University-SCIENCE A (Applied Physics & Engineering)*, 14(3), 155–176. <https://doi.org/10.1631/jzus.A1300029>
- Xue, Y., Gao, B., Yao, Y., Inyang, M., Zhang, M., Zimmerman, A. R., & Ro, K. S. (2012). Hydrogen peroxide modification enhances the ability of biochar (hydrochar) produced from hydrothermal carbonization of peanut hull to remove aqueous heavy metals: Batch and column tests. *Chemical Engineering Journal*, 200–202, 673–680. <https://doi.org/10.1016/j.cej.2012.06.116>
- Yuan, P., Fan, M., Yang, D., He, H., Liu, D., Yuan, A., Chen, T. H. (2009). Montmorillonite-supported magnetite nanoparticles for the removal of hexavalent chromium [Cr(VI)] from aqueous solutions. *Journal of Hazardous Materials*, 166(2–3), 821–829. <https://doi.org/10.1016/j.jhazmat.2008.11.083>
- Zeng, Z., Zhang, S., Li, T., Zhao, F., He, Z., & Zhao, H. (2013). Sorption of ammonium and phosphate from aqueous solution by biochar derived from phytoremediation plants *, 14(12), 1152–1161. <https://doi.org/10.1631/jzus.B1300102>
- Zhang, L., Liu, S., Wang, B., Wang, Q., Yang, G., & Chen, J. (2015). Effect of residence time on hydrothermal carbonization of corn cob residual. *BioResources*, 10(3), 3979–3986. <https://doi.org/10.15376/biores.10.3.3979-3986>
- Zhou, J. L. (2016). Progress in the preparation and application of modified biochar for improved contaminant removal from water and wastewater. *Bioresource Technology*, 214(June), 836–851. <https://doi.org/10.1016/j.biortech.2016.05.057>
- Zhou, N., Chen, H., Feng, Q., Yao, D., Chen, H., Wang, H., ... Lu, X. (2017). Effect of phosphoric acid on the surface properties and Pb(II) adsorption mechanisms of hydrochars prepared from fresh banana peels. *Journal of Cleaner Production*, 165, 221–230. <https://doi.org/10.1016/j.jclepro.2017.07.111>

- Zhou, X., & Zhou, X. (2014). The unit problem in the thermodynamic calculation of adsorption using the langmuir equation. *Chemical Engineering Communications*, 201(11), 1459–1467. <https://doi.org/10.1080/00986445.2013.818541>
- Zhu, X., Liu, Y., Zhou, C., Luo, G., Zhang, S., & Chen, J. (2014). A novel porous carbon derived from hydrothermal carbon for efficient adsorption of tetracycline. *Carbon*, 77, 627–636. <https://doi.org/10.1016/j.carbon.2014.05.067>
- Zhu, Z., Tang, S., Yuan, J., Qin, X., Deng, Y., Qu, R., & Haarberg, G. M. (2016). Effects of various binders on supercapacitor performances. *International Journal of Electrochemical Science*, 11(10), 8270–8279. <https://doi.org/10.20964/2016.10.04>

APPENDIX

1. Publication 1

Perspective sorption evaluation of hydrothermally carbonized *lepironia articulata* for the removal of Ni (II) from aqueous solution.

Asadullah, Lupong Kaewsichan, Kanogwan tohdee



Chiang Mai J. Sci. 2018; 45(5) : 2220-2231
<http://epg.science.cmu.ac.th/ejournal/> Contributed Paper

Prospective sorption evaluation of hydrothermally carbonized *Lepironia articulata* (Grey sedge) for the removal of Ni (II) from aqueous Solution

Asadullah, Lupong Kaewsichan* and Kanogwan Tohdee

Department of Chemical Engineering, Faculty of Engineering, Prince of Songkla University, Hat Yai, Songkhla 90112 Thailand.

* Author for correspondence; e-mail: lupong.k@psu.ac.th

Received: 1 November 2017

Accepted: 30 April 2018

ABSTRACT

As an alternate to pyrolysis, hydrothermal carbonization has been proposed as a promising technique for conversion of different wastes into biofuels, adsorbents and specific chemicals. Different types of biomass wastes were used for converting to adsorbent by researchers and their potential to adsorb heavy metals was reported to be excellent. This paper presents the efficiency of hydrochar produced from an alternate biomass *Lepironia articulata* (LA) through series of activation and carbonization methods for the removal of Ni (II) from aqueous solution, as well as proposed methods of improving hydrochar surface reactivity. Hydrochar produced at 200 °C with a maximum yield of 60% and with an improved surface functional group was selected as an adsorbent. The kinetic study, pH effect, an effect of Ni (II) initial concentration, and adsorbent dose were examined in batch experiments. Fourier Transform Infrared Spectroscopy (FT-IR) was employed to characterize the resulting *lepironia articulata* hydrochar (LAHC). The results of this characterization showed that after the hydrothermal carbonization, the functional groups from fresh biomass were preserved. Based on FT-IR results it can be concluded that the metal binding in biomass of LA takes place by the substitution of Ni (II) ions by an amine, nitro, and carboxylic functional groups. Furthermore, adsorption data for Ni (II) uptake by hydrochar were analyzed according to Langmuir and Freundlich adsorption models. It was noticed from results that maximum uptake percentage of Ni (II) was 72.77% at the initial concentration of 100 mg L⁻¹ and pH 6. The adsorption equilibrium was established in 180 minutes. The maximum adsorption capacity (q_m) calculated is 12.2 mg g⁻¹. Through above evident results it has been proved that the low-cost hydrochar prepared from LA has potential to adsorb Ni (II) from aqueous solution.

Keywords: pyrolysis, hydrothermal carbonization, adsorption, hydrochar

1. INTRODUCTION

Hydrothermal Carbonization (HTC) is a wet biomass conversion technology. It mimics the natural process of coal formation in the lab in just a few hours. During the HTC reaction, water, carbon dioxide, and other compounds are cleaved from the biomass. Subsequently, the energy density is raised significantly and the heating value is estimated to that of dry, high quality brown coal [1, 2]. At the same time, the macromolecular structure of the original biomass will be completely destroyed. This provides a porous, brittle and in part dust-like product that is considerably easier to dry and to be used as an efficient adsorbent in wastewater treatment applications. The HTC process is performed in high-pressure vessels by applying relatively high temperature (generally in the range 180-250 °C) and pressure (approximately 1000-5000 kPa) to biomass in liquid water for a few hours (0.5-8 h) in the absence of air [1]. The main products of HTC are the carbonaceous material hydrochar (HC), process liquid containing various inorganic and organic compounds, and no condensable gases [2]. The extra productive approach, cost effectiveness and efficient methodology for the production of HC has made this material a worth taking for the treatment of wastewater [3].

Although HC exhibits relatively undeveloped porous structure and surface chemistry with acidic properties, high O/C ratio of HC obtained at lower HTC temperatures indicate a greater abundance of surface organic functional groups (OFGs). Another advantage of the hydrothermal method is to allow carbonaceous sphere formation of nano and/or micro size. These carbonaceous spheres have a wide variety of surface functional groups such as -OH, C=O and -COOH [4]. Due to their characteristic structure and abundance of oxygen-

containing functional groups, HC represents suitable alternative lower-cost sorbent for removal of a wide spectrum of water contamination [5]. Therefore, the heavy metal adsorption ability of HC has been reported to be noteworthy [6-8].

Presently there is an exponential increment in the number of studies managing the utilization of various HC as adsorbent of heavy metals including nickel ions.

In recent study, Han *et al.*, [9] from their study concluded that the high sorption capacity of HC obtained from animal manure for the removal of antimony (III) and cadmium (II). In another study Liu *et al.*, [6] have characterized and investigated Cu(II) adsorption properties of pinewood HC. The results indicated the existence of a large amount of OFGs on the HC surface responsible for removal of 4.46 mg g⁻¹ for Cu (II). Still, there are only a few studies for the removal of heavy metals using HC. In most of the previous studies, the HC prepared were only characterized for their surface and structures, further research studies on new biomass for their conversion to HC for the wastewater treatment application is still needed to be filled.

Therefore the objectives of this study were to prepare *Lepironia articulata* hydrochar (LAHC) using optimized HTC process. Further obtained LAHC was characterized according to its functional groups, cation exchange capacity (CEC) and yield to find out its significance for the removal of Ni (II) ions from aqueous solution. The responsible mechanisms for the removal of Ni (II) were elucidated at different pHs, doses, adsorbate initial concentrations and by means of batch adsorption isotherms.

2. MATERIALS AND METHODS

2.1 Material and Equipment

Type of biomass used in this study was *Lepironia articulata* (LA) obtained from Thalae Noi wetland area in Phatthalung, one of the southern provinces in Thailand.

All other chemical reagents were used of analytical grade obtained from Sigma-Aldrich. To prepare stock solution analytical grade heavy metal salt $\text{NiSO}_4 \times 6\text{H}_2\text{O}$ was used.

HTC experiments were carried out in a 1000 mL autoclave reactor equipped with an external resistance heater and internal sensor thermocouple. The internal temperature of the reactor was controlled using electric thermostats single display PID controller in a panel. A pressure gauge was also fitted at the top left of the reactor to monitor inside pressure and release pressure through safety valve if required.

2.2 Preparation of Hydrochar (HC)

The HC preparation method was obtained from [4]. LA obtained was first cut into small pieces of less than 2 cm and then washed several times with distilled water and dried by putting a sample into the heating oven under 80 °C for 3 hours or until the constant weight obtained. 30 gram of dried sample was dispersed into 300 mL distilled water (ratio 1:10) contained in a round bottom flask. 5 % (v/v) sulfuric acid was then mixed as a catalyst. The mixture was shaken vigorously to create a homogenous suspension. The suspension was put into the Teflon chamber which was then fixed into the reactor. Feed stock was heated at 200 °C for a residence time of 24 hours for all experiments [10]. After completing cycle the heater was turned off and the reactor was allowed to cool down to ambient condition. The solid material (HC) and liquid products were collected and subsequently separated by filtration using whatmann no.42 filter paper. HC samples were washed thoroughly with warm distilled water and 0.1 M

hydrochloric acid followed by washing with distilled water until neutral pH appeared. Filtered sample was dried in an oven at 105 °C for 3 hours. Dried samples were ground and sieved up to desired particle size and kept in airtight polyethylene bags for further experiments.

2.3 Physiochemical Characterization

Fourier transform infrared (FTIR) analysis of the biomass feed stock and HC were conducted using Bruker Vortex 70 spectrometer to analyze the modification in functional groups after hydrothermal carbonization. By the application of the standard Brunauer-Emmett-Teller (BET) adsorption-desorption isotherm method, the pore properties and BET surface area (S_{BET}) were accessed using the micromeritics ASAP 2460 model analyzer. In which, the surface area was calculated based on adsorption data in the partial pressure (P/Po) range from 0.0095 to 0.9948 and the total pore volume was determined from the amount of nitrogen adsorbed at a relative pressure of 0.99. The micropore surface area and the micropore volume were obtained via t-plot analysis. The ammonium acetate method was used to determine the cation exchange capacity (CEC). The concentration of the Ni (II) in the aqueous solution was determined using Perkin Elmer AAnalyst 100 flame Atomic Absorption Spectrometer (AAS) by taking results through WinLab software at wavelength of 341.5 nm. A calibration curve was developed using standard Ni(II) solution in the concentration range of 7, 10, 20, 30, 50 and 100 mg L⁻¹, respectively, for the quantification of Ni(II) after the adsorption processes.

2.4. Adsorption Experiments

Batch adsorption experiments were performed in a laboratory incubator shaker (Daihan WIS-20 Shaking Incubator) at 150 rpm under the controlled temperature. Experiments were carried out by allowing an accurately weighed amount of adsorbent (20 g L⁻¹) into 50 mL Ni (II) solution of various initial concentrations ranging (50 - 500 mg L⁻¹) in 250 mL conical flasks. A stock solution of 1000 mg L⁻¹ Ni (II) was initially prepared from analytical grade Nickel sulfate (NiSO₄×6H₂O) crystals using double distilled water. Experiments with variable pH, initial adsorbate concentration and contact time were initially conducted. pH of the sample solutions was adjusted using 0.1N HCl or 0.1N NaOH solution. To calculate the isotherm equilibrium data another set of experiment was performed by varying contact time under the controlled temperature of 303 K. All the above experiments were performed in triplicate. Adsorption capacity of the samples were measured using following equation (Eq. (1)).

$$q_e = \frac{(C_o - C_e)v}{m} \quad (1)$$

Where q_e is the mass of Ni (II) ions adsorbed per mass of LAHC at equilibrium (mg g⁻¹), v is the volume (L) of solution used for batch experiments, m is the mass (g) of adsorbent whereas C_o is the initial concentration (mg L⁻¹) of Ni (II) ions in solution, and C_e is the equilibrium concentration of solution (mg L⁻¹) when amount adsorbed equals to q_e .

2.5 Adsorption Isotherm

2.5.1 Adsorption Isotherm models

Adsorption equilibrium is the set of conditions at which the number of molecules arriving on the surface of the adsorbent equals the number of molecules that are leaving. The relation between the amount of adsorbate adsorbed by an adsorbent (solid) and the concentration of the adsorbate at equilibrium and constant temperature is called adsorption isotherm [11].

Langmuir adsorption isotherm model equation (Eq. (2)) and Freundlich adsorption isotherm model equation (Eq. (3)) were used to fitting the sorption data.

$$q_e = \frac{q_m K_L C_e}{1 + K_L C_e} \quad (2)$$

$$q_e = K_f C_e^{1/n} \quad (3)$$

Where q_m (mg·g⁻¹) is the Langmuir saturated adsorption capacity; K_L is a Langmuir constant (L mg⁻¹); K_f (L g⁻¹) is the Freundlich affinity coefficient, and n is the Freundlich exponential coefficient [12].

3. RESULTS AND DISCUSSION

3.1 Characteristics of Hydrochar (HC)

The prepared LAHC samples were characterized by measuring their surface functional groups, cation exchange capacity (CEC), and HC yield.

(A) Surface functional groups

Large surface area and well-developed porosity do not always indicate greater ability, in the adsorption, besides the structural morphology, surface functional groups perform essential role [13].

The Surface area of the adsorbent used for the removal of heavy metals is another important parameter to be considered before adsorption process. Although in current study functional groups took major part in adsorption ion exchange process, high surface area and pore volume have also contributed towards the maximum capture of Ni (II) ions. The Surface area, pore volume and pore size of LAHC obtained were $69.22 \text{ m}^2 \text{ g}^{-1}$, $0.0800 \text{ cm}^3 \text{ g}^{-1}$ and 4.623 nm respectively, which were found to be high when compared with previous research data (Table 1).

Oxygenated functional groups such as C-O, OH, and COOH are significant for improving hydrochar performance in various applications [14]. For example, surface OH and COOH groups can greatly enhance the adsorption capacity when HC is used as an adsorbent for heavy-metal removal. This is because such groups interact with the metals via hydrogen bonding and complexation [15]. Surface functional groups were improved during hydrothermal synthesis.

A comparison of FTIR spectra of raw biomass and LAHC is illustrated in Figure 1. The absorption peak between 3300 cm^{-1} and 3600 cm^{-1} is assigned to O-H stretching vibrations, the peak between 2850 cm^{-1} and 2920 cm^{-1} represents C-H stretching vibrations [16], the band between 1650 cm^{-1} and 1735 cm^{-1} change is attributed to represent C-O functional groups and aromatic C-O [5], the adsorption band observed at 1512 cm^{-1} corresponds to aromatic C-C, and the peak between 1000 cm^{-1} and 1250 cm^{-1} represents C-O bending vibrations [17]. When comparing with raw biomass some newly

formed peaks at 3420 cm^{-1} in the spectra recorded for LAHC indicates hydroxyl groups which widely play role during the adsorption process. In the main, resulting findings indicate that in the removal of heavy metals, amount of the surface OFGs are closely correlated to the adsorption capacity of HC [13], 200°C and 24 hours residence time.

Figure 1. More oxygenated functional groups developed can be seen in Figure 1 shown on LAHC spectra line. Generally, LAHC is rich in functional groups containing oxygen and aromatic components which are containing C-O and C-C bands, which are the major components of LAHC.

b) Surface area, pore size, and pore volume

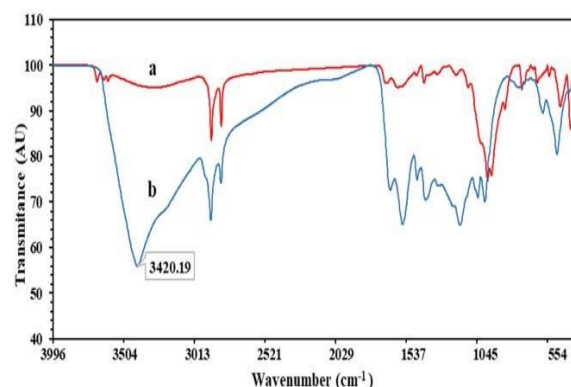


Figure 1. The FTIR spectra of raw LA and LAHC at 200°C

Table 1. Comparison of hydrochars by HTC process using different biomass feed stock.

Feed stock	Metal/ Organic	HTC Time	HTC Temperature (°C)	Surface area ($m^2 g^{-1}$)	Pore volume ($cm^3 g^{-1}$)	Avg pore diameter (nm)	Yield (%)	CEC ($cmol_c kg^{-1}$)	qm ($mg g^{-1}$)	Reference
Seafood waste	NA	1 ^h	150	NA	NA	NA	38.12	NA	NA	[24]
Peanut hu	Ni(II), Pb(II)	5 ^h	300	1.3	NA	NA	38	NA	6.47	[25]
Peels of Carya cathayens sarg	NA	15	280	NA	NA	NA	44.9	NA	NA	[26]
Bamboo hydrochar	Congo red & Naphthol	2 ^h	200	17.94	0.03	3.83	65.7	NA	33.7	[27]
Fresh banana peels	Pb(II)	2 ^h	230	45.27	NA	NA	39.59	NA	14.80	[28]
Municipa waste	PO4-P, NH4-N	NA	250	2	NA	NA	NA	44.5	1.14	[18]
Lepironia Articulata	Ni(II)	24 ^h	200	69.22	0.0800	4.623	60	40	12.1	Current study

c) Cation Exchange Capacity (CEC)

As CEC is said to be a function of surface area and functionality, an increase in hydrochar CEC suggests either the unblocking of pores increasing porosity and surface area or that a higher surface functionality is being revealed by removing tar. The effect of higher surface functionality is being revealed by removing tar may be more important as the surface area had negligible influence on char CEC, with HC possessing low surface areas ($< 6 \text{ m}^2 \text{ g}^{-1}$) [18]. The development of carboxyl and other functional groups can improve CEC [19]. Current study revealed a high CEC value of ($40 \text{ cmol}_c \text{ kg}^{-1}$) listed in Table 1 which is better when compared to HC from different biomass. Improvement in heavy metal removal efficiency in current study is the reason due to the development of negative functional groups on the surface of HC and higher CEC value.

d) Hydrochar yield

Solid mass yield is one of the key characteristics for HC. It is very important to control parameters during hydrothermal treatment to increase the product yield and retaining its adsorption efficiency. Below equation (Eq. (4)) is used to calculate HC yield on dry basis

$$\text{Yield of HC(\%)} = \frac{\text{mass of hydrochar (dry basis)}}{\text{mass biomass before hydrolysis (dry basis)}} \times 100 \quad (4)$$

Yield and CEC along with q_m of the HC are listed in Table 1. Which clearly shows a good yield of 60% achieved in the current study. Low temperature with long retention time can also lead to high yield whereas high temperature may lead to

decrease the yield. Long retention time is helpful to break down the hemicellulose complexes into various functional groups.

3.2 Effect of pH

The pH of the solution has a significant impact on the uptake of heavy metals since it determines the surface charge of the adsorbent and the degree of ionization and speciation of the adsorbate [20]. Figure 2 shows the similar trend as percentage removal of Ni (II) as a function of pH at a heavy metal concentration of 50 mg L^{-1} and a HC dosage of 20 g L^{-1} . Removal efficiency of Ni (II) increases with increase in pH of the solution to 6. After that, a small decrease was observed to pH 7. The percent adsorption of metal ion decreased with the decrease in pH below 5, because protons compete with metal ions for sorption sites on the adsorbent surface and because the contaminant decreases the negative charge of the same surface [21]. On the other hand at higher pH values above 6, the precipitation is dominant or both ion exchange and aqueous metal hydroxide formation (not necessarily precipitation) may become significant mechanisms in the metal removal process. In practice the precipitation can be very small in size sometimes and, upon the neutralization of the wastewater the solubility of the metal ion increases, which leads to re-contamination of the treated water. Therefore the pH of the solution was kept at 6 for rest of the experiments.

3.3 Effect of Initial Concentration of adsorbate

The Initial concentration of adsorbate is one of the effective factors on adsorption efficiency. To calculate the removal efficiency of Ni(II) by varying initial

adsorbate concentration, experiments were done with variable initial Ni(II) concentration (50, 100, 200, 400 and 500 mg L⁻¹) and constant temperature (303 K), pH (6), agitation speed (150 rpm), contact time (2 h) and adsorbent dose (20 g L⁻¹). The experimental results of the effect of initial Ni (II) concentration on removal efficiency were presented in Figure 3. The trend line shown in Figure 3 illustrates a decrease in removal efficiency of Ni (II) from aqueous solution with an increase in initial adsorbate concentration. In case the low concentration of Ni (II) the fractional adsorption become independent of initial Ni (II) ions due to the fact that the ratio of initial number of moles of adsorbate ions to the available surface area of LAHC is large. However, at higher concentration, the uptake rate becomes slower which ultimately decreases the removal efficiency of adsorbent overall, it is likely due to most of the sites on adsorbent are already occupied when the concentration is high.

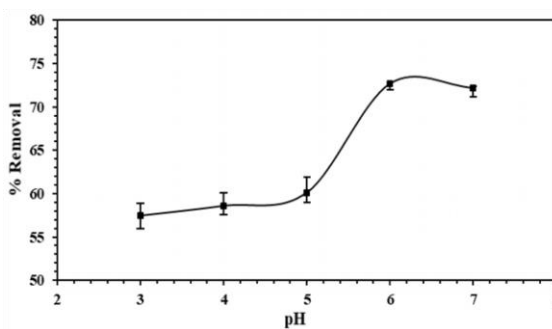


Figure 2. Effect of pH on the percent removal of Nickel; initial metal Concentration of 50 mg L⁻¹ and hydrochar dosage of 20 g L⁻¹.

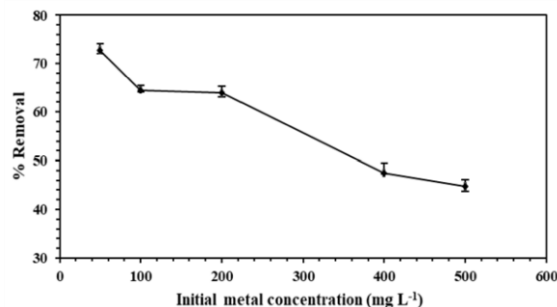


Figure 3. Removal efficiency of Ni(II) with variable initial Concentration of adsorbate (mg L⁻¹).

3.4 Effect of Contact Time on Removal Efficiency

Adsorption of Ni (II) was examined against contact time (min). A 20 g L⁻¹ fixed amount of adsorbent was mixed with 50 mL of the sample solution in a 250 mL conical flask and were shaken with a different interval of time. From Figure 4 a trend of increase in removal efficiency is observed against time 15, 30, 60, 90, 120, and 180 min respectively, the plot illustrates that the percent nickel removal is higher at the start; this is possibly due to a larger surface area of the LAHC being accessible at the beginning for the adsorption of nickel. As soon as the adsorption sites become exhausted, the uptake rate is minimized and controlled by the rate of adsorbate ions which are transported from exterior to the interior available sites of the adsorbent. The maximum percentage removal of Ni (II) was achieved after 120 min of contact time and thereafter no further increment in removal efficiency was observed. From above observations, it was concluded that the maximum time required for the removal of Ni (II) from aqueous solution was 120 min whereas the adsorption of Ni (II) took place immediately after 15 min of starting a process.

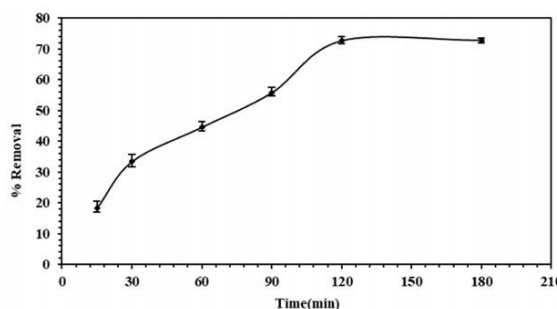


Figure 4. Removal efficiency of Ni(II) against contact time (min) of adsorption process.

3.5 Adsorption Isotherm Models

Modelling of experimental data from adsorption processes is a very important means of predicting the mechanisms of various adsorption systems [21]. Various adsorption isotherm models are being used to identify the adsorption process in detail. To identify the model which best fits the experimental data linearized equations are used to calculate adsorption rate, capacity, and mechanism. Initial values in terms of equilibrium adsorption capacity and adsorbate ion concentration were first calculated before plotting to isotherm model. Adsorption capacity or maximum rate of adsorption can be found in Figure 5. Which shows the linear trend of equilibrium adsorption capacity q_e (mg g^{-1}) against Ni (II) ion concentration in the solution at equilibrium adsorbate concentration in solution C_e (mg L^{-1}). Langmuir and Freundlich isotherm models were studied in this research. Both models were used to identify the surface mechanism of adsorption of Ni (II) onto LAHC.

Langmuir isotherm accounts for the surface coverage by balancing the relative rates of adsorption and desorption (dynamic equilibrium). Adsorption is proportional to the fraction of the surface of the adsorbent that is opened while desorption is proportional to the fraction

of the adsorbent surface that is covered [22]. Freundlich isotherm gives an expression which defines the surface heterogeneity and the exponential distribution of active sites and their energies [23].

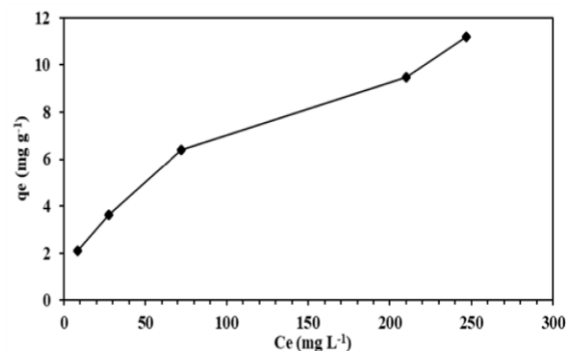


Figure 5. Adsorption capacity q_e (mg g^{-1}) Against Equilibrium adsorbate concentration in solution C_e (mg L^{-1})

Figure 6 (a) and (b) shows that both Langmuir and Freundlich isotherm models fit the experimental data. Still, the trend is better in case of Freundlich isotherm model. The results clearly demonstrate that the adsorption is favorable in terms of higher adsorption capacity with equal distribution of metal ions amongst the active sites of adsorbent. Table 2 Further illustrates the correlation coefficients and constants used in both isotherm models. Value of K_L is 0.0183 which characterizes the ability of LAHC surface to adsorb Ni (II) from the aqueous solution at equilibrium concentration in surface monolayer. Whereas the value of $1/n$ from Freundlich model smaller than 1 represents favorable adsorption condition, and a smaller $1/n$ value indicates an easier adsorption process [22]. In the current study the value of $1/n$ is 0.4856 which is well under 1 and satisfies favorable adsorption process.

Table 2. Langmuir and Freundlich isotherm parameters for the sorption Ni(II) ions onto hydrochar.

Isotherm	Parameter	Value
Langmuir	q_m (mg g ⁻¹)	12.1
	K_L	0.0183
	R_2	0.9913
Freundlich	1/n	0.4856
	K_f	1.33
	R_2	0.9953

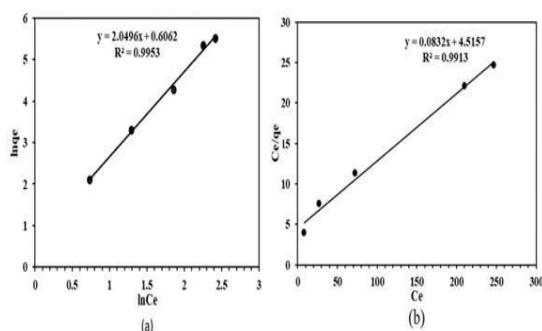


Figure 6. (a) Freundlich adsorption isotherm, (b) Langmuir adsorption isotherm.

4. CONCLUSION

The hydrothermal synthesis process for the preparation of HC from *Lepironia articulata* was found inexpensive and productive. Equilibrium data obtained for LAHC were plotted using Langmuir and Freundlich isotherm linear equations, the later one exhibited the best fit with 1/n calculated 0.4856 and $R^2 = 0.9953$. The maximum removal efficiency obtained was 72.77% with pH 6 and 100 mg L⁻¹ Initial metal concentration. Product yield was calculated to be 60% and was found excellent when compared with different HC obtained from various biomass materials. It was concluded that synthesizing of biomass at 200 °C and 24 h residence time in the presence of a catalyst can lead to highest yield and could help in the development of negative

functional groups on the surface of HC, which is helpful in the removal of cationic heavy metal. Environmental issues concerning to high-temperature pyrolysis methods could be reduced up to a maximum extent, as this process does not allow the gaseous product to release into the open atmosphere and the remaining liquor can be further processed to obtain various other useful products. It is therefore suggested LAHC can be utilized to remove various contaminants in wastewater and the removal efficiency and adsorption capacity of the adsorbent can be enhanced by applying further modification on the structure of HC.

ACKNOWLEDGEMENTS

This research was supported by the Higher Education Research Promotion and Thailand's Education Hub for Southern Region of ASEAN countries (TEH-AC 054/ 2016) Project Office of the Higher Education Commission and graduate school Prince of Songkla University.

REFERENCES

- [1] Lucian M. and Fiori L., *Energies*, 2017; **10**: 211. DOI 10.3390/en10020211.
- [2] Owsianiak M., Ryberg M.W., Renz M., Hitzl M. and Hauschild M.Z., *ACS Sustain. Chem. Eng.*, 2016; **4**: 6783-6791. DOI 10.1021/acssuschemeng.6b01732.
- [3] Girling R.D. and Hassall M., *Agric. For. Entomol.*, 2008; **10**: 297-306. DOI

- 10.1111/j.1461-9563.2008.00379.x.
- [4] Donar Y.O., Caglar E. and Sinag A., *Fuel*, 2016; **183**: 366-372. DOI 10.1016/j.fuel.2016.06.108.
- [5] Mihajlovic M., Petrovic J., Stojanovic M. and Koprivica M., *RAD J.*, 2017; **2**: 65-67. DOI 10.21175/RadJ.2017.01.014.
- [6] Liu Z., Zhang F.S. and J. Wu. J., *Fuel*, 2010; **89**: 510-514. DOI 10.1016/j.fuel.2009.08.042.
- [7] Kang S., Li X., Fan J. and Chang J., *Ind. Eng. Chem. Res.*, 2012; **51**: 9023-9031. DOI 10.1021/ie300565d.
- [8] Regmi P., Garcia Moscoso J.L., Kumar S., Cao X., Mao J. and Schafran G., *J. Environ. Manage.*, 2012; **109**: 61-69. DOI 10.1016/j.jenvman.2012.04.047.
- [9] Han L., Sun H., Ro K.S., Sun K., Libra J.A. and Xing B., *Bioresour. Technol.*, 2017; **234**: 77-85. DOI 10.1016/j.biortech.2017.02.130.
- [9]. Guo S., Dong., Wu T., F. Shi F. and Zhu C., *J. Anal. Appl. Pyrol.*, 2015; **116**: 1-9. DOI 10.1016/j.jaap.2015.10.015.
- [10] Somasundaram S., Sekar K., Gupta V.K. and Ganesan S., *J. Mol. Liq.*, 2013; **177**: 416-425. DOI 10.1016/j.molliq.2012.09.022.
- Bartczak P., Norman M., Klapiszewski L., Karwanska N., Kawalec M., Zdarta J. and Jesionowski T., *Arab. J. Chem.*, 2015. DOI 10.1016/j.arabjc.2015.07.018.
- [11] Mihajlovic M., Petrovic J., Stojanovic M. and Lacnjevac C., *Zastita Materijala*, 2016; **57**: 488-495. DOI 10.5937/ZasMat1603488M.
- [12] Zhu X., Liu Y., Qian F., Zhang S. and Chen J., *Energy Fuels*, 2015; **29**: 5222-5230. DOI 10.1021/acs.energyfuels.5b00512.
- [13] Xu D., Zhao Y., Sun K. and Wu F., *Chemosphere*, 2014; **111**: 320-326. DOI 10.1016/j.chemosphere.2014.04.043.
- [14] Yao Z., Ma Z., Wu Z. and Yao, J. *Anal. Appl. Pyrol.*, 2017; **123**: 40-48. DOI 10.1016/j.jaap.2016.12.031.
- [15] Liu Z. and Zhang F.S., *Desalination*, 2011; **267**: 101-106. DOI 10.1016/j.desal.2010.09.013.
- [16] Takaya C.A., Fletcher L.A., Singh S., Anyikude K.U. and Ross A.B., *Chemosphere*, 2016; **145**: 518-527. DOI 10.1016/j.chemosphere.2015.11.052.
- [17]
- [19] Boehm H.P., *Carbon*, 1994; **32**: 759-769. DOI 10.1016/0008-6223(94)90031-0.
- [20] Cho H., Oh D. and Kim K., *J. Hazard. Mater.*, 2005; **127**: 187-195. DOI 10.1016/j.jhazmat.2005.07.019.
- [21] El-Khariary M.I., *J. Hazard. Mater.*, 2008; **158**: 73-87. DOI 10.1016/j.jhazmat.2008.01.052.
- [22] McQuarrie D.A. and Simon J.D., *Physical Chemistry: A Molecular Approach*, 1st Edn., University Science Books: Sausalito, California, 1997.

- [23] Gunay A., Arsalankaya E. and Tosun I., *J. Hazard. Mater.*, 2007; **146**: 362-371. DOI 10.1016/j.jhazmat.2006.12.034.
- [24] Kannan S., Garipey Y. and Raghavan V., *Energy Fuels*, 2015; **29**: 8006-8016. DOI 10.1021/acs.energyfuels.5b01671.
- [25] Xue Y., Gao B., Yao Y., Zhang M. and Ro K.S., *Chem. Eng. J.*, 2012; **200-202**: 673-680. DOI 10.1016/j.cej.2012.06.116.
- [26] Yang W.T., Shimanouchi T. and Kimura Y., *Desalin. Water Treat.*, 2015; **53**: 2831-2838. DOI 10.1080/19443994.2014.931537.
- [27] Li Y., Meas A., Shan S., Yang R. and Gai X., *Bioresour. Technol.*, 2016; **207**: 379-386. DOI 10.1016/j.biortech.2016.02.012.
- [28] Zhou N., Chen H., Feng Q., Yao D., Chen H., Wang H., Zhou Z., Li H., Tian Y. and Lu X., *J. Clean. Prod.*, 2017; **165**: 221-230. DOI 10.1016/j.jclepro. 2017.07.111.

VITAE

Name Mr. Asadullah

Student ID 5910130002

Educational Attainment

Degree	Name of Institution	Year of Graduation
Master of Engineering (Chemical)	University of Moratuwa Sri Lanka	2015
Bachelor of Science (Chemical Engineering)	Punjab University, Pakistan	2004

Scholarship Awards during Enrolment

Thailand Education Hub (TEH-AC) Scholarship, Prince of Songkla University, Hatyai, Thailand.

Prince of Songkla University Graduate Studies Grant for Ph.D. thesis research

Work – Position and Address

Assistant Professor at Balochistan University of information technology, Engineering and Management science, Quetta, Pakistan.

List of Publication

Asadullah, L. Kaewsichan, Tohdee.k “Prospective Sorption Evaluation of Hydrothermally Carbonized Lepironia articulata (Grey sedge) for the Removal of Ni (II) from Aqueous Solution” August 2018 Chiang Mai Journal of Science 45(5):2220-2231